Fall 2016

Parametric Investigation of a Laboratory Drop Test to Simulate Base Acceleration Induced By Wave Impacts of High Speed Planing Craft

John D. Barber
Old Dominion University

PARAMETRIC INVESTIGATION OF A LABORATORY DROP TEST TO SIMULATE BASE ACCELERATION INDUCED BY WAVE IMPACTS OF HIGH SPEED PLANING CRAFT

by

John D. Barber
B.S.M.E. May 1985, University of Evansville

A Thesis Submitted to the Faculty of
Old Dominion University in Partial Fulfillment of the
Requirements for the Degree of

MASTER OF SCIENCE

MECHANICAL ENGINEERING

OLD DOMINION UNIVERSITY
December 2016

Approved by:

Gene Hou (Director)

Timothy Coats (Member)

Jennifer Michaeli (Member)

ABSTRACT

PARAMETRIC INVESTIGATION OF A LABORATORY DROP TEST TO SIMULATE BASE ACCELERATION INDUCED BY WAVE IMPACTS OF HIGH SPEED PLANING CRAFT

John D. Barber
Old Dominion University, 2016
Director: Dr. Gene Hou

High speed operations in a small craft can be physically punishing and, in some circumstances, even dangerous for the crew. The aspect of small craft operations that make them punishing for the crew is wave slamming generated by wave impacts as the craft is travelling over the seas at high speed.

The initial step of this thesis effort was to perform a literature survey to determine what knowledge existed within the technical and academic community about wave slamming and simulating them with drop tests.

Eventually, a final experiment strongly influenced by the experiment model found in (Protocol 1, 2014) was formulated. Technical drawings were produced which in turn were given to the NSWCCD DN waterfront fabrication shop at Naval Station Norfolk for fabrication. The fabricated hardware was assembled and instrumented. A predetermined series of drops were performed and data was recorded and analyzed.

Once the reduced data was obtained, trends were observed and conclusions of the research were drawn. Finally, the math models were generated using tools in MATLAB. The math models can be used as a tool to customize a drop test that can simulate a single wave impact. An example of how to customize a drop test to simulate a single wave impact is provided.

This thesis is dedicated to my wife, Vivian, my daughter, Rachel, and my son, Michael. Thank you all for your patience, love, strength and encouragement while I completed this journey.

ACKNOWLEDGMENTS

I would like to thank my wife, Vivian, and children, Rachel and Michael for their unwavering support and love throughout this academic journey. They all have endured the cost of tuition and countless nights when I have been in class or on campus for various other reasons. They never complained and listened with interest when I talked about what I was doing. I thank them so much.

I would like to thank Mr. Dave Pogorzelski for his support in getting the experiment complete.

I would like to thank Mr. Dan Holmes for his help with instrumentation and data collection. His expertise was greatly appreciated. It would have been impossible to complete this effort without him.

I would like to thank Mr. Ernest Roscoe, Mr. Mark Sedaca and Mr. Duran Slinde for their work in completing the experiment.

I would like to thank Mr. Mike Riley for his valuable assistance in this effort. I would like to thank Mike for his patience as he taught me just a fraction of what he knows about this interesting subject. I know there must have been times when he thought that I would never understand this subject (I had those same feelings too), but he stayed the course and helped me from start to finish. I owe him so much.

Finally, I would like to thank Dr. Gene Hou for his assistance in completing this thesis. Most of all, I thank him for giving me the initial opportunity to pursue a graduate degree. No other instructors or department heads would even consider me as a candidate. He saw my potential and opened the door for me to pursue a graduate degree. I will be forever in his debt.

TABLE OF CONTENTS

Chapter Page

LIST OF FIGURES

Figure Page

Figure Page

LIST OF TABLES

Table Page

CHAPTER 1

1. INTRODUCTION

1.1 Problem Statement and Motivation

High speed operations in a small craft can be physically punishing and in some circumstances, even dangerous for the crew. This fact can be easily understood when considering the vastness of the sea itself in relation to the physical dimensions and characteristics of a small craft. The design tradeoffs that make these small craft so popular for commercial, search and rescue, law enforcement and military purposes are the acceleration, the high top speed and the small drafts that these craft typically draw. These qualities are of great importance to law enforcement agencies and military special operations forces.

Unfortunately, the sea can be a hostile and unforgiving environment. The sea can often turn from a very pleasant place to work in to one of great turmoil and danger within a matter of minutes. This situation typically arises because of rapidly changing weather fronts in the local area and also because of the craft's position relative to a safe harbor at the time that the weather front arrives. When adverse weather strikes, the crew of a small craft is forced to endure rough sea conditions until the mission is over or until they arrive at a safe harbor to seek refuge. Even conditions that are benign for large ships can become hazardous for small craft. A photograph of a Naval Special Warfare 11 Meter Rigid Inflatable Boat operating at high speed in a low sea state is provided as Figure 1.

Figure 1. Naval Special Warfare 11 Meter Rigid Inflatable Boat (NSWCCD Photograph)

As illustrated in Figure 1, even a combination of high speed and a low sea state can result in significant craft motion. Craft motion is not random; rather, it is the response of the craft to a number of input factors such as wave interaction, craft speed, craft weight, hull shape, etc. A complete study of all design parameter interactions with craft motion is outside the scope of this document; rather, the focus of this study is the interaction of 3 specific parameters based on a laboratory test. The specific parameters to be investigated are (a) weight, (b) drop height and (c) wedge angle. The laboratory test and the decision making process that resulted in choosing these 3 parameters will be discussed.

1.2 Approach

The initial step of this thesis effort was to perform a literature survey to determine what knowledge existed within the technical and academic community regarding the wave slam phenomena and the procedures necessary to evaluate impulse signals. The findings of this effort help to refine further research and the objectives of this thesis.

The next step was to design the experiment. Eventually a final experiment design was strongly influenced by the experiment model found in (Protocol 1, 2014). The unique hardware used in the described experiment was modeled in GeoMagic Design Expert, and technical

drawings were produced which in turn were given to the NSWCCD DN waterfront fabrication shop at Naval Station Norfolk for fabrication.

The fabricated hardware was assembled and instrumented. A predetermined series of drops were performed, and data was recorded on a National Instruments, Inc., data acquisition system with a sampling rate of no less than 2,000 Hz. The recorded data was post processed and converted into a text file using a script written in National Instruments, Inc. LABVIEW by Naval Surface Warfare Center, Carderock Division, Norfolk Detachment (NSWCCD DN), Code 835 personnel.

Once the reduced data was obtained, trends were observed and conclusions about the proposed research were drawn. Finally, the math models were generated using tools in MATLAB.

1.3 Contribution Of The Thesis To The Technical Community

The contributions of this research to the technical community are primarily that it presents a study that describes the effects of (a) wedge angle, (b) drop weight and (c) drop height upon the acceleration amplitude and acceleration duration produced by dropping a test fixture whose design and test procedure was influenced by (Protocol 1 2014). The results of the parametric variation observed in the experiments will help other researchers better understand the physics of drop tests performed with sand impact surfaces to better simulate wave impacts in a laboratory test. A secondary product of this thesis will be a pair of math models. Each model will have wedge angle, drop weight and drop height as the inputs. The output for one model will be predicted acceleration amplitude, and the output for the other model will be predicted acceleration duration. An example of how to use the empirical models to formulate a single event impact will be provided. Additionally, topics for further investigation based upon this thesis will also be provided in the conclusions and recommendations chapter.

1.4 Scope Of Thesis

Chapter 1 presents motivation and background information that is necessary in order to understand the purpose and goals of this thesis. Chapter 2 provides more background information regarding wave slam events and the procedure for analyzing wave impact events.

This background and wave impact analysis procedure allows the reader to develop a further appreciation for the physical events that occur during a wave slam event and how these events are tied to the proposed test procedure. Chapter 3 describes the experimental setup used and provides a discussion of the initial results. Chapter 4 is a discussion of the results. Chapter 5 presents the conclusions and important findings of this study.

1.5 Review of Previous Works

A significant amount of analysis work concerning the rigid body motion response of small, high speed craft in a seaway has been performed by Naval Surface Warfare Center, Carderock Division, Norfolk Detachment (NSWCCD DN). The mission of NSWCCD DN is to provide complete small craft support to the US Navy. This support includes, but is not limited to, design, acquisition, in-service support and asset tracking. The analysis work of rigid body motion response was performed by NSWCCD DN in support of the above mentioned design tasking. The overall goal of this analysis work was to better understand the rigid body motion response of small craft and ultimately to promote a standardized method of analyzing vertical acceleration.

A problem that has existed within the small craft community is a general disagreement between technical experts regarding the method to analyze data obtained from an accelerometer secured to the deck of a high-speed craft while underway in a seaway. As an example of this lack of consistency, one analyst could look at vertical acceleration data recorded in the time domain and count every noticeable peak while another analyst could decide to pick only those peaks that he considered to be significant. In this case, the number of peaks counted by the two analysts when looking at the same vertical acceleration data could differ by thousands of peaks counted. Since there was no standard method to identify what constituted a peak, there was no method to determine which of the two peak counts were more applicable. In the same manner, there also existed no guidance regarding data filtering or any guidance regarding a minimum time interval between significant peaks.

Engineers at NSWCCD DN began a process to rectify the situation concerning the lack of a standardized method for evaluating vertical acceleration data (Riley, Haupt, Jacobson 2010).

The first step was to review the many sets of time history acceleration data for small craft that have been tested at NSWCCD DN. During this review process, the engineers at NSWCCD DN noticed that the craft encounters with waves (hereafter referred to as wave impacts) exhibited a relatively constant periodicity for a given speed and sea state. Specifically, the engineers noticed and then verified that for craft in seas greater than 1.6 feet significant wave height and at speeds between 10 and 50 knots, the wave impact frequency was less than 2 waves per second. Engineers then made the observation that using a time duration peak discriminator instead of an amplitude threshold as the peak discriminator made further calculations more predictable and intuitive. Based on the wave impact frequency of less than 2 waves per second, the engineers surmised that when looking a Fast Fourier Transform (FFT) of any vertical acceleration data, any frequency content in the acceleration record greater than 2 Hertz must be coming from a source other than rigid body encounters with the waves.

As stated above, the engineers did notice some frequency content greater than 2 Hertz. During the review process, engineers routinely performed a FFT on the many time history acceleration data sets and noticed a trend. The trend was that the largest spectral amplitudes corresponded to frequencies below 10 Hertz, and smaller spectral amplitudes occurred between 20 Hertz and 80 Hertz. The engineers came to the conclusion that these smaller spectral amplitudes were the result of local deck flexure and machinery vibration. In order to isolate the rigid body motion component from the time history acceleration data sets, engineers concluded that in most cases, a 10 Hertz low pass filter provided optimum results. This conclusion was arrived at by performing many Fast Fourier Transforms (FFT) of actual small craft test data. Any person using this method should always perform an FFT analysis of their specific data to determine the most appropriate low pass filtering level. Engineers also noted that a Butterworth filter, a Bessel filter and a Kaiser Window filter produced results within a few percent of each other. Therefore, the filter type used was not as critical as selecting the appropriate cut off frequency value. As stated above, the selection of a 10 Hertz low pass filter was a good starting point in most cases based on the observation of many FFT analyses.

The final step of this process was determining a reasonable acceleration baseline level for analyzing and counting higher acceleration peaks induced by wave impacts. This

acceleration level should be high enough so as to ignore small incidental wave impacts and not be so large as to ignore slightly larger yet significant wave impacts. Engineers concluded that a convenient and effective baseline would be the Root Mean Square (RMS) of all of the data points in the data set. Strictly speaking, the RMS is a measure of the average fluctuation about the mean for a time varying signal. It was observed that the RMS value tends to correlate well with the average upward acceleration due to buoyancy and hydrodynamic lift after each impact is over.

In this document (Riley, Haupt, Jacobson 2010), engineers laid the foundation for a standardized method to evaluate vertical acceleration data obtained from small high-speed craft in a seaway. The foundation of this method was to (a) demean the data set, (b) apply a 10 Hertz low pass filter to the data set, (c) compute the RMS value for the demeaned and filtered data set and (d) identify peaks. The peaks were identified by selecting the first peak of interest that demonstrated a value greater than the RMS value. The next peak and all subsequent peaks needed to satisfy two conditions. The first condition was that the next peak shall have a value greater than the RMS value and the peak shall occur at a time value greater than 0.5 seconds from the previously identified peak. For the edification of a reader that is not familiar with the term demean, demean is the process of removing the +1 G bias that an accelerometer produces while it sits still and level. Following the demean process, the average value of an acceleration data set would be 0 G instead of +1 G.

Following the method described in (Riley, Haupt, Jacobson 2010), engineers at NSWCCD DN began to closely inspect many filtered data sets from the NSWCCD DN historical test data files. During this inspection, it became evident that all individual acceleration spikes would fit into one of three patterns. It was also noted that the patterns appeared to be scalable, but the patterns were there nonetheless. The fact that the patterns continually appeared proved to be interesting.

Further investigation yielded an equation that related average peak acceleration to significant wave height and craft speed that could partially explain the scalability phenomena (Savitsky and Brown October 1976). Algebraic manipulation of this equation lead to the conclusion that the ratio of acceleration responses for two specific test conditions was directly

proportional to the ratios of the kinetic and potential energies of the two specific test conditions. This fact confirmed that the responses of small craft in a seaway were not random but rather predictable based upon the input characteristics of the wave impact.

The next step in this investigation was to theorize about what was physically happening to the craft during each of the three acceleration spike patterns. Data from vertical accelerometers, longitudinal accelerometers and inertial measurement units that provided pitch, roll, and yaw data were used to provide clues about physical movements and orientations. Based upon this data, the conclusion was drawn that the patterns were either Alpha slams, Bravo slams or Charlie slams. Slams where the craft becomes airborne and lands stern first in the water were classified as Alpha slams. Slams where the craft becomes airborne and lands on an even keel were classified as Bravo slams. Slams where the craft impacts an incident wave with very little or no free fall but having a noticeable negative longitudinal acceleration at impact were classified as Charlie slams (Riley, Haupt, Jacobson,2012).

The thoughts and processes presented in the above works were refined and expanded (Riley, Coats, Murphy 2014). In this document, the term “modal decomposition” is introduced. Modal decomposition refers to the process of separating unfiltered vertical acceleration data into a rigid body component and a higher frequency vibration component. The authors expand upon their case to primarily analyze the low frequency, rigid body content (Riley, Haupt, Jacobson 2010) and (Riley, Haupt, Jacobson,2012) by presenting a mathematical study of selected sinusoidal vibration frequencies and calculating their relative displacements and velocities. As an example, a pure sine wave with an acceleration of 4 g and a frequency of 1 Hz will have a displacement of 39.120 inches and a velocity of 20.440 feet per second. In contrast, a pure sine wave with an acceleration of 4 g and a frequency of 40 Hz will have a displacement of 0.024 inches and a velocity of 0.511 feet per second. Comparing these values, it becomes evident that the greater damage potential to small craft operating at speed in a seaway will come from rigid body motions instead of higher frequency vibrations.

Based on the concept that more damage could be caused by the rigid body component of motion and the impact velocities associated with the rigid body motion, (Riley, Coats, Murphy 2014) show how vertical velocity data could be inverted by multiplying the velocity

data by -1 and inputting it into a script developed by the authors which could identify the highest impact velocity peaks associated with the vertical acceleration data. With the highest impact velocity identified, a laboratory drop test could be designed to simulate specific wave impacts. This simulation would require dropping an object from an applicable height to replicate the impact velocity and the desired deceleration pulse (both amplitude and duration). This duration could be replicated if an appropriate energy absorbing material was used to provide the proper acceleration duration (Riley, Coats, Murphy 2014).

The United Kingdom's Ministry of Defense addressed the issue of replicating acceleration amplitude and acceleration duration by preparing a test standard for testing shock mitigating seats (Protocol 1 2014) that uses a specific test fixture design that impacts sand. The sand impact medium was selected because it results in a half-sine shock pulse shape that simulates the shape of severe wave impact pulses in high-speed craft (Military Test Procedure 5-2-506, *Shock Test Procedures*). This test standard called for shock-mitigating seats to be secured to the base of a wedge shaped fixture. Then the fixture is dropped wedge first into a bin of sand. A photograph of the drop test fixture specified in Protocol 1 is provided as Figure 2. This test standard allows the user the latitude to adjust the height of the drop until the desired acceleration amplitude is achieved. However, there is no latitude regarding the angle of the wedge. The angle of the wedge is fixed at 55°. The dimensions, material and configuration of the test fixture that is dropped are specified (Protocol 1 2014).

Figure 2. Drop Test Fixture As Described In Protocol 1 (Protocol 1 2014)

(Protocol 1 2014) provides a model for a drop test that could be used as a vehicle to learn how the interaction of drop height, test fixture weight and wedge angle could possibly affect acceleration amplitude and acceleration duration. The drop test apparatus shown in Figure 2 was used to test and evaluate the shock response of several different test items; however, systematic drop tests designed to evaluate how systematic parametric variations in payload weight, drop height, and impact wedge angle affect impact shock severity have not yet been performed. This lack of knowledge related to the drop test methodology provided the primary motivation for the tests described in the following section.

1.6 Objectives

The primary objective of this thesis is to understand the effect that (a) adjusting the wedge angle, (b) varying the drop weight and (c) varying the drop height would have on the

acceleration amplitude and acceleration duration produced by dropping a test fixture into a sand impact medium. After the series of drops are complete, the data will be reduced and analyzed to determine the correlation of these 3 factors. The final report shall include math models whose inputs will be wedge angle, weight and drop height with an output of predicted acceleration magnitude and predicted acceleration duration.

CHAPTER 2

2. BACKGROUND

2.1 Statistical Method Versus Deterministic Method of Data Analysis

(Riley, Haupt, Jacobson,2012) introduced a new approach to wave impact data analysis that they call a deterministic approach for wave impact data analysis. The deterministic method of wave impact data analysis gleans each individual, significant wave impact in a data set for more data than in previous data analysis methods. That data can take the form of empirical data or observational data. Observational data is where the analyst examines the general shape of curves and compares them to other dataset curves in order to identify patterns of recurring curves. An example of using this data as observational data was the identification of the Alpha, Bravo and Charlie slams (Riley, Haupt, Jacobson,2012). A deterministic analysis approach is one that assumes that the relationship in a physical system involves no randomness in the development of the future state (Riley, Haupt, Jacobson,2012). Simply stated, the deterministic method has concluded that the state of the craft at any time is directly affected by many inputs of the wave impact that the craft has just experienced The term deterministic refers to a significantly different method of analysis than the more traditional statistical method of wave impact data analysis.

Statistical methods look at a complete data set and calculate average values and RMS values using a peak to trough methodology adopted from ocean wave measurement techniques (Riley, Haupt, Jacobson,2012). In this method, only peak values are recorded using a qualitative method to define the threshold above which the data is considered to be important enough for the design or comparative study. Typically, once these peak values have been obtained, they would be sorted and the highest one-third, one-tenth and one-hundredth values would be calculated and reported. These values would then be used as a measure of the average impact severity for a given speed and wave height for the design of a small craft.

To understand exactly how the technical community began the shift from a statistical method of data analysis to a deterministic method of data analysis, the reader must first

understand the history of craft motion measurement techniques and the limitations that each of these methods presented to technical personnel.

2.2 A Brief History of Craft Motion Measurement Techniques

Many design equations that Naval Architects use to design hulls are developed with pressure as one of the design parameters. As such, Naval Architects prefer hull data given in terms of pressure. However, gathering pressure data can be difficult if not impossible to obtain. Difficulties with clogging of pressure tubes, inconsistencies with surface pressures and even difficulties with pressure data reduction make the gathering of meaningful pressure data difficult for the test engineer. Another option is to gather acceleration data and use this data to model the rigid body motions of the craft. Gathering acceleration data in various locations throughout the test craft is much easier for test engineers. Fortunately there is a direct relationship between recorded pressure loads and recorded rigid body acceleration responses (Riley, Coats, Murphy 2014).

The ability to capture, record and analyze craft motion and acceleration data has increased in parallel with the ongoing development of the personal computer. During the 1960s, craft motion data was sensed with servo-type accelerometers and collected on reel to reel magnetic tape recorders. The collected data was analyzed by hand with personnel printing out the data on long paper strips, placing the paper on the floor and manually measuring the height of each peak using calibrated scales, and recording peak accelerations on a separate piece of paper.

By the early 1990s, computer based, digital data acquisition systems were introduced to the marketplace. As with any new product, the equipment provider began to understand the unique equipment requirements of their customers and the ability of the hardware to meet those requirements. In the case of high-speed craft testing, computer based data acquisition systems did not prove as robust as necessary to meet the maritime environment. When testing in the maritime environment, it is necessary for the equipment to be highly shock resistant, salt water resistant and compact enough to be conveniently placed in small spaces.

A self-contained unit data sensor and acquisition unit was introduced to the marketplace in the late 1990s by Instrumented Sensor Technology (IST). The IST model EDR-2 included a tri-axial accelerometer, signal conditioning, a 10 bit digital-to-analog converter (DAC), microprocessor, and 1 megabyte (MB) of memory all contained in a rugged, environmentally sealed, portable unit. Custom software written exclusively for the EDR-2 allowed the user to define recording control parameters and analyze the data. IST continued to improve their line of EDR systems, but a lagging problem was the lack of memory. This lack of memory had to be overcome by creative testing techniques. One technique was to establish a trigger comprised of vertical acceleration levels and acceleration duration. While this system helped it was impossible to tell when a shock event occurred in real time. Another data acquisition system was introduced in the late 1990s by a company known as IOTech. This system was modular and also provided the ability to filter acceleration data prior to storage. An additional feature of this system was increased memory and adjustable data sampling speeds.

In the early 2000s, NSWCCD adopted the National Instruments, CompactRIO system as their standard data acquisition system. The CompactRIO is the combination of a real-time controller, reconfigurable Input/Output Modules, a Field Programmable Gate Array module and an Ethernet expansion chassis. When encased in a plastic protective case, the CompactRIO has proven itself to be very rugged. With high capacity, inexpensive, solid-state memory, the CompactRIO is capable of storing thousands of times more data than the older IST systems. This translates into days, rather than minutes, of recording time at sampling rates beyond 2,000 samples per second.

With the introduction of more capable data acquisition systems with increased storage capacity, the ability to capture more data began to open up new methods of analyzing data sets. The availability of new analysis techniques written into commercial software and into software authored by personnel at NSWCCD DN allowed for the transition from statistical methods of data analysis to deterministic methods of data analysis.

2.3 Wave Slam Sequence of Events

With the introduction of the deterministic data analysis method, it is possible to use this data to determine, in detail, what a small craft is doing physically as it impacts a wave. The dynamic load acting upon any structure is typically described in units of pressure and/or force. The response of that structure to the applied force or pressure is typically described in (a) displacement, (b) velocity and/or (c) acceleration (Riley, Coats, Murphy 2014). In the realm of high speed craft testing, the best way to mathematically describe the environment that the craft is experiencing at any moment is via pressure data derived from a matrix of pressure gauges along the bottom surfaces of the craft. The process of getting pressure data along this matrix of pressure gauges is expensive in test execution and becomes even more expensive and complex when trying to correlate the pressure distribution data to the dynamic response data of the craft (Riley, Coats, Murphy 2014).

Instead of trying to correlate pressure distribution to dynamic response, an alternative method would be to use rigid body heave acceleration values and correlate that to pressure distribution. The net vertical force at a hull cross-section of the pressure distribution at any instant in time is directly proportional to the heave acceleration response at that cross-section (Riley, Coats, Murphy 2014). The heave acceleration can be extracted from recorded acceleration data using concepts of response mode decomposition. In the absence of pressure data or force measurements, the amplitude and duration of the rigid body heave acceleration at any location can be used as a measure of the severity of a wave impact load in units of “G” in the vertical direction (Riley, Coats, Murphy 2014).

One of the most useful locations to place a vertical accelerometer on a high-speed craft is at the Longitudinal Center of Gravity (LCG). In practice, test personnel determine the location of the LCG of a craft with a scale weighing test. The raw load data from the scale weighing test is substituted into a moment balance equation which results in the location of the LCG on the craft. The LCG location is marked, and one of the many locations for accelerometer placement becomes the LCG. Typically the LCG accelerometer is secured to the main deck as a matter of

convenience. This convenience is derived because the main deck, in most cases, is parallel to the keel.

Figure 3 shows four different curves measured by vertical accelerometers for four different craft. Each craft was in different sea states and moving at different speeds. For each craft, the accelerometer that provided the data was located at the LCG and orientated vertically.

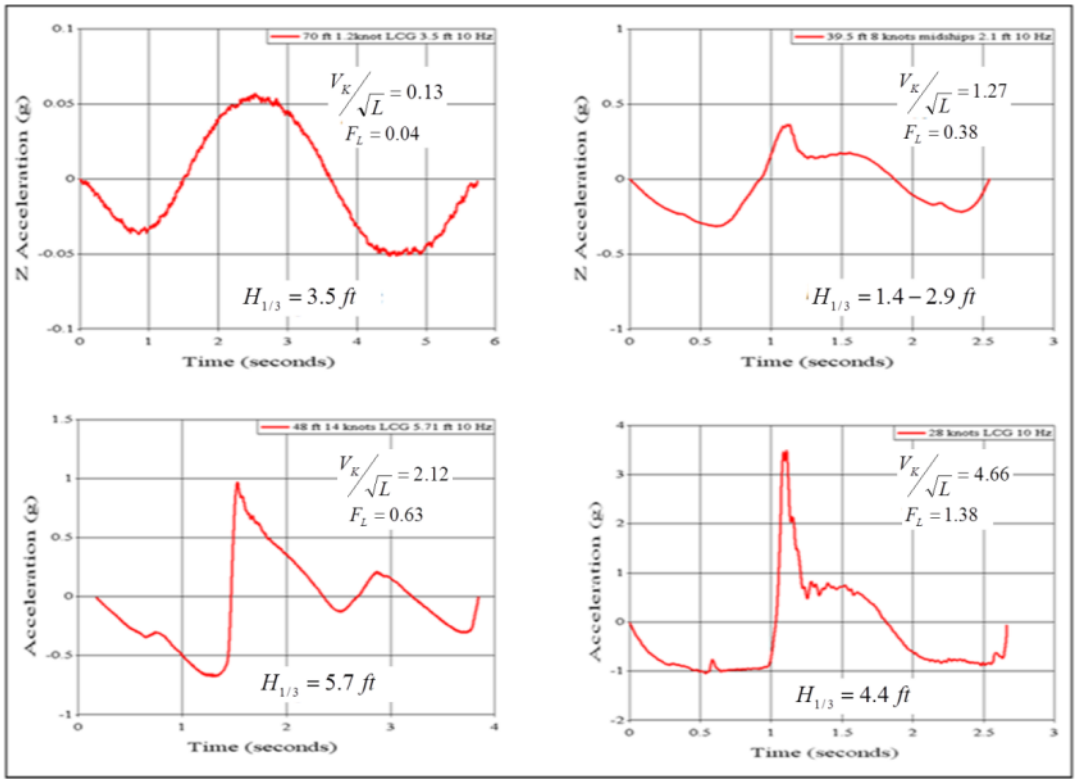

Figure 3. Various Speed Wave Encounters (Courtesy of Authors (Riley, Coats, Murphy 2014))

Figure 3, references three mathematical parameters in each of the four curves. Those parameters are (a) the speed ratio, (b) the length Froude number and (c) significant wave

height. In order to appreciate the significance and relevance of each curve, an explanation of each of the parameters is provided.

In 1868, a researcher named William Froude proposed a set of theories that predicted the wave making potential and total hull resistance of ships based on scale model testing. The connective tissue between the models tested by Mr. Froude and full-scale ships is a non-dimensional number called the length Froude Number (F_L). The F_L is defined as:

$$F_L = \frac{v}{\sqrt{g * L}}$$

where

v = craft speed,

g = acceleration of the craft due to gravity,

L = craft length.

Although the use of the F_L is predominant with hydrodynamicists, naval architects are more likely to use a number called Speed-Length (SL) Ratio. The SL ratio is defined as:

$$SL = \frac{V_k}{\sqrt{L}}$$

where

V_k = speed of the craft in knots,

L = length of the craft in feet.

The SL ratio is commonly used in the United States simply because it uses the more common unit of velocity knot in place of the less common velocity unit feet per second. Additionally, it doesn't use the gravity term, which makes it easier to work with. If one so desires, the SL ratio can be converted back to the F_L simply by multiplying the SL by 0.298.

Another number that is important to naval architects is called Significant Wave Height ($H_{1/3}$). $H_{1/3}$ is traditionally described as the mean wave height of the highest third of all measured wave heights for a given period of time. Technical documents in the maritime domain often define the environment that craft must function in as a sea state requirement. A common reference among test engineers is the Wilbur Marks Scale for Fully Risen Seas. Within this table is a cross reference between $H_{1/3}$ and sea state number. Part of the method that the Wilbur Marks Scale uses to define sea states is with a lower limit $H_{1/3}$ value and an upper limit $H_{1/3}$ value.

During at sea tests, the $H_{1/3}$ value is not known but simply estimated based on the experience of the test coxswains who roughly determine if the sea state at the test location is near the desired test conditions. A wave height measuring and recording device, such as a wave buoy, is thrown into the water prior to testing. As the test continues, the wave buoy measures and records the wave height data. After the test is concluded, the wave buoy is recovered, and its data is retrieved. The wave buoy data is post processed and statistically evaluated. Only after these calculations have been completed can the actual $H_{1/3}$ be determined.

The upper left curve of Figure 3 depicts a craft that is moving slowly. This condition is best described as “underway but not making way” (Riley, Coats, Murphy 2014). As the craft is sitting in the water and moving slowly or not moving at all, it is supported by buoyant forces, and the only movement experienced by the craft is the up and down motion of the passing waves. As the wave is approaching the location of the accelerometer, the acceleration level is positive as the craft is climbing the approaching wave face and negative as the craft falls down the back face of the wave.

For the purposes of this document, the hump region of a craft speed versus craft trim curve refers to the point where the trim angle of a planing craft has reached its maximum and has begun to decrease. What this means physically to a planing hull is that prior to achieving the hump speed, the planing hull acts more like a displacement hull. As the speed of the hull increases through the water, hydrodynamic lift eventually begins to lift the hull from the water.

When this happens, the craft will typically experience a noticeable increase in speed with very little additional power applied. The upper right curve of Figure 3 depicts a craft still in the pre-hump region, but the craft is picking up speed (Riley, Coats, Murphy 2014). The smooth sinusoidal shape that was evident is essentially still there, but the appearance of a small magnitude impact can be observed near the 1.1 second mark. This craft has a speed ratio of 1.27 which puts it clearly in the pre-hump region where the effects of buoyant forces dominate the effects of dynamic forces. It is apparent, though, that the effects of dynamic forces are increasing because of the emergence of a small but noticeable spike in the acceleration level near the 1.1 second mark.

The lower left curve of Figure 3 depicts a craft in the pre-hump region approaching the planing region (Riley, Coats, Murphy 2014). The smooth sinusoidal shape noticed with simply buoyant forces has begun to disappear and is now being replaced with a saw tooth shaped curve with noticeable impact spikes. The impact observed at time 1.5 seconds is an impact, and as the craft recovers from the impact and momentarily sinks deeper in the water, buoyant forces become more dominant, causing the craft to oscillate up and down slightly as the craft prepares to encounter the next impact.

The lower right curve of Figure 3 depicts a craft that is transitioning into the planing region (Riley, Coats, Murphy 2014). In this curve, the most dominant feature is the impact feature that occurs at the 1-second mark. After the impact spike that tends to look like a half-sine pulse, the lower amplitude smooth part of the acceleration curve is caused by hydrodynamic lift and buoyancy. The craft is experiencing a near free fall condition in the 2 to 2.5 second region. This observation is based on the near constant -0.9 G acceleration level. During this period the craft is ready for the next impact.

Guidelines have been presented to determine which forces are most prevalent upon a hull based on the value of the SL ratio (Savitsky and Brown October 1976). The guidelines are summarized in tabular form as Table 1.

Table 1. SL Ratios and Its Effect Upon Craft

SL Ratio	Effect Upon Craft
$0 < SL \leq 2$	Pre-hump region. The effect of buoyancy forces dominate the effect of hydrodynamic forces.
$2 < SL \leq 4$	Pre-hump region and approaching the planing region. Both dynamic forces and buoyant forces are present but the effect of the buoyant forces are greater than the effect of the dynamic forces
$4 < SL \leq 6$	Transition into the planing region. Both dynamic forces and buoyant forces are present but the effect of the dynamic forces are greater than the effect of the buoyant forces
$SL > 6$	Planing region. The effect of impact forces dominate the effect of hydrodynamic and buoyant forces

The severe wave impact in the lower right of Figure 3 is the one of interest when studying the effects of wave slam shock on the hull, installed equipment, and personnel. The next step is to look closer at one wave impact like the one shown in Figure 4 to understand in more detail the characteristics of the motion in terms of acceleration, velocity, and absolute displacement.

Figure 4 consists of three curves. The top curve is a small section that was extracted from a typical unfiltered vertical LCG accelerometer large data set. This specific section contains the characteristic large impact spike that is seen when the subject craft is transitioning into the planing region as illustrated in the lower right curve of Figure 3 (Riley, Coats, Murphy 2014). The middle curve of Figure 4 is a velocity versus time curve that was generated by integrating the acceleration curve. In the same manner, the bottom curve of Figure 4 is a displacement curve obtained by integrating the velocity curve. These three curves were then

aligned and shown together so that the relationship between craft motions and acceleration, velocity and displacement can be made (Riley, Coats, Murphy 2014).

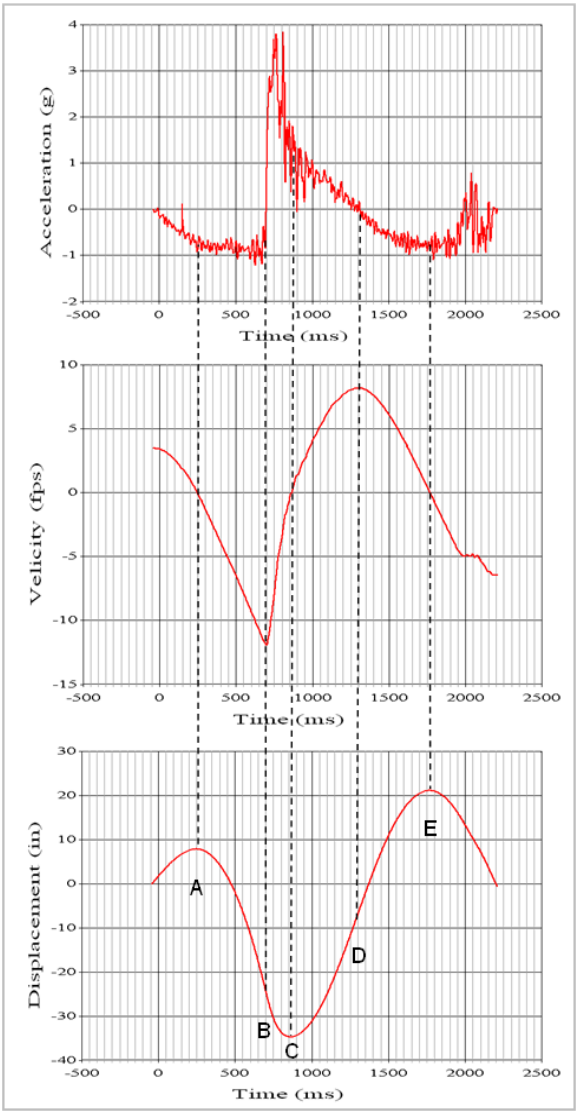

Figure 4. Wave Impact Sequence Of Events (Courtesy of Authors (Riley, Coats, Murphy 2014))

Visual inspection of the top curve from point A to point B yields an average value of acceleration of -0.9 G's. This value is very close to the value of -1.0 G, which would indicate a free fall condition. Additionally, visual inspection of the middle curve from point A to point B shows that there is a linear decrease of velocity from 0 feet per second to the absolute minimum value of -12 feet per second. During this phase, impact with the water has not yet occurred, but water entry is imminent.

Point B is where the vertical velocity reaches its absolute minimum value. Also at point B, the acceleration curve experiences a rapid increase to a maximum value of 3.8 G's. Because of these 2 observations, it is observed that point B is when the craft comes into contact with the next incident wave.

Point C is identified as the point where the displacement of the craft experiences its minimum displacement value of -34 inches. Also at point C, buoyancy, hydrodynamic lift and drag combine to produce a positive effect which brings the relative velocity of the LCG to 0 feet per second. Once the craft reaches the zero value, the impact event is complete.

Point D is where the maximum vertical velocity is reached immediately following the incident wave impact. Traveling from point C to point D, the craft experiences a positive change in displacement, and the negative slope of the acceleration becomes less severe. This behavior is explained by a combination of buoyancy and hydrodynamic lift, with components of thrust and drag (Riley, Coats, Murphy 2014).

As the craft travels from point D to point E, it continues to decelerate with an expected linear decrease in velocity. At point E, the craft reaches maximum vertical displacement. Following point E, gravity begins to have a greater affect upon the craft, and the craft is poised to begin another wave encounter sequence.

2.4 Wave Slam Event To Be Modeled Via The Experiment

For the purposes of this thesis, the specific area of interest in the entire wave encounter sequence is from point B to point C on Figure 4. The shape of this acceleration spike will be attempted to be replicated with a half sine pulse. However, the peak acceleration magnitude and acceleration duration will be allowed change as the variables within the experiment are

allowed to change. The variable conditions and the value of the acceleration magnitude and the acceleration duration will be noted and recorded.

CHAPTER 3

3. EXPERIMENT SET UP

3.1 Basic Experiment Description

The basic experiment was not conducted in accordance with Protocol 1; rather, the experiment and the procedure were heavily influenced by it. The primary characteristic of the experiment that was influenced was the use of sand to control the impact pulse shape. Using sand as an impact surface was in response to the following statements: "In order to simulate the vertical rigid body acceleration of a wave impact, the falling equipment item must experience an acceleration pulse upon impact with a shape that simulates the first half-sine acceleration pulse (Riley, Coats, Murphy 2014)" and "This is typically achieved at drop test facilities by placing a pliable object or energy absorbing material under the test fixture. When the test fixture impacts this object or material, the desired first half sine pulse may be produced" (Military Test Procedure 5-2-506, Shock Test Procedures, 1966).

Where deviations took place with equipment or procedures, the deviations were made in order to minimize the test cost or to achieve test data outside the window of acceptable data specified by Protocol 1. For example, the Protocol 1 drop test fixture was constructed from a mild steel plate with a thickness of 6 mm. Since the mild steel plate measured in English units was cheaper to procure, this experiment was conducted with a drop test fixture constructed from steel plate with a thickness of ¼ inch. As an example of gathering test data outside the window of acceptable data, Protocol 1 states that the maximum acceptable value of vertical acceleration that may be obtained in a vertical drop shall be $1.2*100\ ms^{-2}$ which equates to $393.7\ fts^{-2}$ or 12.2 G's. During this test, acceleration levels of greater that 20 G's were recorded.

The sand used in this test was fine washed masonry. The sand box used for an impact pit was 6 feet wide by 6 feet long by 4 feet deep.

A total of 4 different wedges were used in this experiment. The wedges were 45°, 55°, 65° and 75°. The mass of the drop fixture was another variable in this experiment. The mass was varied by affixing 1 to 7 plates to the top of the drop test fixture. Each plate had a nominal weight of 29 pounds. A drawing of the test fixture with a 45° wedge and 4 plates is provided as

Figure 5. The complete drawing package used to fabricate the drop test fixture is included in this document as appendix A.

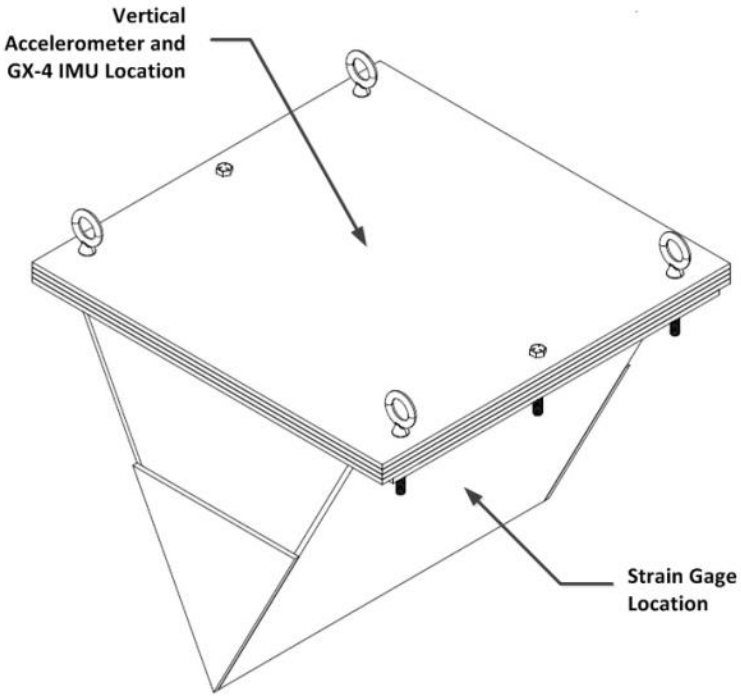

Figure 5. Drop Test Fixture With 45° Wedge

3.2 Detailed Experiment Description

For this experiment, the drop heights selected were 3 feet, 5 feet, 7 feet and 9 feet. The test fixture was raised to the specified drop height via a bridge crane. The height of the drop was measured by means of a length of cord cut to length and taped to the bottom of the wedge. A photograph of the test fixture suspended above the sand box is provided as Figure 6.

Figure 6. Drop Test Fixture Suspended Above The Sand Box.

The test fixture was dropped from the hook of a bridge crane. A shackle was attached to the crane hook. Beneath the shackle was a load cell that continually sensed the weight of the test fixture. Beneath the load cell was a quick release mechanism that was activated by pulling a lanyard. Prior to attaching the test fixture to the quick release mechanism, test personnel raised the quick release from the floor and then zeroed the weight thus eliminating the weight of the quick release from the displayed weight of the test fixture. A photograph of the load cell and quick release mechanism used in testing is provided as Figure 7.

Figure 7. Load Cell and Quick Release Mechanism Used During Testing.

A Silicon Designs model 50 accelerometer and a MicroStrain GX3 Inertial Measurement Unit was attached to the top plate. These sensors were used to sense the orientation of the fixture prior to release and to sense the acceleration of the fixture throughout the test event. Prior to dropping the fixture, test personnel would ensure that the pitch and roll angles of the fixture were at 0° ± 1°. A bi-axial strain gauge was attached to each side of the wedge that sensed strain during impact. Strain data was collected for informational purposes only. All of the data was collected and stored using a National Instruments CompactRIO data acquisition and signal conditioning system. Following each drop, the electronic data was stored and the penetration depth into the sand was noted and recorded. The wedge was then lifted from the sand; the sand in the immediate area of the impact was turned over several times with a shovel to reduce the potential effects of sand compaction and then the sand was leveled. The wedge was then dusted off, and test personnel prepared for the next test drop. A photograph of the 45° wedge fixture immediately after coming to rest in the sand box is provided as Figure 8.

Figure 8. 45° Wedge Fixture Following A Drop Into The Sand Box

A total of 112 individual test conditions existed for this experiment (4 wedges x 7 weight plates x 4 drop heights = 112 test conditions). To minimize cost, only one drop at each of the 112 separate test conditions was initially authorized. At the conclusion of these 112 drops, further authorization was granted to increase the number of drops from 1 at each test condition to a total of 5 drops at each test condition. With this additional authorization, a total of 560 drops would be completed. However, only the additional drops for the 45° wedge were completed, which resulted in another 112 drops being performed (1 wedge angle (45°) x 7 weight plates x 4 drop heights x 4 drops = 112 drops). These additional drops combined with the initial 112 drops resulted in a total of 224 drops completed. One of the 224 drops had an instrumentation problem that was not discovered until test completion. As a result, data was analyzed from a total of 223 valid drops. These two series of drop tests resulted in a completed test matrix of 5 drops for the 45° wedge and only 1 drop at each of the other test conditions for the 55° wedge, the 65° wedge and the 75° wedge.

One feature that was added to the top plate of the test fixture following the first series of 112 drops was a symmetrical and center mounted aluminum plate that protected the sensor

package from potential damage from a falling shackle. This aluminum plate and mounting hardware weighed a total of 3.8 pounds. This additional weight was noted in the total weight of the fixture.

CHAPTER 4

4. EXPERIMENT RESULTS

4.1 Data Analysis

Data generated during this experiment was analyzed using the modal decomposition method (Riley, Coats, Murphy 2014). Raw data was obtained from the cRIO system in its raw TDMS file format. It was then converted to a text file using a file conversion utility written by personnel at NSWCCD DN Code 835. The text file was then imported into MS Excel, and all headers were removed. The resulting file was then saved as a Comma Separated Variables (CSV) file. The CSV file was then imported into a software package identified as UERDTools (Mantz, Costanzo, Howell III, Ingler, Luft, Okano). UERDTools is a software package that was written by personnel at Naval Surface Warfare Center, Carderock in West Bethesda, Maryland that was designed to analyze wave forms generated by underwater explosive events. For this experiment, UERDTools was used to demean, zoom in on, and to perform 10 Hz low pass filtering of the test event. A sample of a filtered waveform event that was generated by dropping the 55° wedge loaded with seven plates from a height of 7 feet is provided as Figure 9.

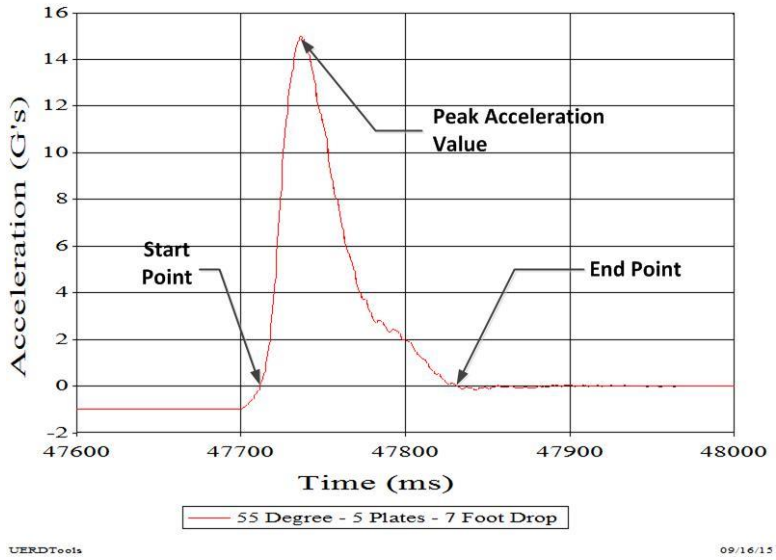

Figure 9. Filtered Half Sine Pulse For The 55° Wedge, 5 Plates and a 7 Foot Drop

A standard method of analyzing the filtered waveforms was adopted for this experiment in order to maintain consistency. The starting point for the event to be measured was defined as that point where the trace increases from its steady state -1 G value and crosses the 0 G axis. The end point for the event was defined as that point where the trace next came into contact again with the 0 G axis. The shock pulse duration was defined as the time differential between the end point and start point values. The peak acceleration value was defined as the maximum acceleration level found between the identified start point and the identified end point. For each test event, these values were collected using this method.

4.2 Data Disparity

Data for this experiment was collected during two distinct periods. The initial data collection was conducted in August of 2015. The initial data collection consisted of 112 individual drops. Those test drops consisted of 1 drop each for each of the 112 specific test conditions. The second series of 112 drops consisted of testing for the 45° wedge only. These two series of drop tests combined for a total of 224 drops. An instrumentation problem was

noted with one of the test drops but was not discovered until after the test was complete. Therefore, data was obtained for a total of 223 valid drops.

For each series of drops, the same equipment, the same fixtures, the same instrumentation and the same personnel were used to collect the data. During the period between the experiments, August 2015 and June 2016, the impact sand box remained inside the waterfront facility of Naval station Norfolk, Building V-47 protected from the effects of rain and snow.

The data from both data collection periods were analyzed as described in the above section of this document. All of the data from the 2 series of drop tests were merged into a single file and sorted by wedge angle, number of plates and drop height. A small sample of the sorted master data file is provided as Table 2. Following the merging and sorting of data, inspection of the master data file revealed an interesting trend. The data collected in August of 2015 consistently had a higher acceleration magnitude and consistently had a smaller acceleration duration than the data collected in June of 2016. This trend can be seen in the data tabulated in Table 2. Drop number 16 was performed on 8 August 2016. When analyzed, this drop had an acceleration magnitude of 19.8 G's. This acceleration magnitude was 174% higher than the average value of drops 17, 18, 19 and 20. Drop number 16 also had an acceleration duration of 88.5 milliseconds. This acceleration duration was only 67% of the average value of drops 17, 18, 19 and 20. A complete listing of the raw data collected in this effort is provided as appendix B.

Table 2. Master Data File Sample

Drop Number	Wedge Angle (Degrees)	Number of Top Plates	Drop Height (Feet)	Weight (Lbs)	Acceleration Magnitude (G's)	Acceleration Duration (Milliseconds)	Acceleration Magnitude Percent Difference	Acceleration Duration Percent Difference
16	45	1	9	104.0	19.8	88.5	174.5	67.3
17	45	1	9	102.5	11.5	136.3		
18	45	1	9	102.5	11.2	132.2		
19	45	1	9	102.5	11.5	120.1		
20	45	1	9	102.5	11.1	137.4		
21	45	2	3	130.0	10.3	98.5	173.1	64.5
22	45	2	3	137.0	5.9	137.0		
23	45	2	3	137.0	6.1	147.9		
24	45	2	3	137.0	5.9	175.9		
25	45	2	3	137.0	5.8	149.9		

Of particular note, the values of acceleration magnitude for the data collected in 2015 were, on average, 162% higher than the values collected in 2016. In the opposite manner, the values of acceleration durations for the data collected in 2015 were on average 72% lower than the values collected in 2016.

Additionally, another interesting observation can be made by looking solely at the test data values collected in 2016. The observation that was made is how consistent the data collected in 2016 appeared. For example, looking at the values for acceleration magnitude for drops 17, 18, 19 and 20 in Table 2, the average value of those acceleration magnitudes is 11.3 G's with a standard deviation of only 0.2 G's. As an additional example, looking at the values for acceleration duration for drops 17, 18, 19 and 20 in Table 2, the average value of those acceleration durations is 131.5 milliseconds with a standard deviation of 7.9 milliseconds. This

calculation was performed for all sets of the 45° wedge data collected in 2016, and the average of all standard deviation calculations for acceleration magnitude was only 0.2 G's, and the average of all standard deviation calculations for acceleration duration was only 8.6 milliseconds.

For the purposes of comparison, the standard deviations for all of the data for the 45° wedge were calculated. In this case, when combining the 2015 and the 2016 45° wedge data, the average standard deviation for acceleration magnitude rose to 2.4 G's, and the average standard deviation for acceleration duration rose to 21.0 milliseconds.

Since there was no difference in any of the equipment or personnel that was used in both the 2015 and 2106 drops, it is hypothesized that the sand dried during the year between the two series of drop tests. This theory would stand to reason since the sand that was used in this test was washed masonry sand and had some water in it for the 2015 test. Since the impact box sat dormant and was not exposed to rain and snow for approximately 1 year, it had time to dry. The absence of water could certainly explain why impact magnitudes in wet sand had a higher magnitude than dry sand. It could also explain why the acceleration durations for wet sand were smaller for wet sand than for dry sand.

4.3 Wedge Angle, Weight and Drop Height Effects Upon Acceleration Magnitude

4.3.1 Data Exclusion

Data for the 112 drops gathered in 2015 was plotted in order to determine trends. The 2016 data was not included in the plots because as discussed in section 4.2 of this document, there is a noticeable disparity between the two data sets. This disparity could unduly influence the plots and negatively influence the trend recognition process. Exclusion of the 2016 data set from the plotting process was made simply to remove the possible effects of moisture content in the sand as a possible variable. However, a set of empirical equations using a combination of the 2015 data and the 2016 data has been provided and will be discussed later in this document.

4.3.2 Wedge Angle Effects Upon Acceleration Magnitude

The effect of wedge angle upon acceleration magnitude was plotted by sorting the data by wedge angle, drop height and then by the number of plates mounted to the test fixture. As depicted in Figure 10, the plots of 3 foot drops represent roughly a horizontal pattern. The exceptions to this pattern are the light blue 3 foot drop with one plate that has an unusually high value associated with the 75° wedge and the orange 3 foot drop with 6 plates that had an unusually low value associated with the 55° wedge.

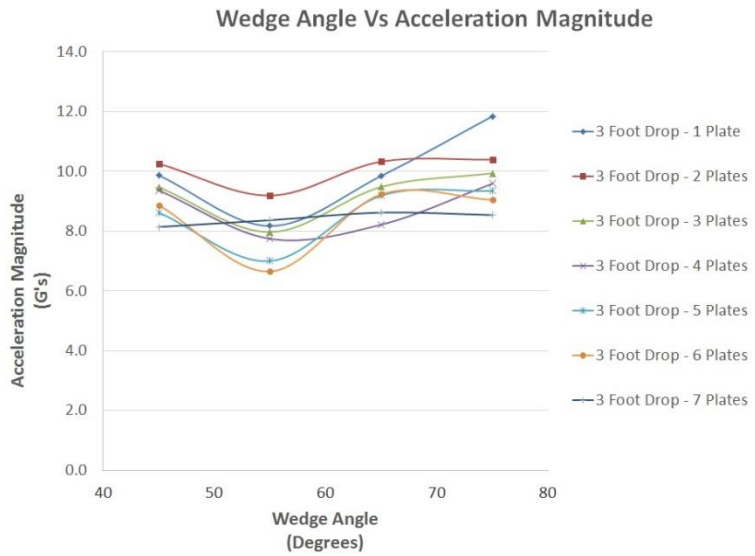

Figure 10. Wedge Angle Versus Acceleration Magnitude For The 3 Foot Drop

Examination of the 5 foot drop data, the 7 foot drop data and the 9 foot drop data revealed the effects of wedge angle upon acceleration magnitude becomes noticeably more linear as the drop height increases. Figure 11 is a plot of the 5 foot drop data. Figure 12 is a plot of the 7 foot drop data. This trend can be seen in Figure 13, which is a plot of the 9 foot

drop data. Most of the plots are parallel with the exception of the purple 9 foot drop with 4 plates.

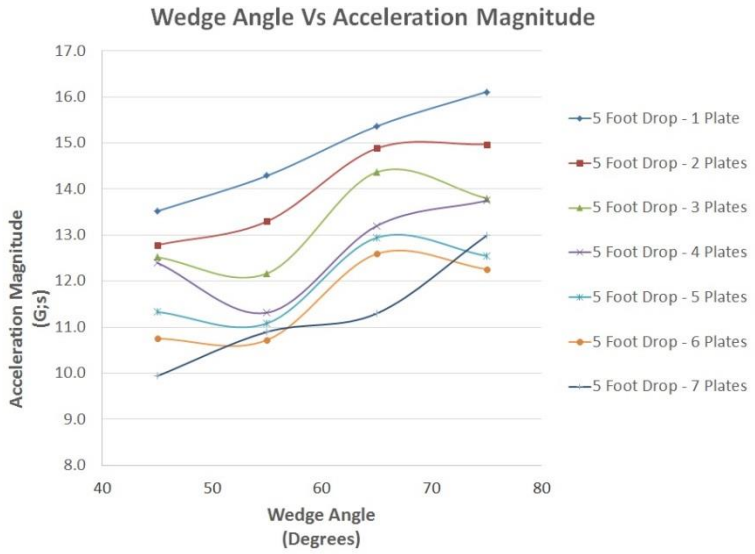

Figure 11. Wedge Angle Versus Acceleration Magnitude For The 5 Foot Drop

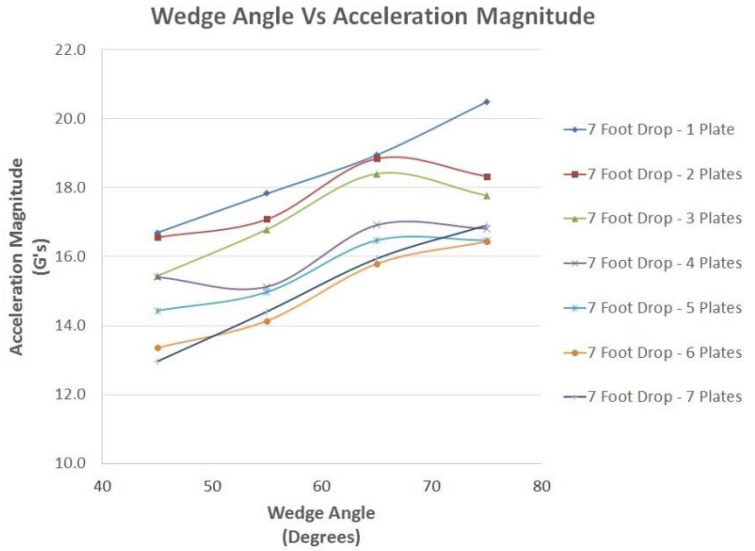

Figure 12. Wedge Angle Versus Acceleration Magnitude For The 7 Foot Drop

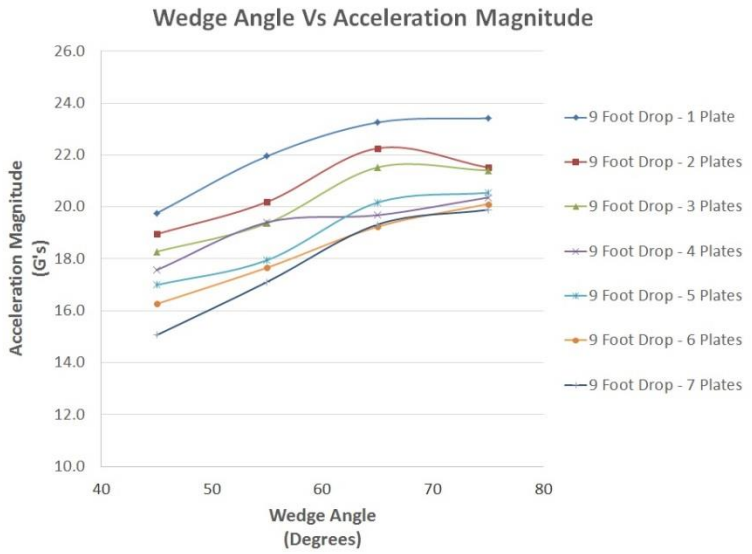

Figure 13. Wedge Angle Versus Acceleration Magnitude For The 9 Foot Drop

4.3.3 Weight Effects Upon Acceleration Magnitude

The test data plots demonstrate linear behavior throughout the test parameter region. The plots of the 45 ° wedge, the 55 ° wedge, the 65 ° wedge and the 75 ° wedge all demonstrate that increasing weight has a linear effect on acceleration magnitude. This effect can clearly be seen in Figure 14, Figure 15, Figure 16 and Figure 17. Figure 14 depicts the weight versus acceleration magnitude data for the 45° wedge. Figure 15 depicts the weight versus acceleration magnitude data for the 55° wedge. Figure 16 depicts the weight versus acceleration magnitude data for the 65° wedge. Figure 17 depicts the weight versus acceleration magnitude for the 75° wedge.

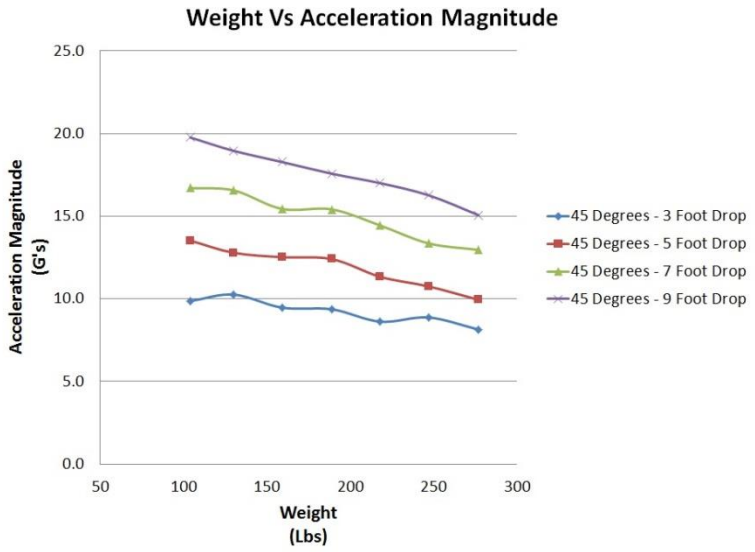

Figure 14. Weight Versus Acceleration Magnitude For The 45° Wedge

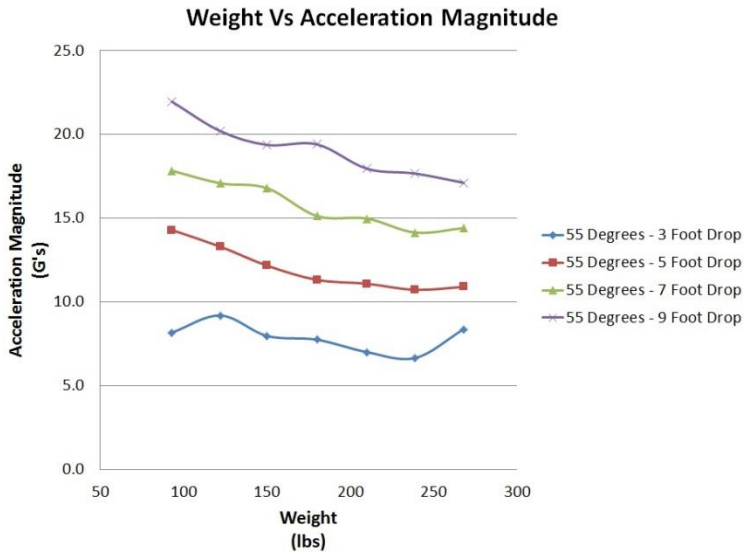

Figure 15. Weight Versus Acceleration Magnitude For The 55° Wedge

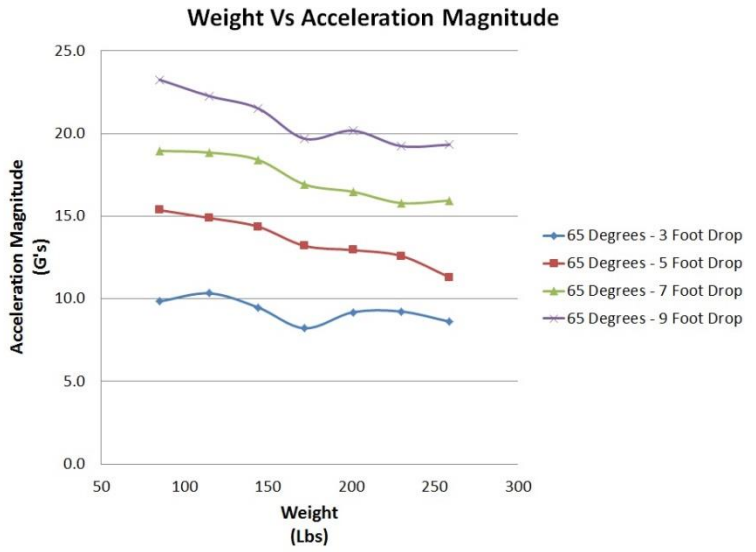

Figure 16. Weight Versus Acceleration Magnitude For The 65° Wedge

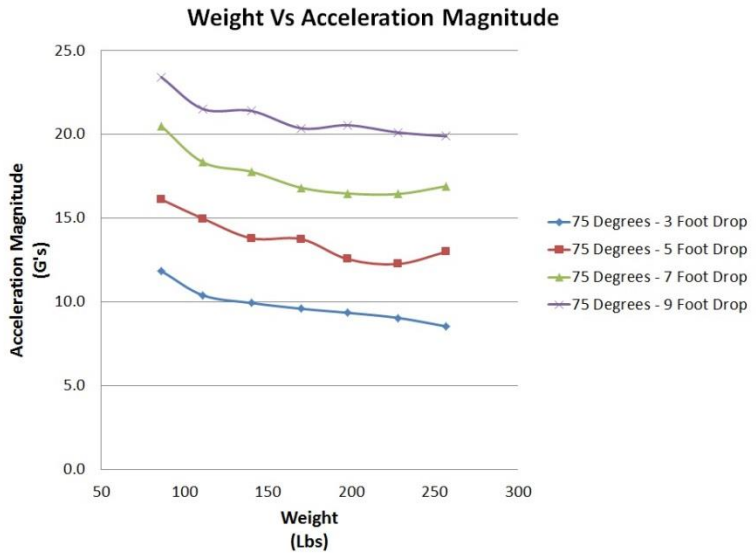

Figure 17. Weight Versus Acceleration Magnitude For The 75° Wedge

4.3.4 Drop Height Effects Upon Acceleration Magnitude

The test data plots indicate linear behavior. The plots of the 45° wedge, the 55° wedge, the 65° wedge and the 75° wedge all demonstrate that increasing drop height has a linear effect upon acceleration magnitude. This effect can clearly be seen in Figure 18, Figure 19, Figure 20 and Figure 21. Figure 18 depicts the drop height versus acceleration magnitude data for the 45° wedge. Figure 19 depicts the drop height versus acceleration magnitude for the 55° wedge. Figure 20 depicts the drop height versus acceleration magnitude for the 65° wedge. Figure 21 depicts the drop height versus acceleration magnitude for the 75° wedge.

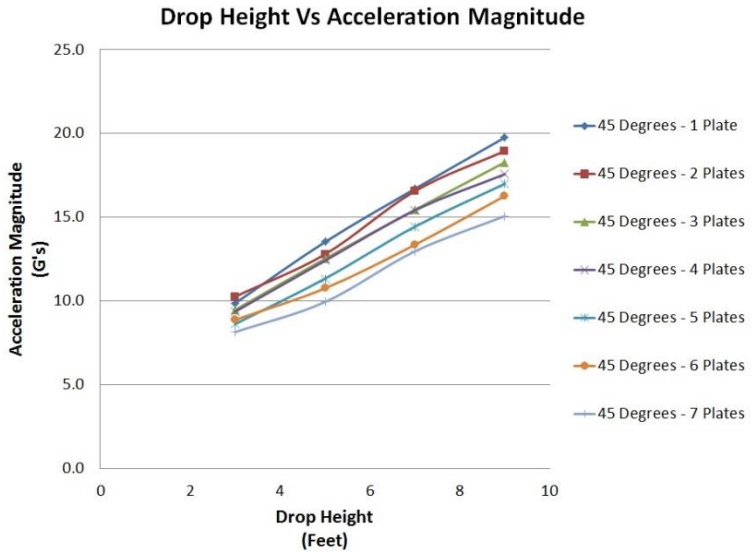

Figure 18. Drop Height Versus Acceleration Magnitude For The 45° Wedge

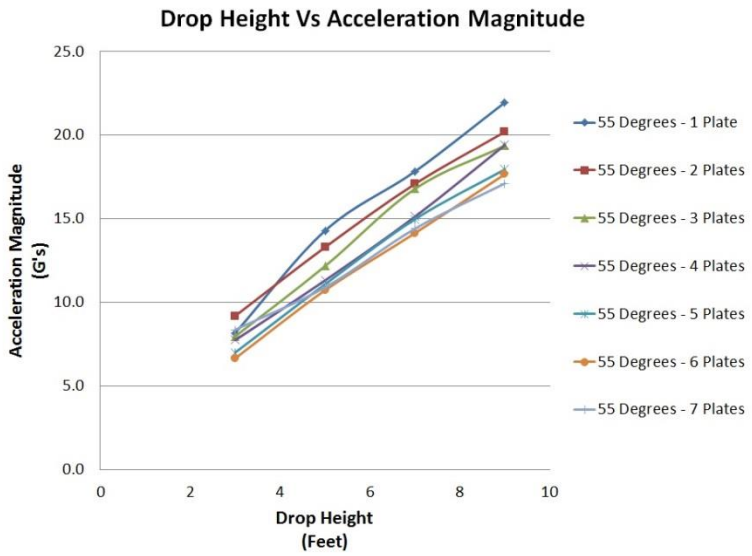

Figure 19. Drop Height Versus Acceleration Magnitude For The 55° Wedge

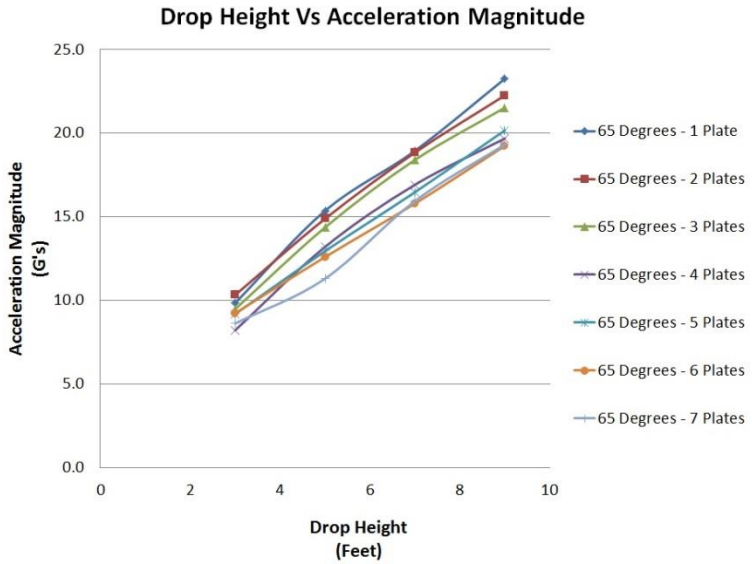

Figure 20. Drop Height Versus Acceleration Magnitude For The 65° Wedge

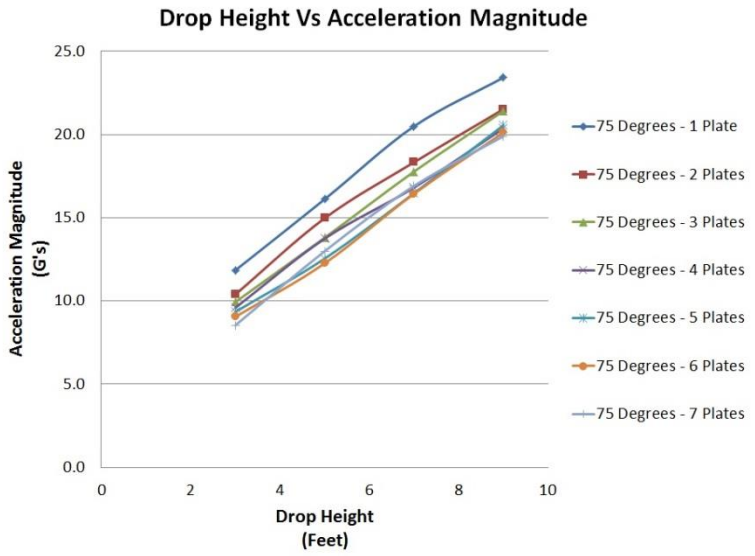

Figure 21. Drop Height Versus Acceleration Magnitude For The 75° Wedge

4.4 Wedge Angle, Weight and Drop Height Effects Upon Acceleration Duration

4.4.1 Wedge Angle Effects Upon Acceleration Duration

The effect of wedge angle upon acceleration duration was plotted by sorting the data by wedge angle, drop height and then by the number of plates mounted to the test fixture. As depicted in Figure 22, the plots of 3 foot drops represent roughly a horizontal pattern. The exceptions to this pattern are the blue 3 foot drop with one plate that has an unusually high value associated with the 55° wedge and the orange 3 foot drop with 6 plates that also had an unusually high value associated with the 55° wedge.

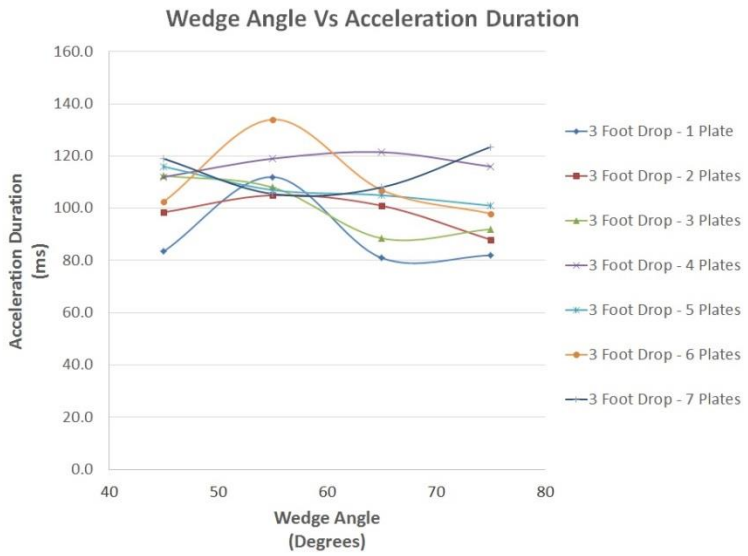

Figure 22. Wedge Angle Versus Acceleration Duration For The 3 Foot Drop

The effect of wedge angle upon acceleration duration became more random as the drop height increased. This trend was noted in the 5 foot drop data, the 7 foot drop and the 9 foot drop data. The randomness of the data was at its most extreme in the 9 foot drop data. A plot of the 5 foot drop data is provided as Figure 23. A plot of the 7 foot drop data is provided as Figure 24. A plot of the 9 foot drop data is provided as Figure 25.

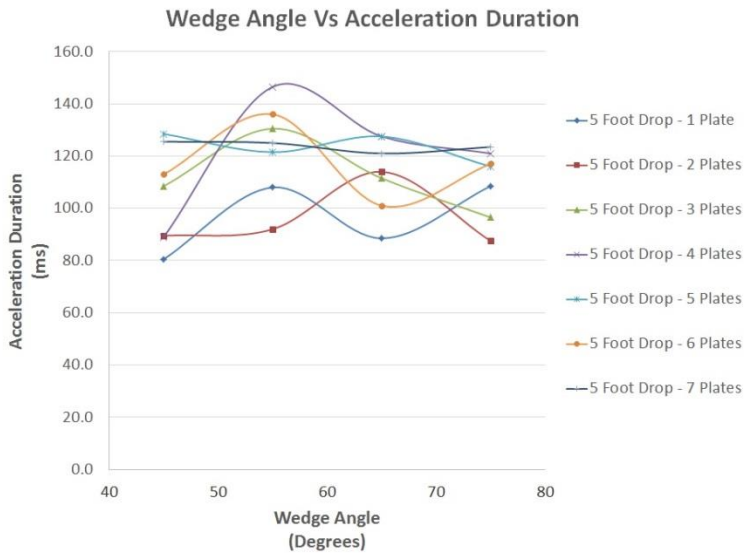

Figure 23. Wedge Angle Versus Acceleration Duration For The 5 Foot Drop

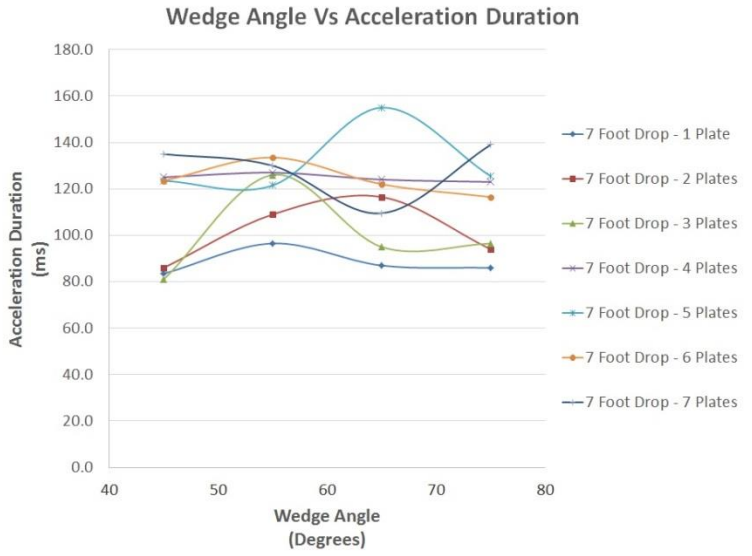

Figure 24. Wedge Angle Versus Acceleration Duration For The 7 Foot Drop

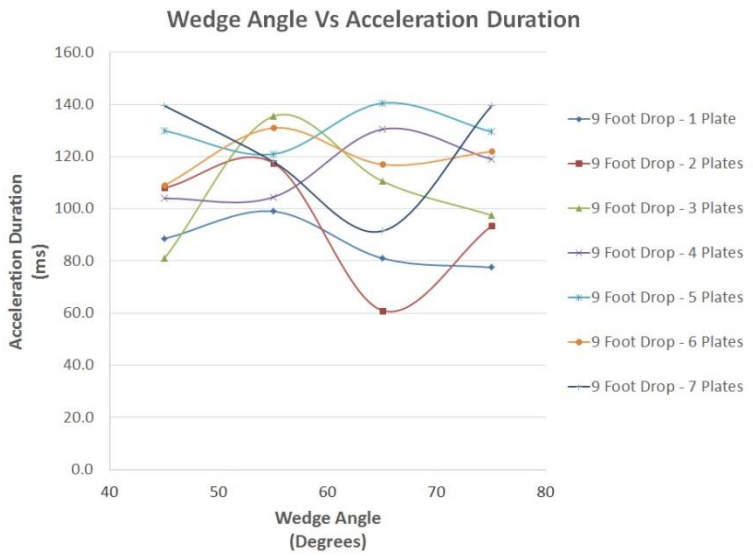

Figure 25. Wedge Angle Versus Acceleration Duration For The 9 Foot Drop

4.4.2 Weight Effects Upon Acceleration Duration

The test data plots indicate linear behavior for the 45° wedge and the 75° wedge but with a noticeable scattering of data about the linear fit. The test plots for the 55° wedge and the 65° wedge appear to be much more random. Figure 26 depicts the weight versus acceleration duration data for the 45° wedge. Figure 27 depicts the weight versus acceleration duration data for the 55° wedge. Figure 28 depicts the weight versus acceleration duration data for the 65° wedge. Figure 29 depicts the weight versus acceleration duration data for the 75° wedge.

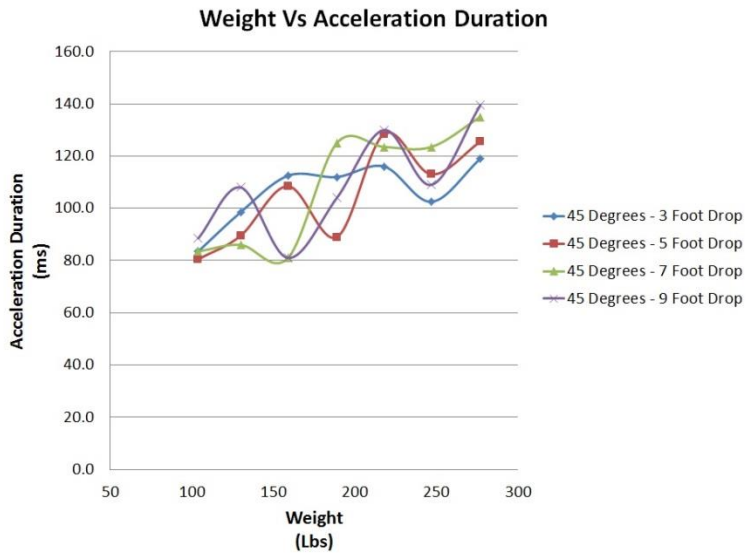

Figure 26. Weight Versus Acceleration Duration For The 45° Wedge

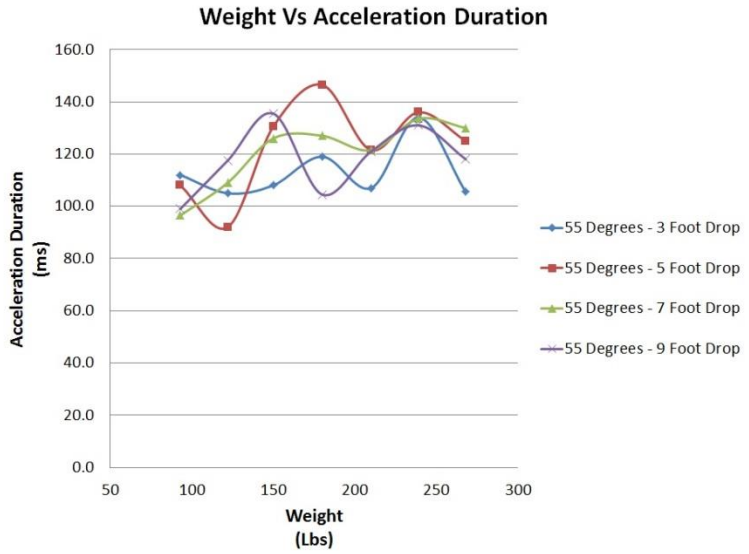

Figure 27. Weight Versus Acceleration Duration For The 55° Wedge

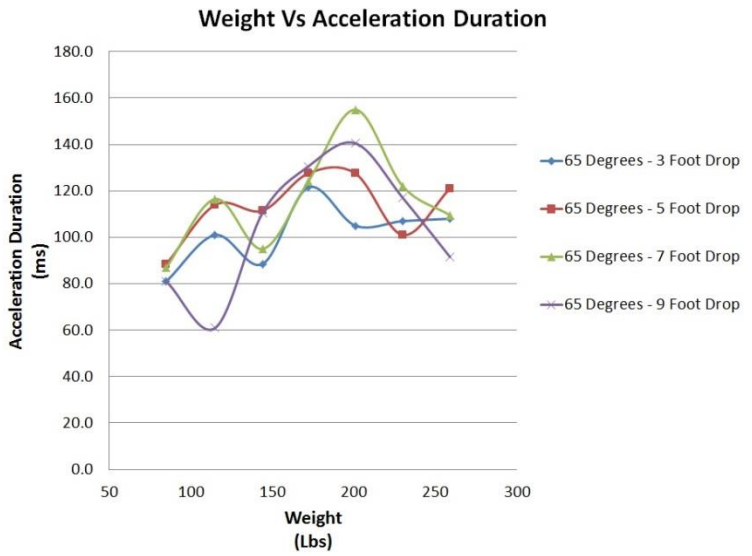

Figure 28. Weight Versus Acceleration Duration For The 65° Wedge

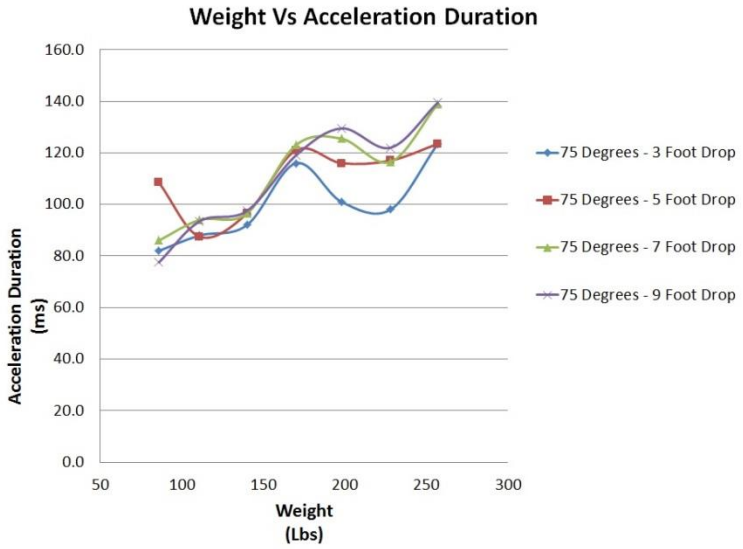

Figure 29. Weight Versus Acceleration Duration For The 75° Wedge

4.4.3 Drop Height Effects Upon Acceleration Duration

The test data plots show random behavior. If a linear regression data fit was fitted through the data in Figure 30 and in Figure 31, the slope of both of those lines would be minimal. In fact, the slope of the line for the linear fit of data in Figure 30 was 0.867, and the slope for the linear data fit in Figure 31 was 1.746. Figure 30 depicts the drop height versus acceleration duration data for the 45° wedge. Figure 31 depicts the drop height versus acceleration duration for the 75° wedge. Since the slope of the lines is minimal, this would suggest that drop height was not a major contributing factor to acceleration duration.

One obvious factor to performing linear fits to the data in Figure 30 and Figure 31 was the amount of error that would be observed about the linear data fit. For the linear fit for the data in Figure 30, the standard error was 11.377. For the linear fit for the data in Figure 31, the standard error was 17.3905. Since no other data trends are obvious in the data, it is assumed that the data follows a linear trend with a large error about the best fit line.

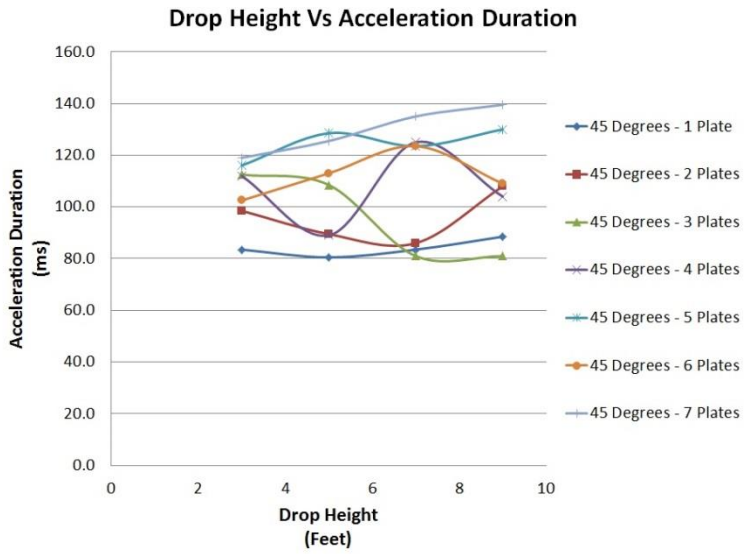

Figure 30. Drop Height Versus Acceleration Duration For The 45° Wedge

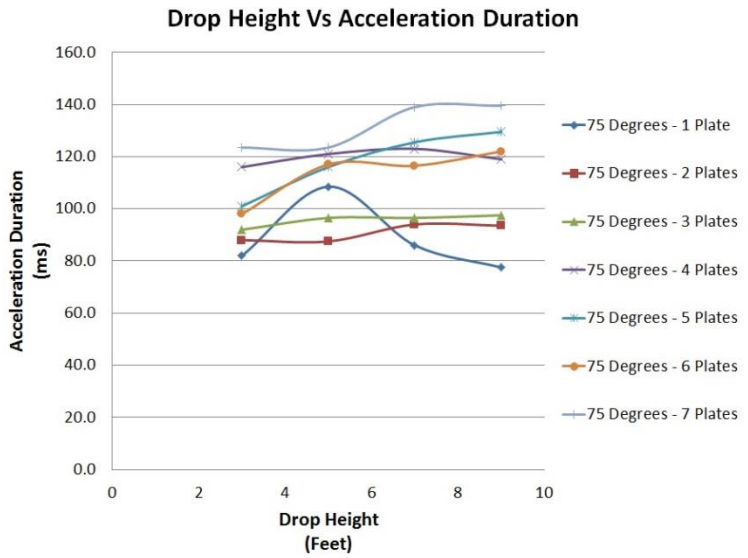

Figure 31. Drop Height Versus Acceleration Duration For The 75° Wedge

Figure 32 and Figure 33 are provided for informational purposes. Figure 32 depicts the drop height versus acceleration duration data for the 55° wedge. Figure 33 depicts the drop height versus acceleration duration data for the 65° wedge

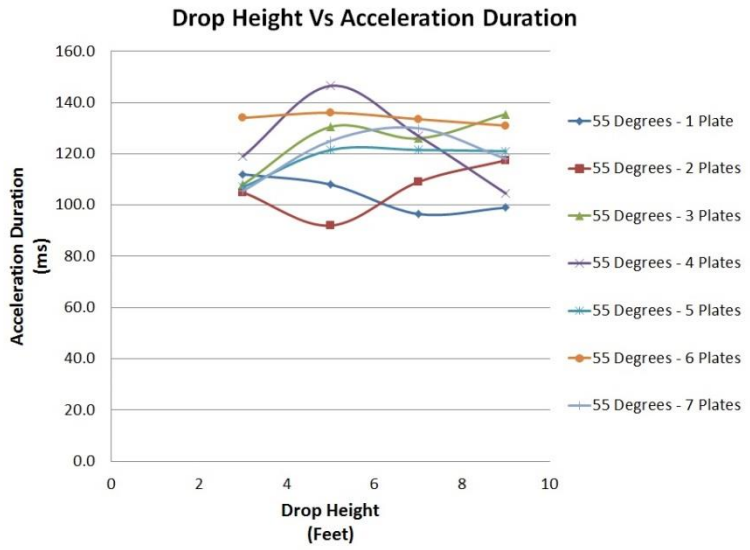

Figure 32. Drop Height Versus Acceleration Duration For The 55° Wedge

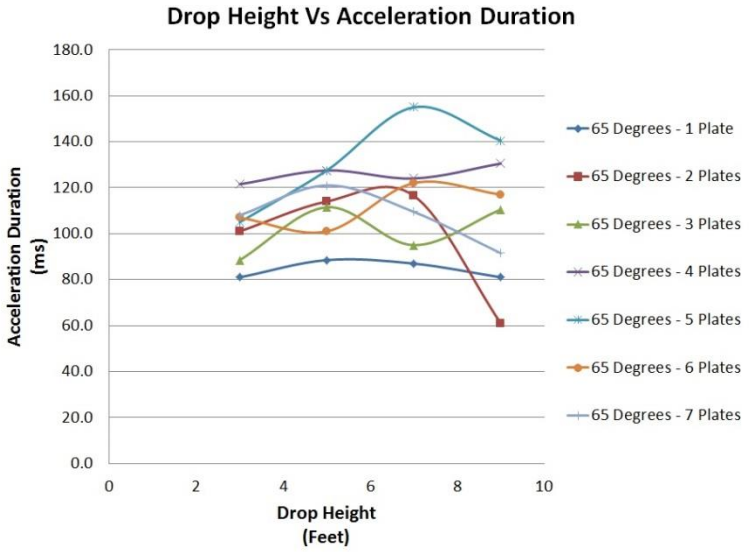

Figure 33. Drop Height Versus Acceleration Duration For The 65° Wedge

4.4.4 Acceleration Duration Data Dispersion

It is evident that there is much variation in the acceleration duration for each of the plots shown above. Intuitively, one would think that for a given wedge angle and weight, such as 65° with 2 plates as shown in Figure 33, that as drop height increases so would acceleration duration. However, the exact opposite behavior has been noticed for this example. In this particular case, a decrease of approximately 50 ms has been observed.

During the data analysis process of this effort, it was observed that there was little consistency in the time differential from the transition point until the time where the curve crossed the zero axis at the end point. For the purposes of this document, the transition point is defined as being where the steep slope of the rear half of the sinusoidal acceleration pulse begins to flatten out. Figure 34 illustrates the location of a transition point in data from a sample full-scale craft, rough water test that was not part of this effort. The selection of Figure 34 was only to provide the reader with a clear example of an easily defined transition point. In most cases, the data from this effort did not have such clearly defined transition points. This observation can be easily seen in Figure 9 where determining the location of the transition point would require some subjective judgment. The inconstancies within the acceleration duration data for this effort were chiefly located in the region from the transition point to the time where the curve crossed the zero axis at the end point. In some cases, the time from the transition point to the end point was up to 50 ms longer than expected. No reason for this disparity was observed.

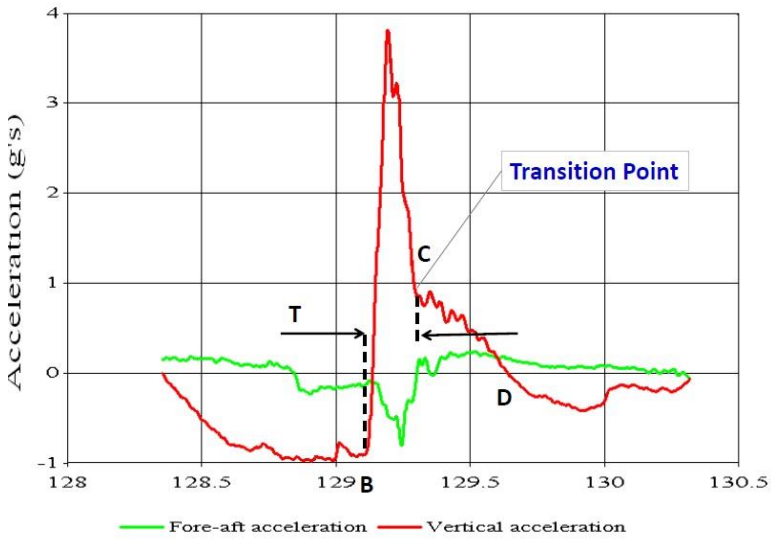

Figure 34. Transition Point Illustration

When looking at full-scale planing craft motion data, it is not uncommon to see acceleration pulse durations ranging from 75-200 ms. This could happen for a variety of reasons: rolling or pitching at the time of impact, the size variations in the waves, differences in the impact velocity, etc. Considering this with respect to the drop tests performed, given that there was no apparatus to maintain zero pitch or roll during the drop, given that there may have been variations in the sand surface between drops, and understanding that the sand consistency would likely vary with depth, it is not unlikely that there should be variations in duration from one drop to the next.

4.5 Compliance With Protocol One

Since the test that was performed in this effort was based upon the test method described in Protocol One, it is not surprising that some of the time history curves generated could fit within the allowable region of a valid Protocol One compliant test. Where there was discrepancy with Protocol One, it was due to exceeding the maximum acceleration magnitude limit. The maximum acceleration magnitude allowed in Protocol One is 12.2 G's, and many of the time history curves generated in this effort exceeded this maximum level. An example of

this can be seen in Figure 35 where the curve generated from a 55° wedge, 5 plate and 7 foot drop had a maximum acceleration value of 15.0 G's. In Figure 35, the line in green that lies above the curve is the Protocol One upper limit line. In Figure 35, the line in blue that lies below the curve is the Protocol One lower limit line. As described with Protocol One, any acceleration magnitude time history curve that fits within these limits is considered a valid Protocol One test. However, there was no intent in the work herein to comply completely with Protocol One as this was not an effort to test equipment for a military acquisition program. Protocol One compliance was not a requirement for this thesis, though it is good to see that the acceleration time history profile aligns well with the Protocol One profile limits.

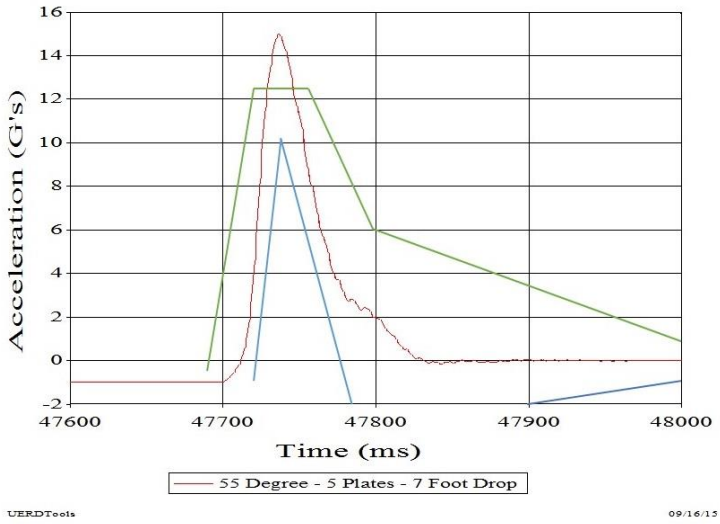

Figure 35. Sample Curve With Protocol One Compliance Envelopes Inserted

4.6 Empirical Models

As discussed above, some of the trends observed in the data, especially the data regarding acceleration magnitude, appeared to be linear; therefore, the formulation of the

empirical models for acceleration magnitude and acceleration duration would be accomplished using linear regression techniques. The linear regression tool selected for this task was the MVREGRESS tool located in MATLAB. Two separate sets of empirical models were generated. One set of empirical models was generated that would model only the first 112 drops conducted in 2015. The second set of empirical models was generated using the entire data set, consisting of 2015 and 2016 data that would model all 224 drops conducted. Equations 1 and 2 model the 112 drops conducted in 2015. Equations 3 and 4 model all 224 drops conducted in both 2015 and 2016. In both sets of equations the following variables are defined as:

A = Wedge angle, measured in degrees;

W = Drop test fixture weight, measured in pounds;

H = Drop height, measured in feet;

Acceleration Magnitude, measured in G's;

Acceleration Duration, measured in milliseconds.

For 112 drops:

$$0.0667A - 0.0189W + 1.7686H + 3.2206 = Acceleration\ Magnitude \text{ (Eqn 1)}$$

$$0.0610A + 0.1890W + 0.8670H + 68.1380 = Acceleration\ Duration \text{ (Eqn 2)}$$

For 224 drops:

$$0.2279A - 0.0143W + 1.2931H - 5.7473 = Acceleration\ Magnitude \text{ (Eqn 3)}$$

$$-1.1195A + 0.1367W + 0.2694H + 161.4086 = Acceleration\ Duration \text{ (Eqn 4)}$$

Both sets of equations were evaluated and compared to the actual data values collected. Table 3 summarizes the statistical results of empirical model comparison with the collected test data. Equations 1 and 2 were compared with the test data for the 112 drops conducted in 2015. Equations 3 and 4 were compared with the test data for all 224 drops

conducted in 2015 and 2016. As can be observed in Table 3, equations 1 and 2 demonstrate greater statistical accuracy than equations 3 and 4. The greater statistical error demonstrated with these models can be attributed to the data disparity discussed earlier.

Table 3. Empirical Model Statistical Summary

Equation	Average Error	Standard Deviation	Maximum Error	Minimum Error
Eqn 1	0.0	0.8	2.0	-2.3
Eqn 2	0.0	14.2	38.8	-40.6
Eqn 3	0.0	2.2	5.1	-3.6
Eqn 4	0.0	19.2	55.0	-54.2

Another check of the accuracy of the derived equations would be to plot the actual results versus the predicted results. The results were segregated by drop height. The decision to group the data in this method was based on the assumption that the error within the data would grow smaller as drop height increased. Figure 36 depicts the plotted data for equation 1, which predicts acceleration magnitude. Figure 37 depicts the plotted data for equation 2, which predicts acceleration duration. Equations 1 and 2 were selected for this accuracy check because they demonstrated lower error values than equations 3 and 4.

Once the data was plotted, a least squares curve fit was applied to each group of data. A slope of 1 would indicate a perfect math model prediction. A slope greater that 1 would indicate that the math model over predicts the results. A slope less than 1 would indicate that the math model under predicts the results. Additionally, the R squared value was calculated for each least squares fit to determine the goodness of fit.

The plotted data in Figure 36 demonstrated linear patterns. An interesting observation is that the goodness of fit increased from 0.41 for the 3 foot drop to 0.91 for the 9 foot drop. This confirms the original assumption discussed above. Conversely, the math model begins to more consistently under predict as drop height increases. This can be observed with a slope for the least squares fit of 0.84 for the 3 foot drop and a slope for the least squares fit of 0.67 for the 9 foot drop.

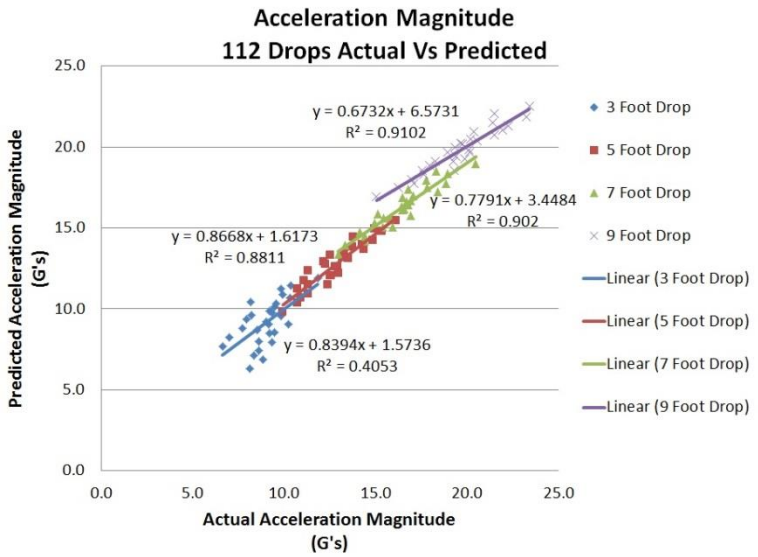

Figure 36. Acceleration Magnitude, 112 Drops Actual Vs Predicted Results

No further analysis was performed with equation 2 since no data patterns were observed in Figure 37.

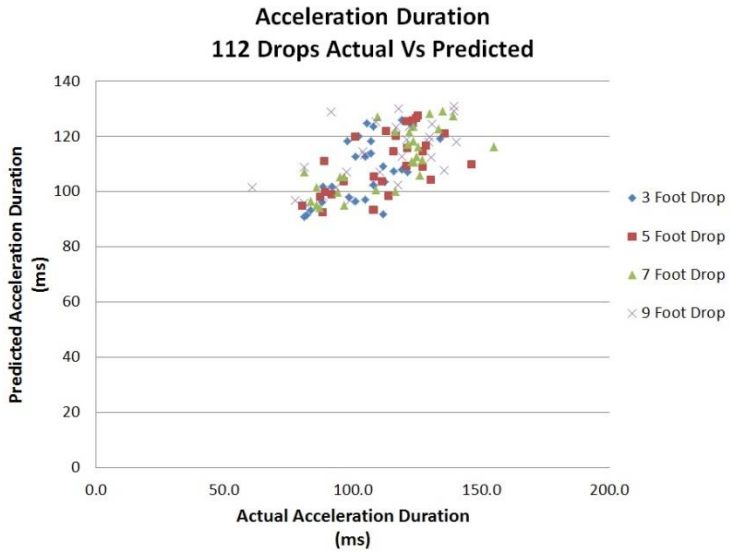

Figure 37. Acceleration Duration, 112 Drops Actual Vs Predicted Results

4.7 Application Example

Equations 1 and 2 can be used by interested parties to simulate, in the laboratory, single impact events based upon the measured rough water performance of a craft in a seaway. For example, suppose that a marine radio manufacturer has built a prototype Very High Frequency (VHF) radio and, with it, a specialty mounting system designed to mitigate the effects of the wave slamming that the radio will be subjected to during rough water operations. The VHF radio manufacturer wants to know how efficient the mounting system is in reducing shock. The VHF radio manufacturer does not have access to craft or personnel that can perform a rough water test that will allow them the opportunity to learn this information under real world conditions, but assume that they do have access to some rough water data for a particular craft. After review of the rough water test data, the VHF radio manufacturer has determined that the worst case shock that their system will see in a particular craft would be at an acceleration level of 15.4 G's and at an acceleration duration of 120 milliseconds.

Assume that the prototype VHF radio weighs 4 pounds and that the corresponding shock absorbing mount weighs 9 pounds. This combined system weighs 13 pounds. Also

suppose that the radio manufacturer has a warehouse with a high enough ceiling to allow a series of 6 foot drops from a roof truss. It is also assumed that the radio manufacturer has access to appendix B of this thesis and, as such, knows the weight of all of the wedges and plate combinations. With these pieces of information and by using equations 1 and 2, the radio manufacturer can modify appendix C into a simple spreadsheet and select a wedge angle, fixture weight combination that when dropped from a 6 foot height can produce the shock environment that is targeted. In this particular case, selecting the 75° wedge with 4 plates and the mounted radio system (total weight = 170 pounds + 13 pounds = 183 pounds) and dropping it from a height of 6 feet can produce an acceleration magnitude of 15.4 G's and an acceleration duration of 112.5 milliseconds. The radio manufacturer can install an accelerometer on the top deck of the fixture and upon the radio itself. By comparing the data generated by the two accelerometers during a series of drop tests, the radio manufacturer can cheaply determine the effectiveness of the shock absorbing mount before subjecting it to an expensive and time consuming rough water test. After determining what combination of wedge angle, weight and drop height to use, it would be wise if the radio manufacturer performed a series of tuning drops where the manufacturer would tune the three parameters in order to get as close to the desired acceleration level and acceleration magnitude as possible.

CHAPTER 5

5. CONCLUSIONS AND RECOMMENDATIONS

It was observed that the effect of wedge angle upon acceleration magnitude was roughly linear. It was also observed that the effect of wedge angle upon acceleration duration was random and the randomness became more pronounced as the drop height increased.

It was observed that the effect of weight upon acceleration magnitude was linear throughout the test variable region. It was also observed that the effect of weight upon acceleration duration was linear but with a large error about a best fit line.

It was observed that the effect of drop height upon acceleration magnitude was linear throughout the test variable region. It was also observed that the effect of drop height upon acceleration duration was roughly a horizontal line with a large error about the best fit line.

It was observed that a plot of actual versus predicted acceleration magnitudes results in linear behavior. When these results were sorted by drop height, the error became smaller as the drop height increased. It was also observed that the slope of a best fit line through these data plots resulted in a decreasing slope as drop height increased. This trend would suggest that the math model for acceleration magnitude increasingly under predicts as drop height increases.

It was observed that a plot of actual versus predicted acceleration durations resulted in no visibly discernable pattern.

As demonstrated in section 4.7, equations 1, 2, 3 and 4 can be used as a tool to customize a drop test that can simulate a single wave impact. It should be noted that these equations are only valid in the regions of weight from 110 pounds to 297 pounds, regions of drop heights from 3 feet to 9 feet, regions of wedge angle from 45° to 75° and in a consistent sand moisture content. It should also be noted that for the 112 drops conducted in 2015, only one drop at each test condition was conducted. Even though the data set was expanded to 5 drops in each test condition for the 45° wedge, these additional test drops demonstrated that there was disparity in test results when the tests were conducted with different sand

conditions. Therefore, it is recommended that the presented equations be used as a general guide to test personnel designing a drop test to simulate wave impacts. It is recommended that test personnel conduct preliminary drops to verify and tune the performance of their test setup prior to conducting a specific test.

There are potential areas where the results of this research could be improved and refined. As discussed above, an issue noted during the execution of this thesis effort was the accuracy of the empirical models. The generation of these models was based on limited data. In the case of equations 1 and 2, 112 valid data points were used for model generation. In the case of equations 2 and 3, 223 valid data points were used for model generation. A way to refine the accuracy of empirical models by using more data would be for an interested party to conduct further tests based upon the methods, drawings and procedures provided within this thesis.

Another issue that should be investigated is determining how the moisture content of the sand affects the peak acceleration magnitude and acceleration duration upon impact. A method for measuring the moisture content should be included in the test procedure. This information should be collected and then integrated into the empirical model generation.

REFERENCES

GeoMagic Design Expert, Version 12, 333 Three D Systems Circle, Rock Hill, SC 29730

National Instruments cRIO Post Processing Data Script, NSWCCD, Code 835

Riley, Michael R., Haupt, Kelly D., Jacobson, Donald R. (2010). "A Generalized Approach and Interim Criteria for Computing $A_{1/n}$ Accelerations Using Full-Scale High-Speed Craft Trials Data", Naval Surface Warfare Center Carderock Division Report NSWCCD-23-TM-2010/13, April 2010

Savitsky, Daniel and Brown P.W. (October 1976). "Procedures for Hydrodynamic Evaluation of Planing Hulls in Smooth and Rough Water", Marine Technology, Volume 13, No. 4.

Riley, Michael R., Haupt, Kelly D., Jacobson, Donald R. (2012). "A Deterministic Approach For Characterizing Wave Impact Response Motions Of A High-Speed Planing Hull", Naval Surface Warfare Center Carderock Division Report NSWCCD-23-TM-2012/05, January 2012

Riley, Michael R., Coats, Dr. Timothy W., Murphy, Heidi (2014). "Acceleration Response Mode Decomposition For Quantifying Wave Impact Load In High Speed Planing Craft", Naval Surface Warfare Center Carderock Division Report NSWCCD-23-TR-2014/007, April 2014

Protocol 1 (2014). "Maritime Whole Body Vibration, Shock Mitigating Seat Test", PQQ Reference JK6KHJ8427, United Kingdom Ministry Of Defense, 08/01/2014

UERDTools, Version 4.4. Mantz, Paul, Costanzo, Fredrick, Howell III, Jamie, Ingler, Dave, Luft, Eric, Okano, Steve, Naval Surface Warfare Center, Carderock Division, Underwater Explosion and Research Development, 9500 MacArthur Boulevard, West Bethesda, MD 20817-5700

MATLAB, Version 8.2, MathWorks Inc., Natick, Massachusetts

Military Test Procedure 5-2-506, *Shock Test Procedures*, U.S. Army Test and Evaluation Command, White Sands Missile Range, New Mexico, December 1966.

Appendix A - Technical Drawing Package of Drop Fixture

REVISIONS				
ZONE	REV	DESCRIPTION	DATE	APPROVED

NOTES

1. Assembled Weight - 183 Pounds

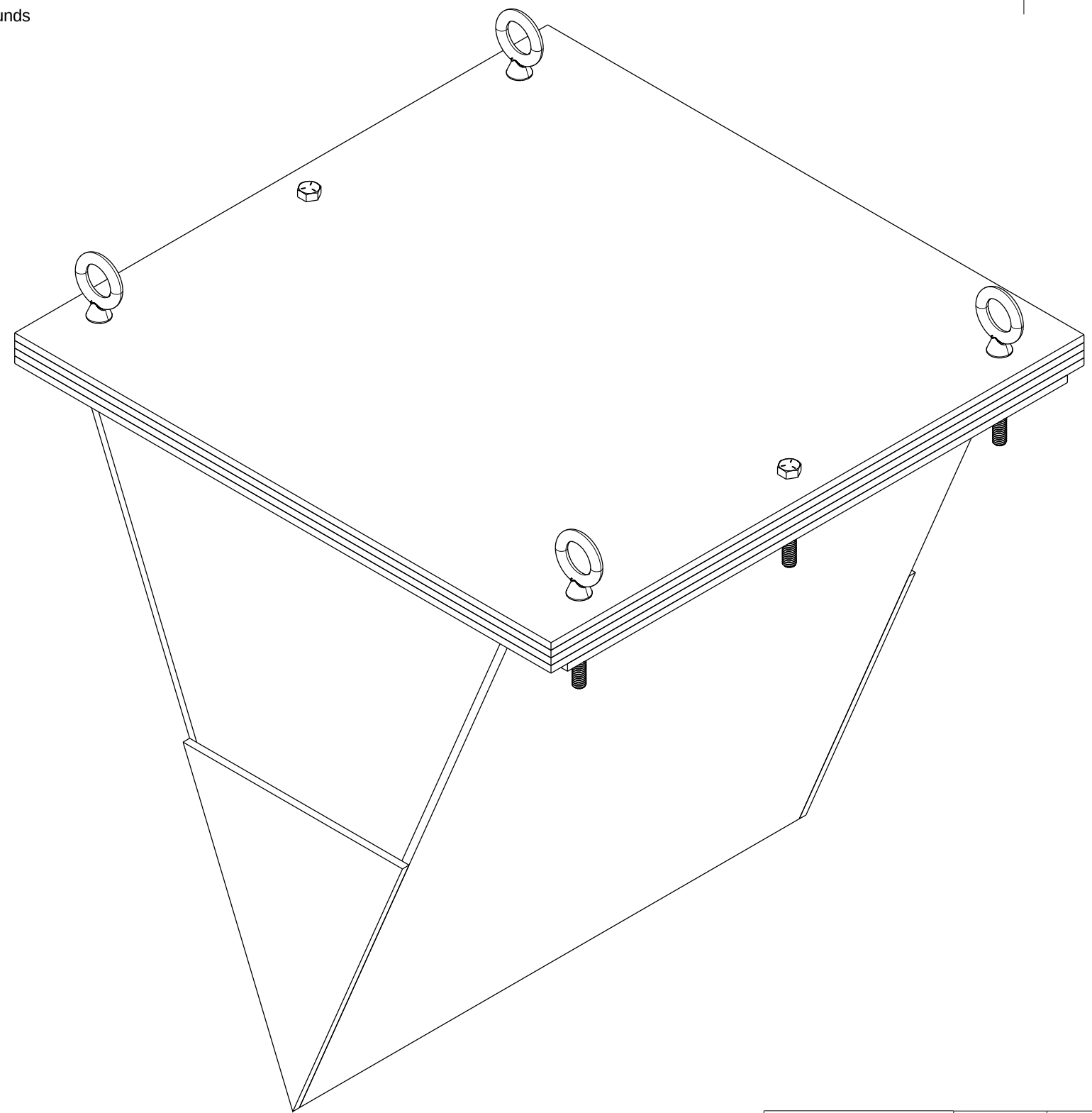

	DRAWN: John Barber	DATE: 1 May 2015	
	CHECKED		
	QA		Drop Fixture - 45 Degree Wedge
	MFG		SIZE: C / FSCM NO. / DWG NO.: SK-001 / REV
	APPROVED		SCALE / SHEET: 1 of 3

REVISIONS				
ZONE	REV	DESCRIPTION	DATE	APPROVED

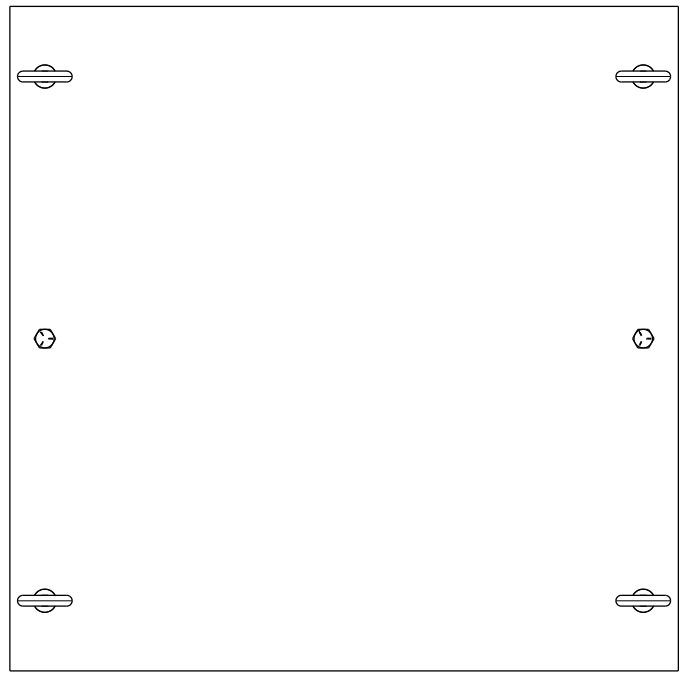

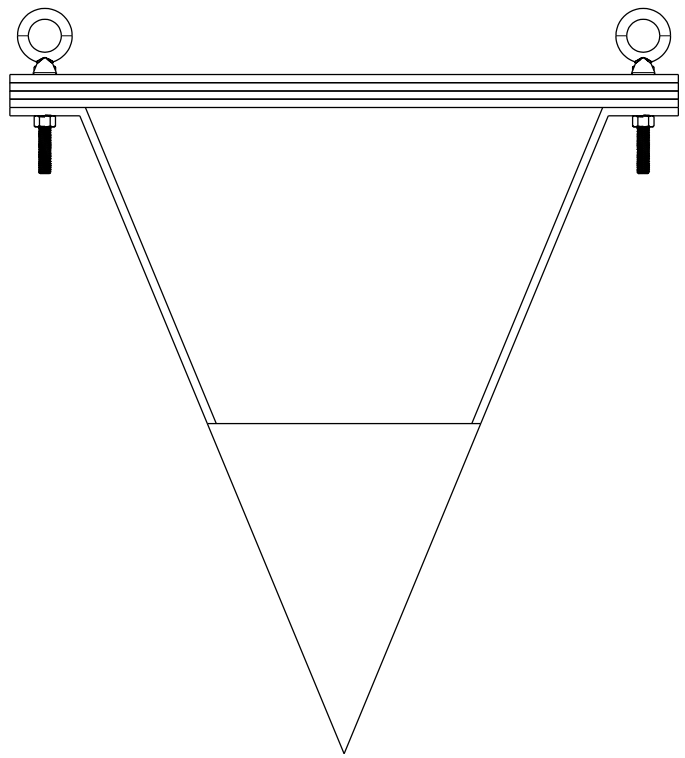

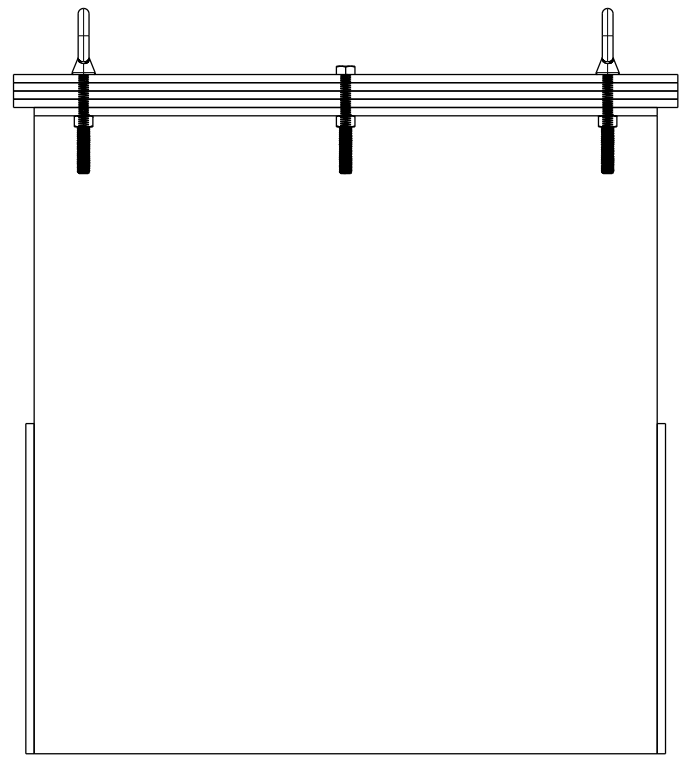

	DRAWN: John Barber	DATE: 1 May 2015	
	CHECKED		
	QA		Drop Fixture - 45 Degree Wedge
	MFG		SIZE: C / FSCM NO. / DWG NO.: SK-001 / REV
	APPROVED		SCALE / SHEET: 2 of 3

Item Number	Quantity	Part Number	Part Name	Revision	Comment
1	1		Wedge - 45 Degree		
2	4		Top Plate		
3	2	92865A636	Hex Head Bolt - 3 Inches Long - 3/8 UNC-16		McMaster Carr
4	2		End Plate - 45 Degree		
5	6		Hex Nut - 3/8 UNC-16		
6	4	3014T63	Eye Bolt - 3 Inch Long - 3/8 UNC-16		McMaster Carr

REVISIONS				
ZONE	REV	DESCRIPTION	DATE	APPROVED

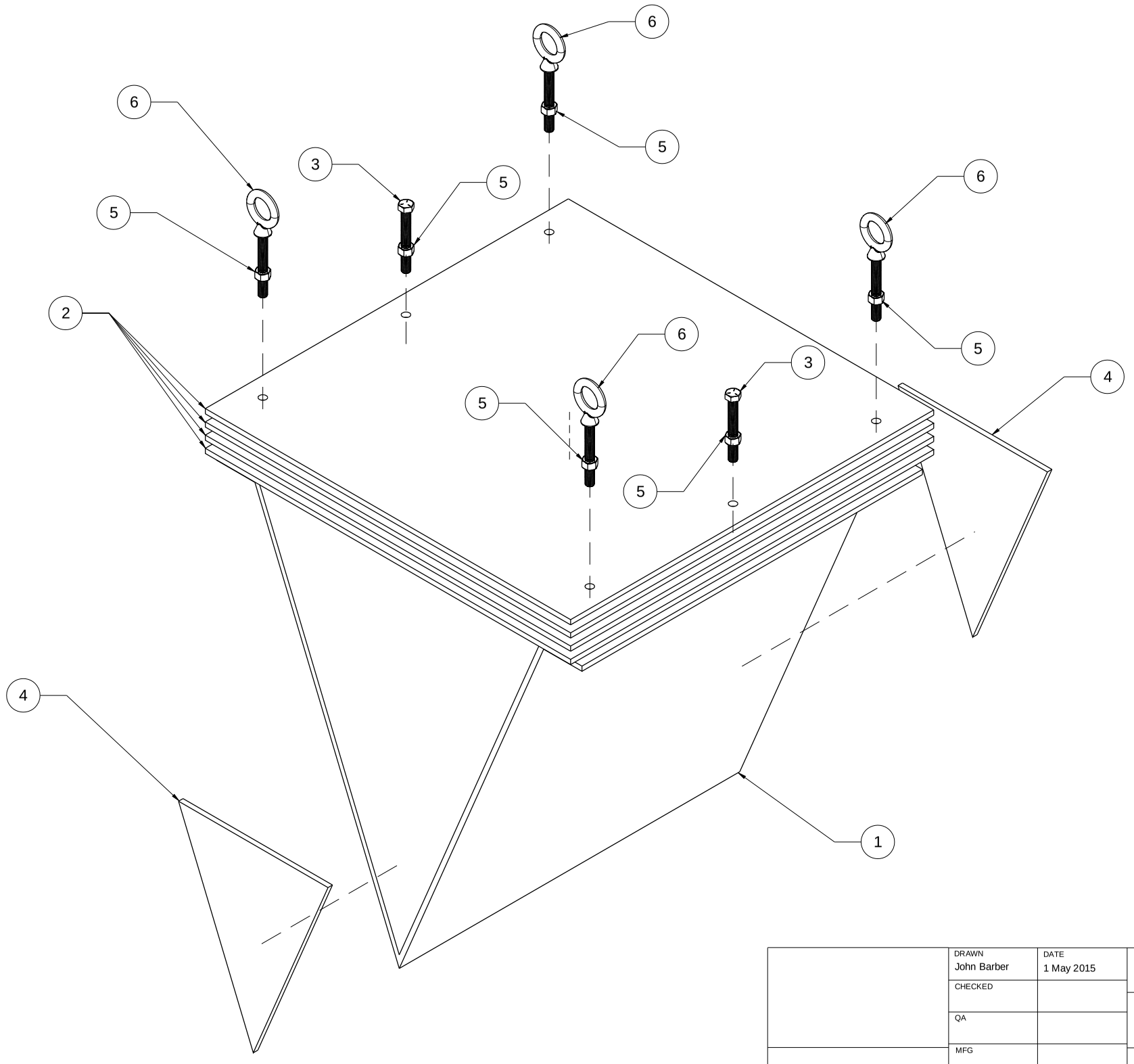

	DRAWN: John Barber	DATE: 1 May 2015	
	CHECKED		Drop Fixture - 45 Degree Wedge
	QA		
	MFG		SIZE: C | FSCM NO. | DWG NO.: SK-001 | REV
	APPROVED		SCALE | SHEET: 3 of 3

REVISIONS				
ZONE	REV	DESCRIPTION	DATE	APPROVED

Notes

1. Assembled Weight - 174 Pounds

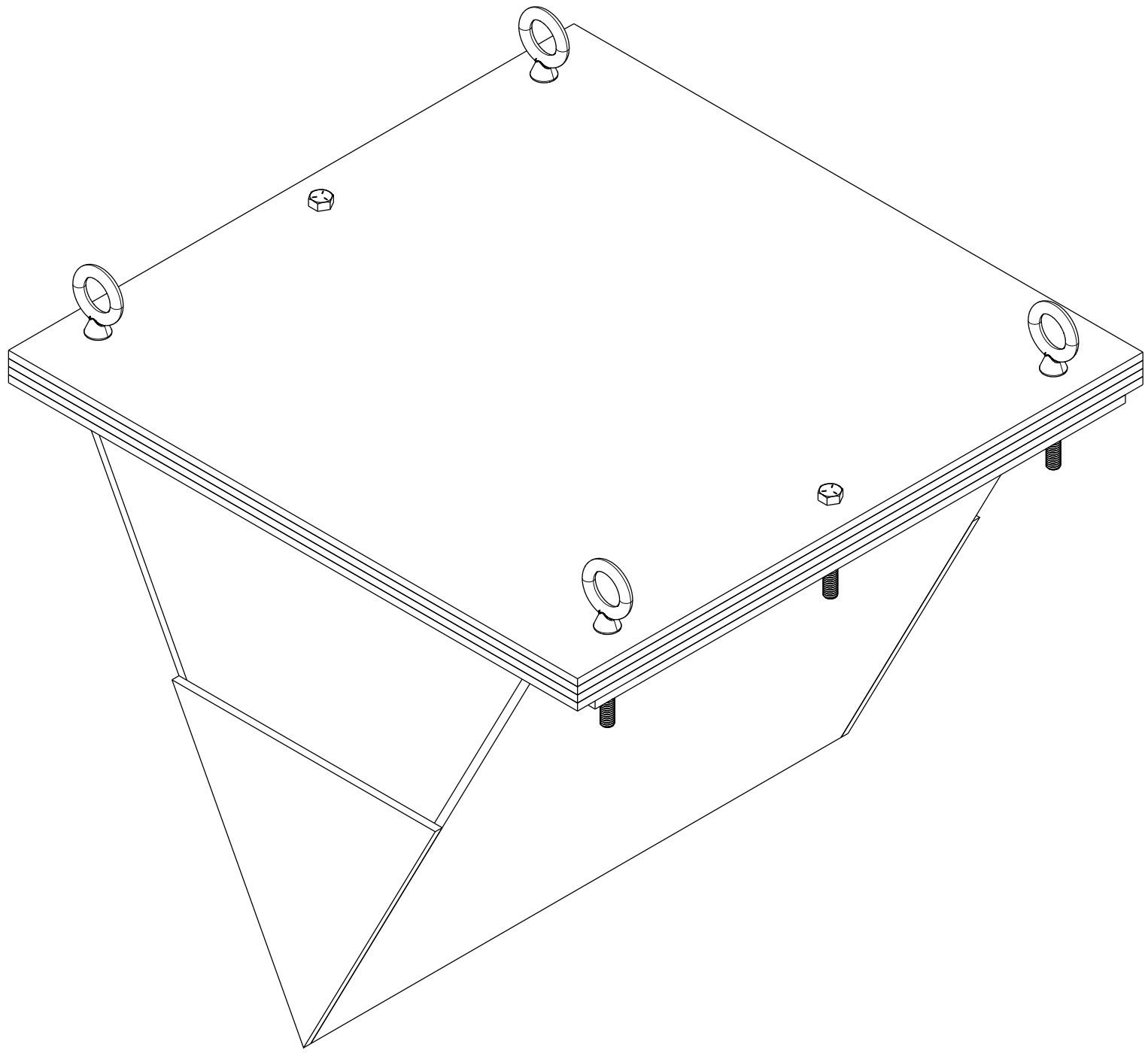

	DRAWN: John Barber	DATE: 2 May 2015	
	CHECKED		Drop Fixture - 55 Degree Wedge
	QA		
	MFG		SIZE: C / FSCM NO. / DWG NO.: SK-008 / REV
	APPROVED		SCALE / SHEET: 1 of 3

REVISIONS				
ZONE	REV	DESCRIPTION	DATE	APPROVED

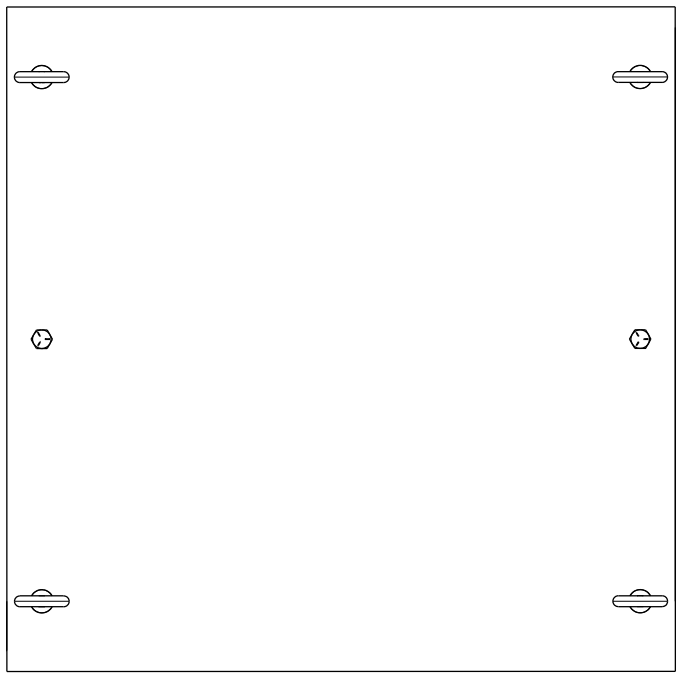

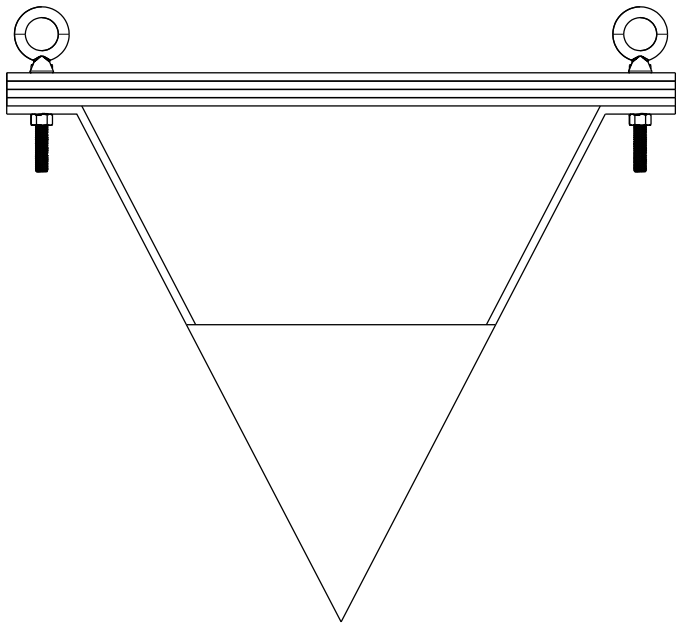

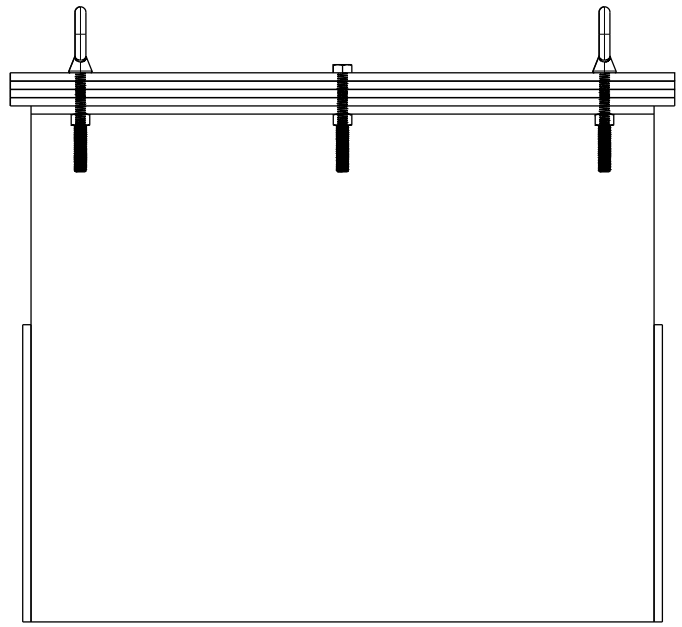

	DRAWN: John Barber	DATE: 2 May 2015	
	CHECKED		
	QA		Drop Fixture - 55 Degree Wedge
	MFG		SIZE: C / FSCM NO. / DWG NO.: SK-008 / REV
	APPROVED		SCALE / SHEET: 2 of 3

Item Number	Quantity	Part Number	Part Name	Revision	Comment
1	1		Wedge - 55 Degrees		
2	4		Top Plate		
3	2	92865A636	Hex Head Bolt - 3/8 Inch - 16 UNC - 3 Inches Long		McMaster Carr
4	2		End Plate - 55 Degrees		
5	6		Hex Nut - 3/8 Inch - 16 UNC		
6	4	3014T63	Eye Bolt - 3/8 Inch - 16 UNC - 3 Inch Long		McMaster Carr

REVISIONS				
ZONE	REV	DESCRIPTION	DATE	APPROVED

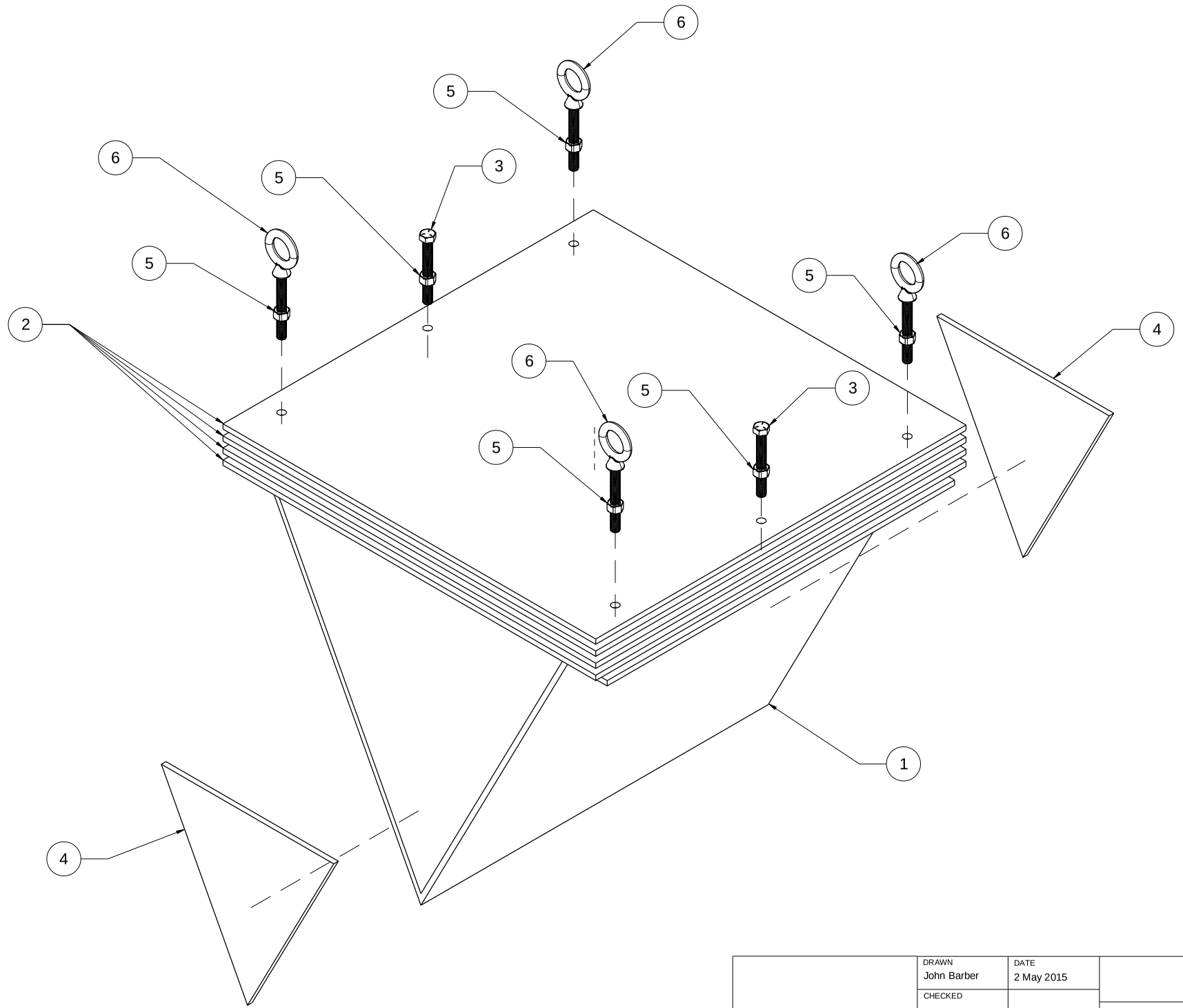

	DRAWN: John Barber	DATE: 2 May 2015	
	CHECKED		Drop Fixture - 55 Degree Wedge
	QA		
	MFG		SIZE: C | FSCM NO. | DWG NO.: SK-008 | REV
	APPROVED		SCALE | SHEET: 3 of 3

REVISIONS				
ZONE	REV	DESCRIPTION	DATE	APPROVED

NOTES

1. Assembled Weight - 167 Pounds

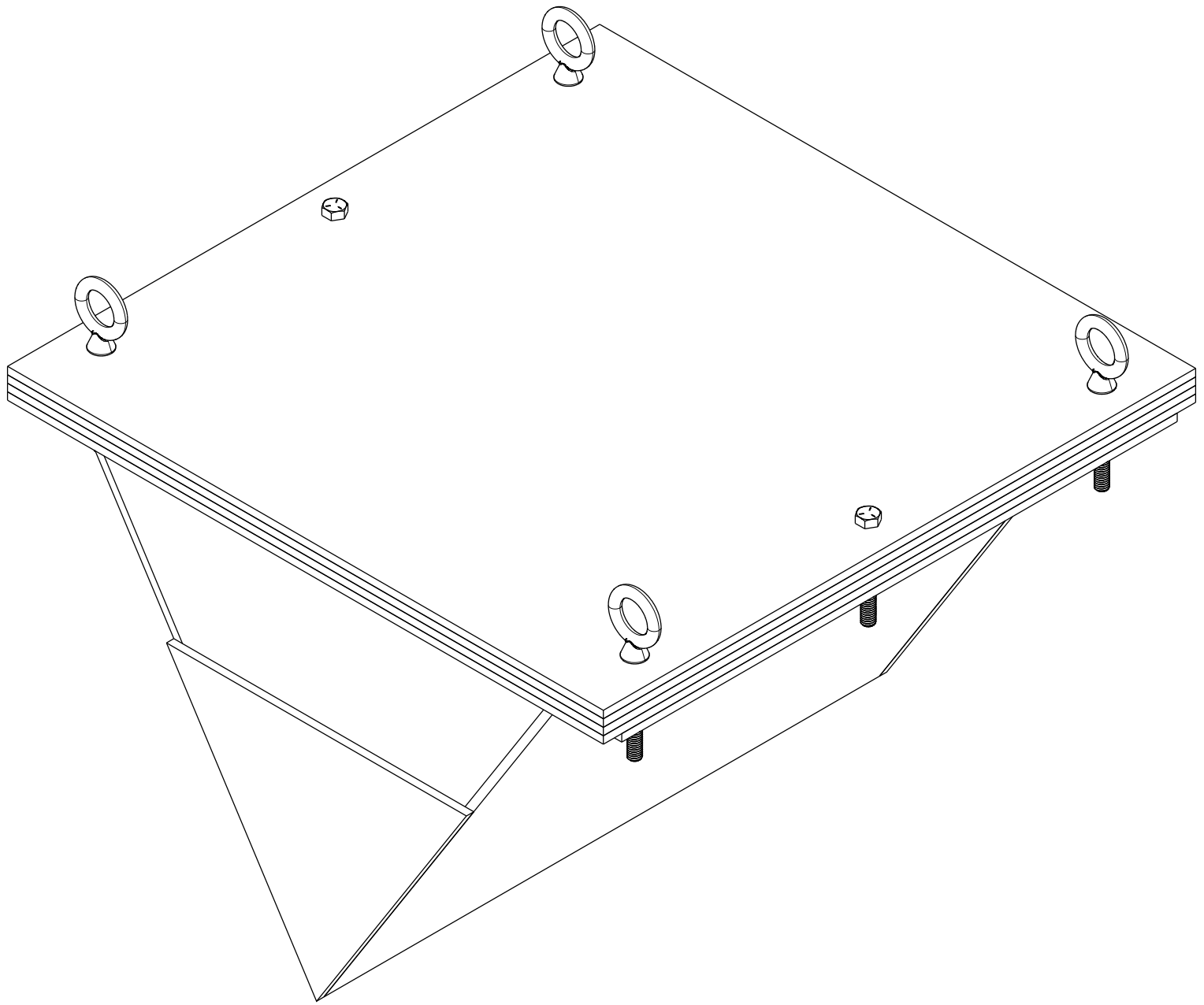

	DRAWN	John Barber	DATE	3 May 2015
	CHECKED			
	QA			
	MFG			
	APPROVED			

Drop Fixture - 65 Degree Wedge

SIZE	FSCM NO.	DWG NO.	REV
C		SK-011	

SCALE | SHEET 1 of 3

REVISIONS				
ZONE	REV	DESCRIPTION	DATE	APPROVED

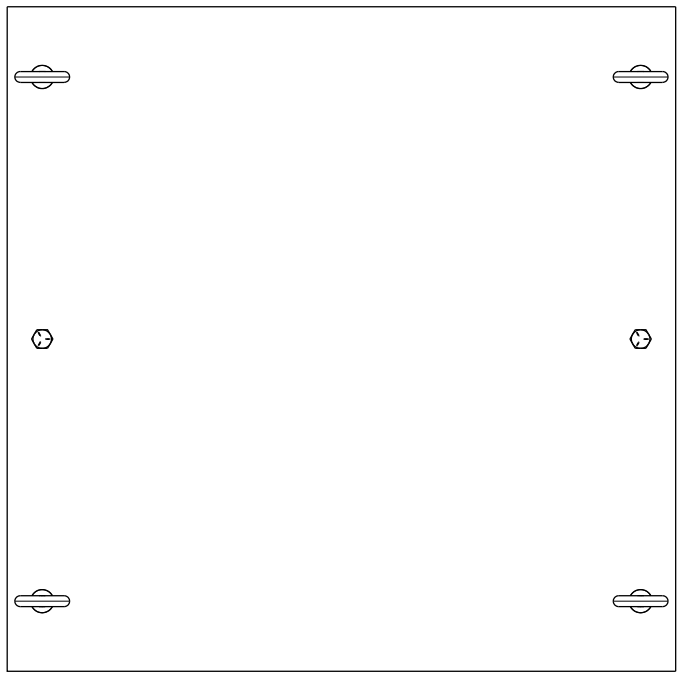

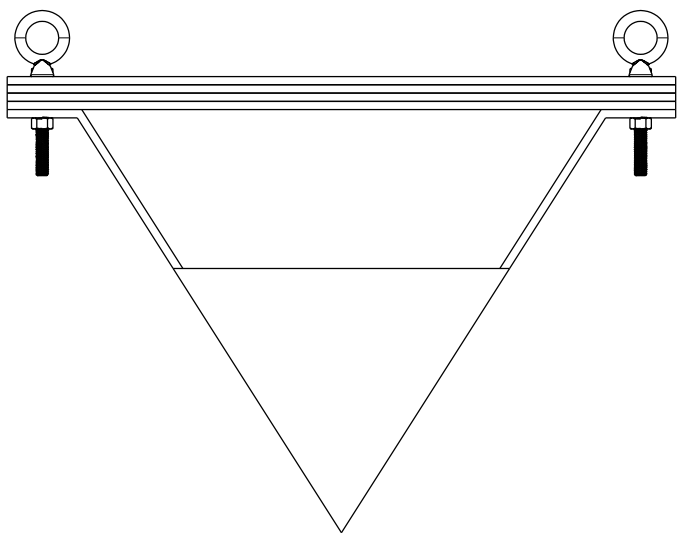

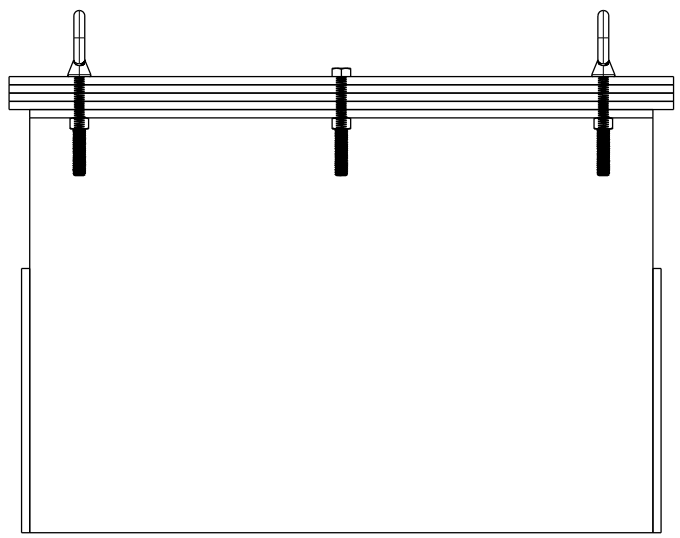

	DRAWN: John Barber	DATE: 3 May 2015	
	CHECKED		
	QA		Drop Fixture - 65 Degree Wedge
	MFG		SIZE: C / FSCM NO. / DWG NO.: SK-011 / REV
	APPROVED		SCALE / SHEET: 2 of 3

Item Number	Quantity	Part Number	Part Name	Revision	Comment
1	1		Wedge - 65 Degree		
2	4		Top Plate		
3	2		End Plate		
4	2	92865A636	Hex Head Bolt - 3/8 UNC-16 - 3 Inches Long		McMaster Carr
5	6		Hex Nut - 3/8 UNC-16		
6	4	3014T63	Eye Bolt - 3/8 UNC-16 - 3 Inches Long		McMaster Carr

REVISIONS				
ZONE	REV	DESCRIPTION	DATE	APPROVED

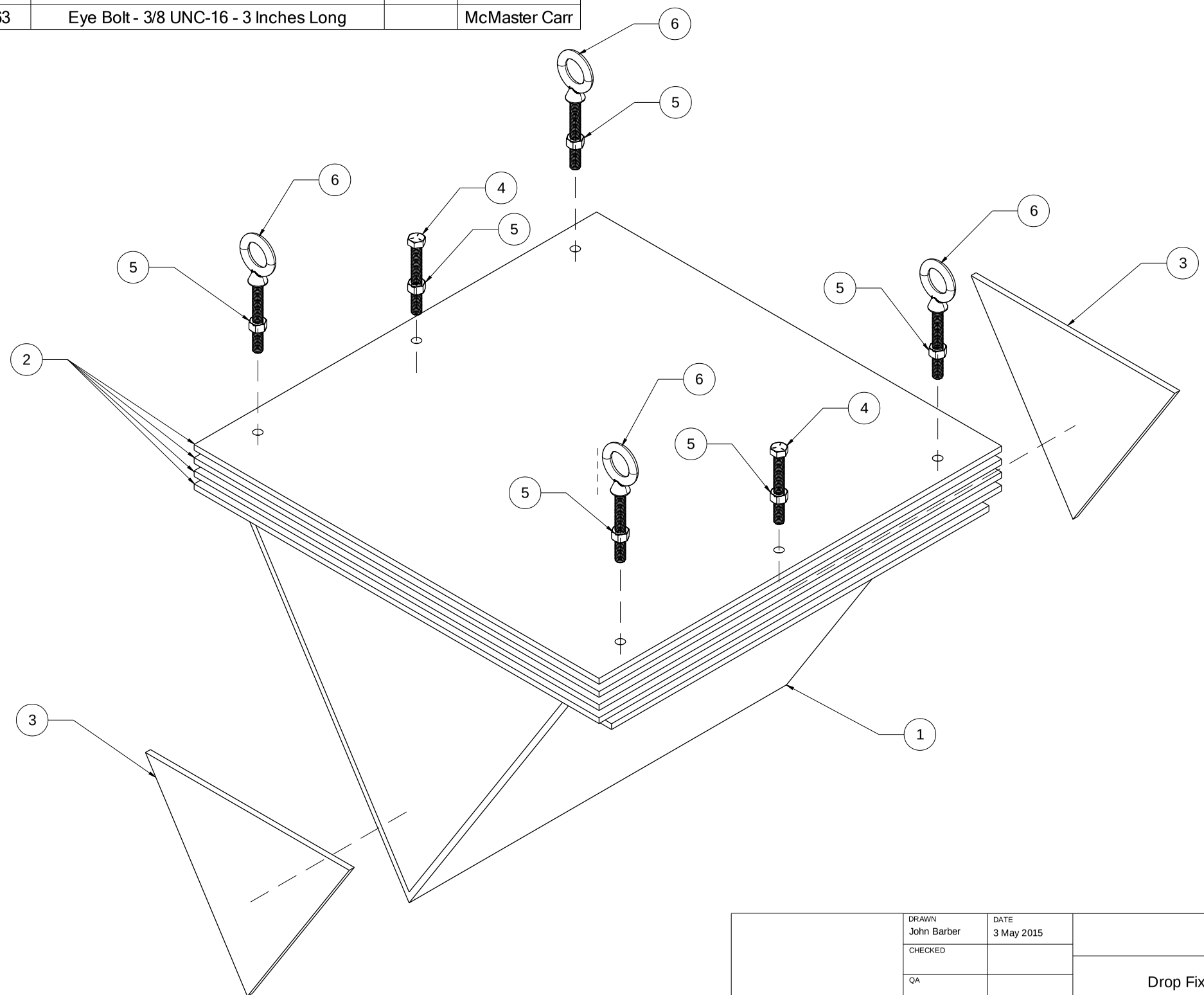

	DRAWN: John Barber	DATE: 3 May 2015	
	CHECKED		Drop Fixture - 65 Degree Wedge
	QA		
	MFG		SIZE: C | FSCM NO. | DWG NO.: SK-011 | REV
	APPROVED		SCALE | SHEET: 3 of 3

REVISIONS				
ZONE	REV	DESCRIPTION	DATE	APPROVED

NOTES

1. Assembled Weight - 164 Pounds

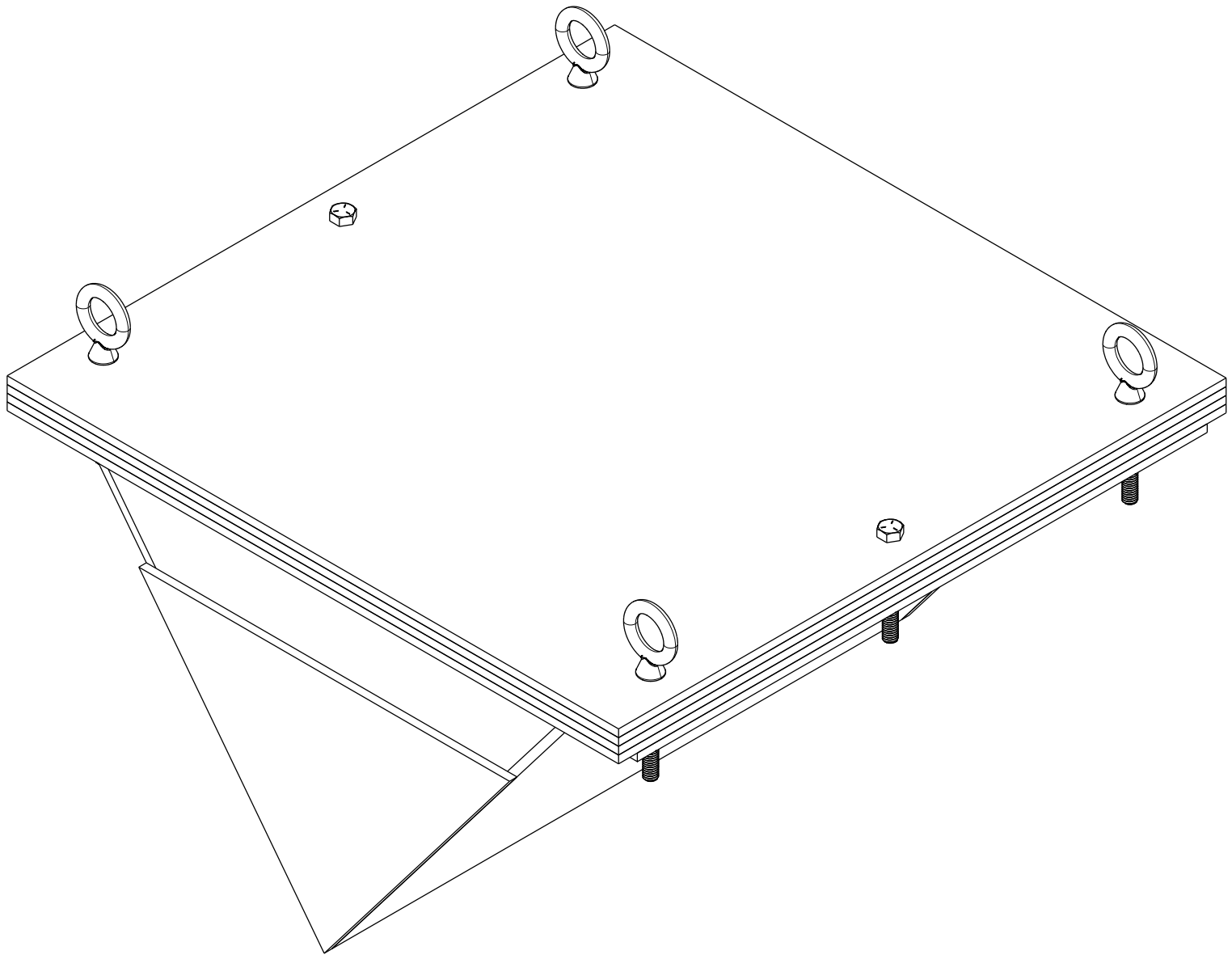

	DRAWN: John Barber	DATE: 10 May 2015	
	CHECKED		Drop Fixture - 75 Degree Wedge
	QA		
	MFG		SIZE: C / FSCM NO. / DWG NO.: SK-014 / REV
	APPROVED		SCALE / SHEET: 1 of 3

REVISIONS				
ZONE	REV	DESCRIPTION	DATE	APPROVED

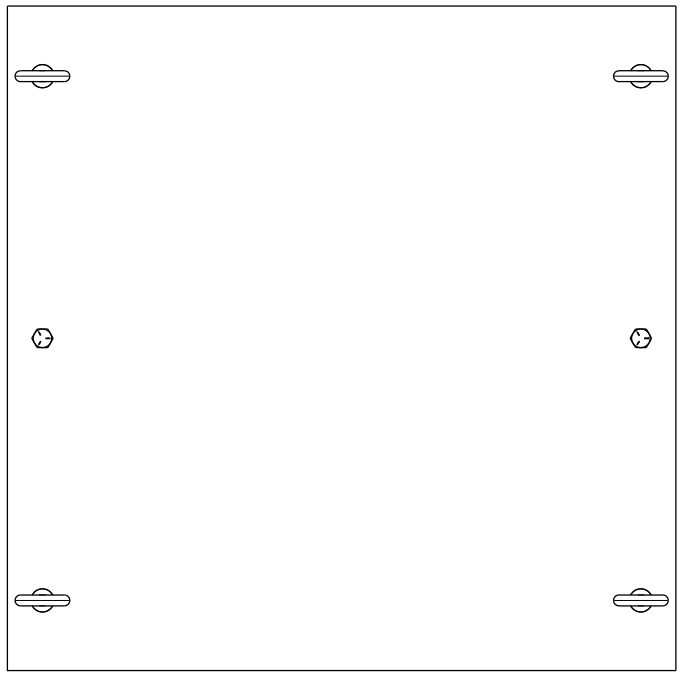

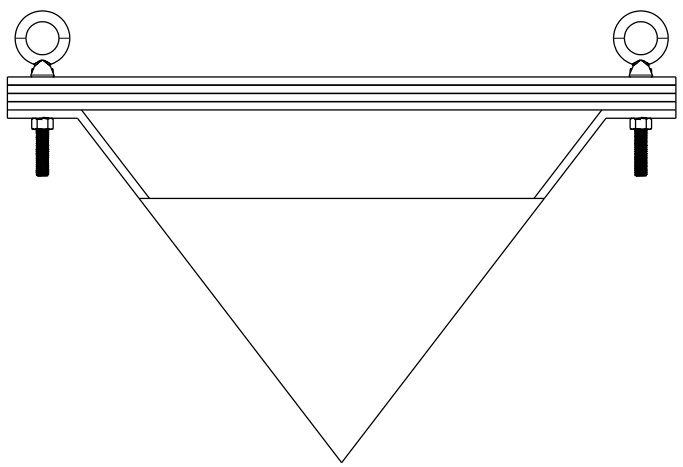

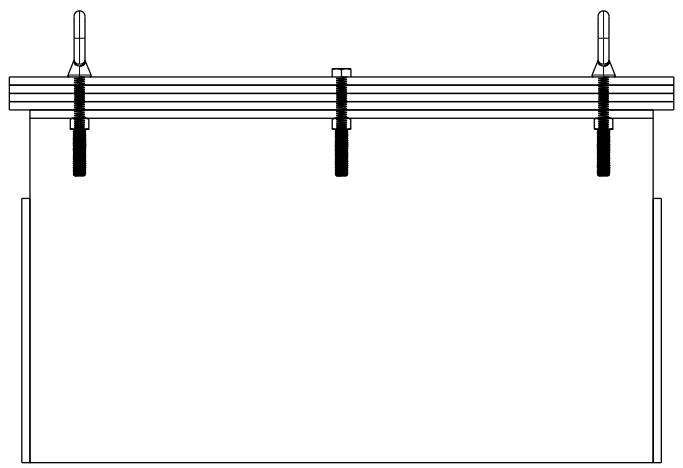

	DRAWN: John Barber	DATE: 10 May 2014	
	CHECKED		
	QA		Drop Fixture - 75 Degree Wedge
	MFG		SIZE: C / FSCM NO. / DWG NO.: SK-014 / REV
	APPROVED		SCALE / SHEET: 2 of 3

Item Number	Quantity	Part Number	Part Name	Revision	Comment
1	1		Wedge - 75 Degree		
2	4		Top Plate		
3	2		End Plate - 75 Degrees		
4	2	92865A636	Hex Head Bolt - 3/8 -16 UNC x 3 Inches Long		McMaster Carr
5	6		Hex Nut - 3/8 - 16 UNC		
6	4	3014T63	Eye Bolt - 3/8 - 16 UNC x 3 Inch Long		McMaster Carr

REVISIONS				
ZONE	REV	DESCRIPTION	DATE	APPROVED

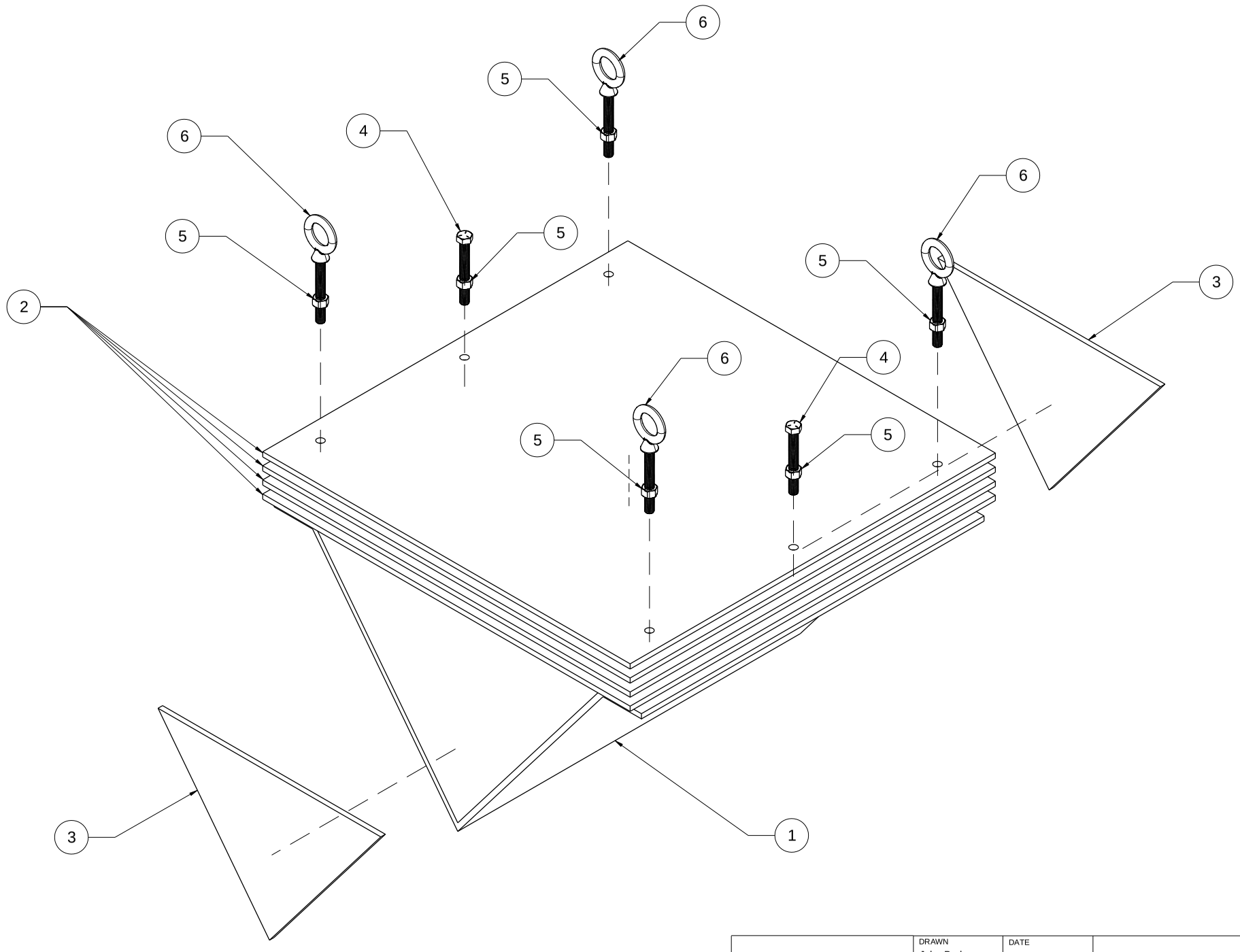

	DRAWN: John Barber	DATE: 10 May 2015	
	CHECKED		Drop Fixture - 75 Degree Wedge
	QA		
	MFG		SIZE: C | FSCM NO. | DWG NO.: SK-014 | REV
	APPROVED		SCALE | SHEET: 3 of 3

REVISIONS				
ZONE	REV	DESCRIPTION	DATE	APPROVED

NOTES

1. Material - Steel Plate, 1/4 Inch
2. Finished Weight - 61 Pounds
3. Qauntity Required - 1 Each

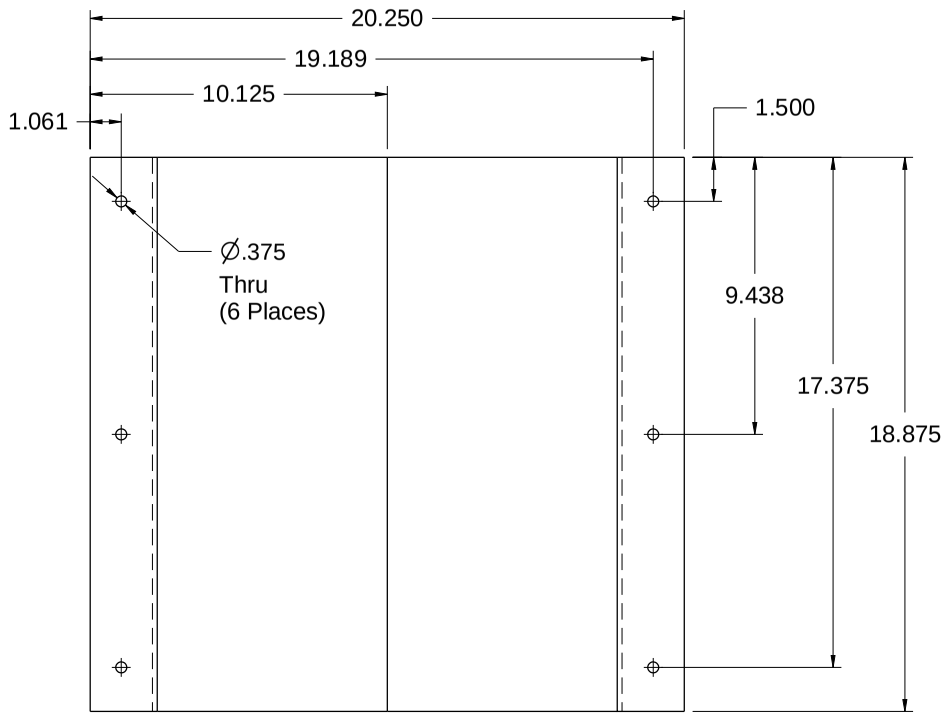

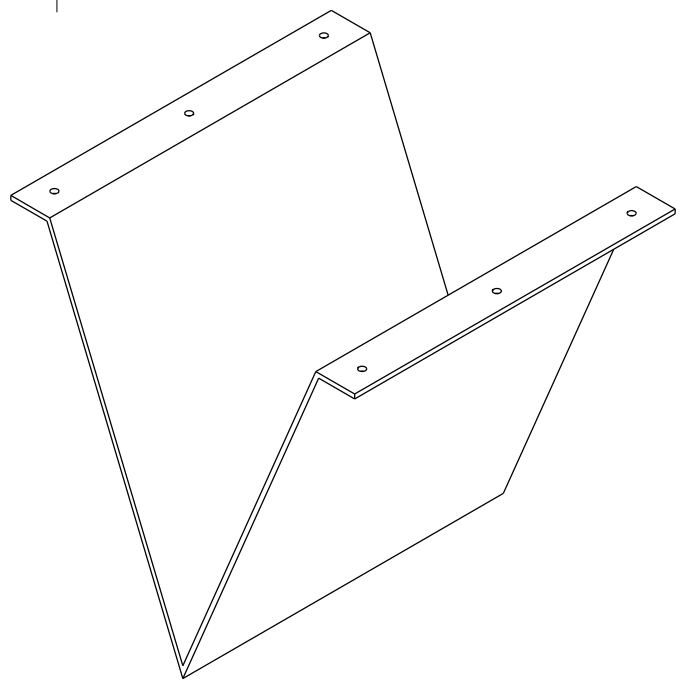

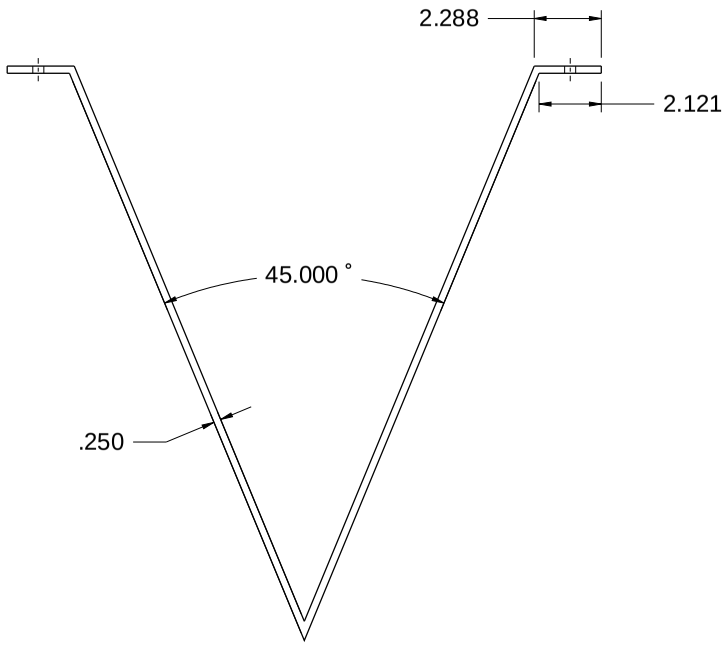

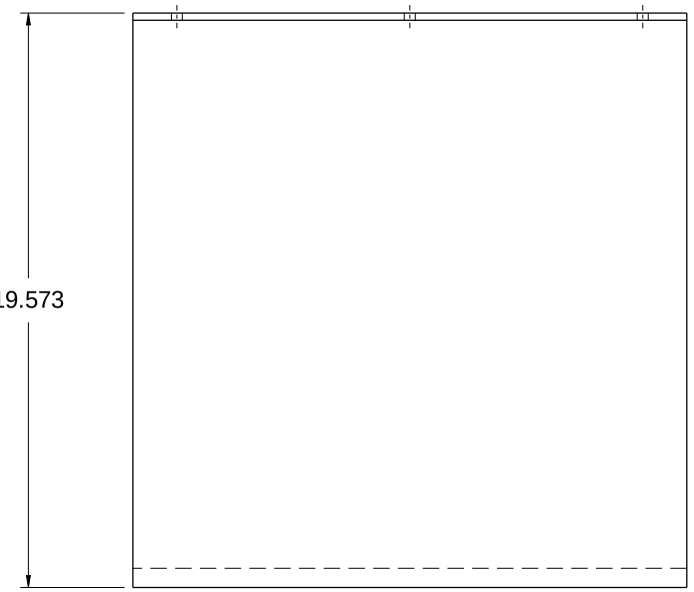

	DRAWN: John Barber	DATE: 2 May 2015	
	CHECKED		
	QA		Wedge - 45 Degrees
	MFG		SIZE: C / FSCM NO. / DWG NO.: SK-002 / REV
	APPROVED		SCALE / SHEET

REVISIONS				
ZONE	REV	DESCRIPTION	DATE	APPROVED

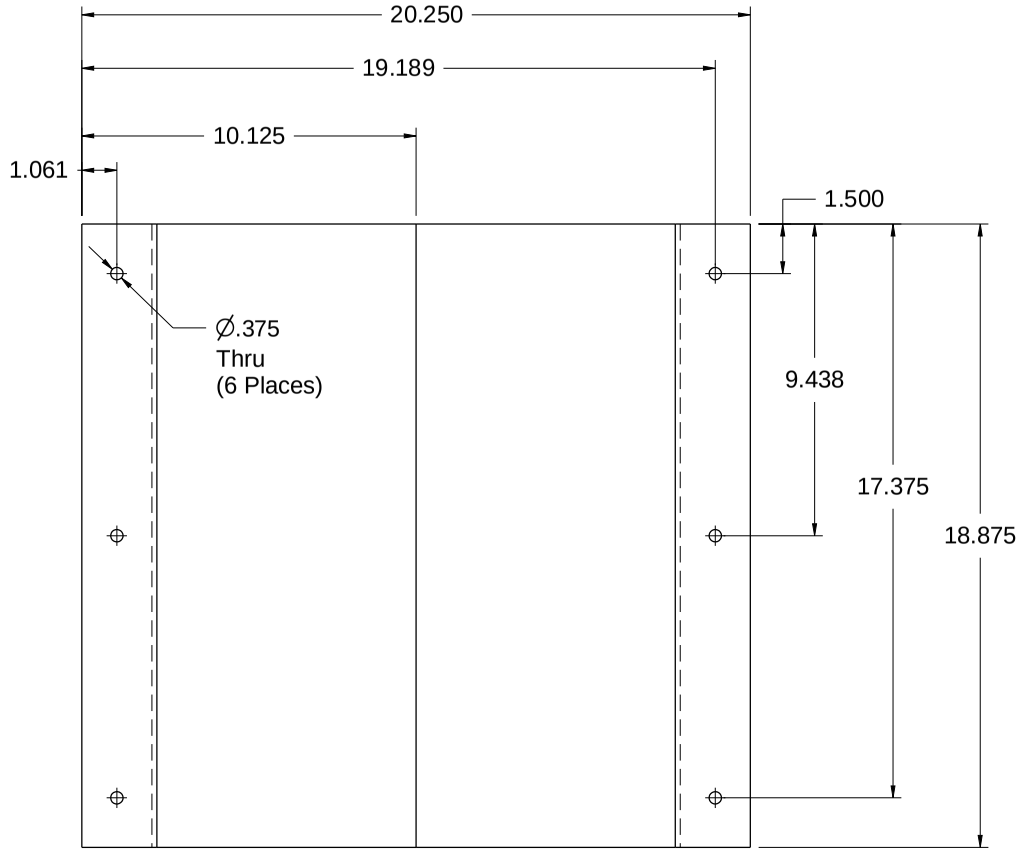

NOTES

1. Material - Steel Plate, 1/4 Inch
2. Finished Weight - 52 Pounds
3. Quantity Required - 1 Each

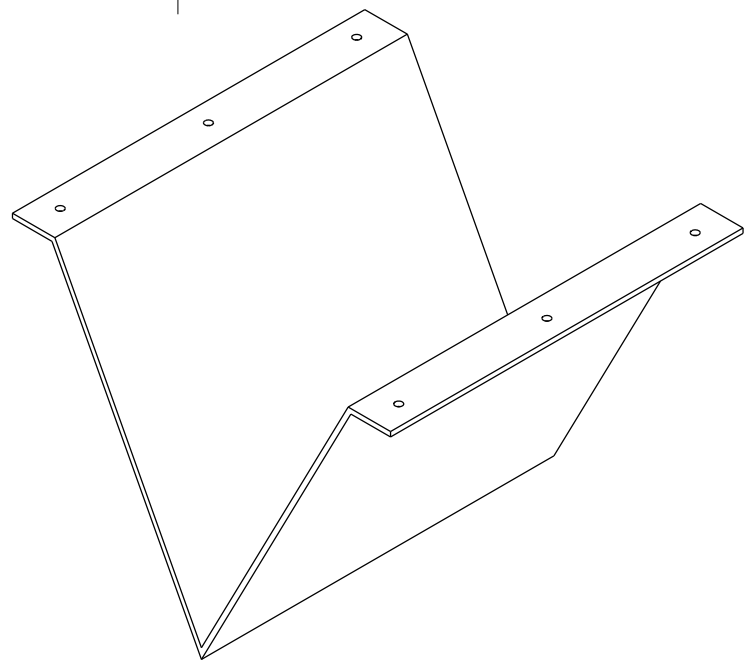

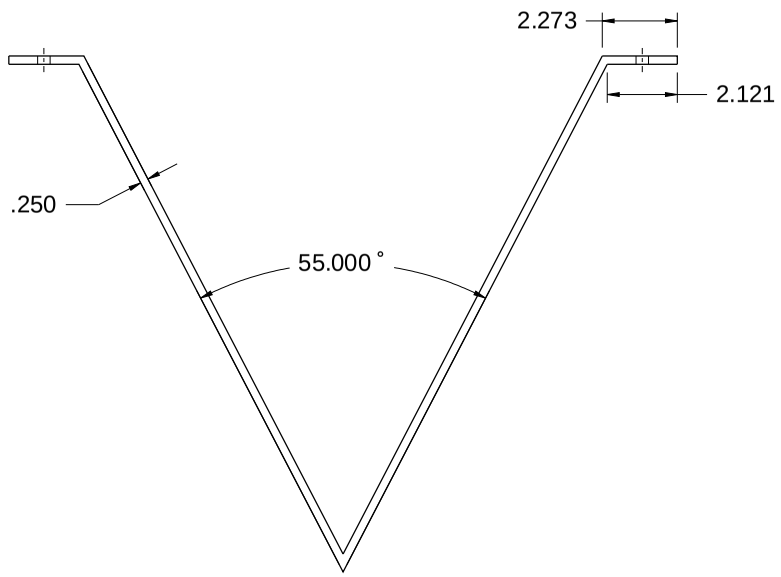

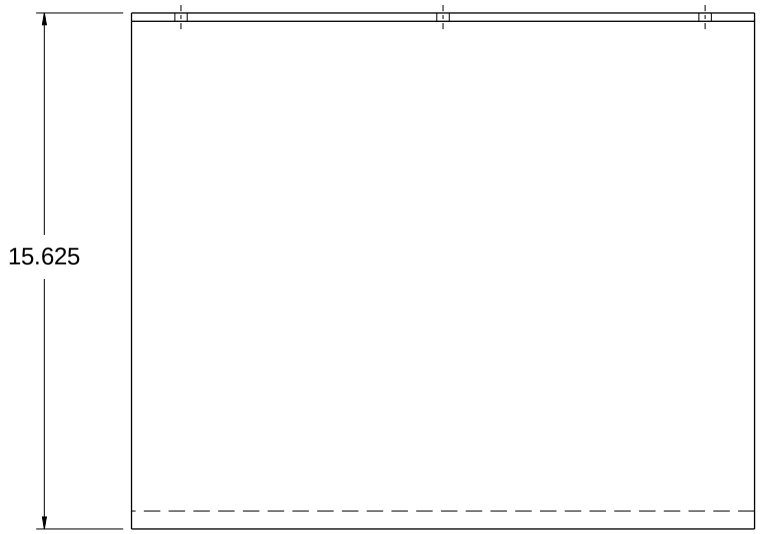

	DRAWN: John Barber	DATE: 2 May 2015	
	CHECKED		
	QA		Wedge - 55 Degrees
	MFG		SIZE: C / FSCM NO. / DWG NO.: SK-009 / REV
	APPROVED		SCALE / SHEET

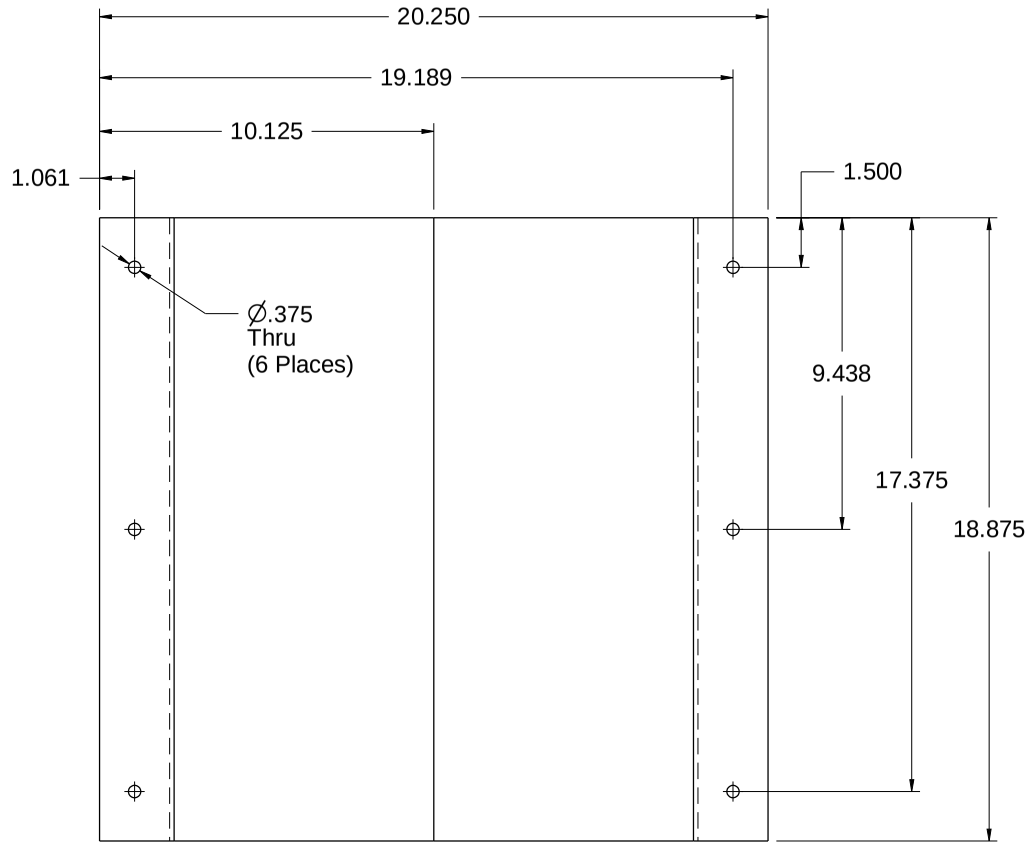

NOTES

1. Material - Steel Plate, 1/4 Inch
2. Finished Weight - 42 Pounds
3. Quantity Required - 1 Each

REVISIONS				
ZONE	REV	DESCRIPTION	DATE	APPROVED

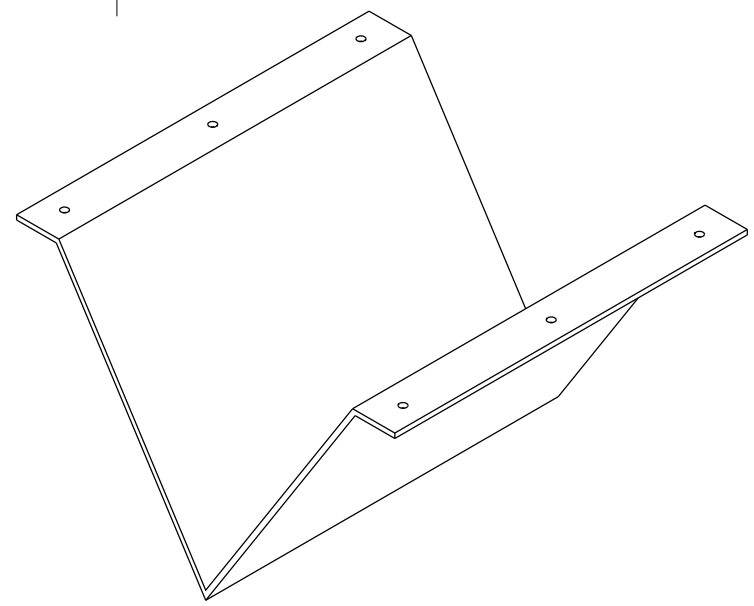

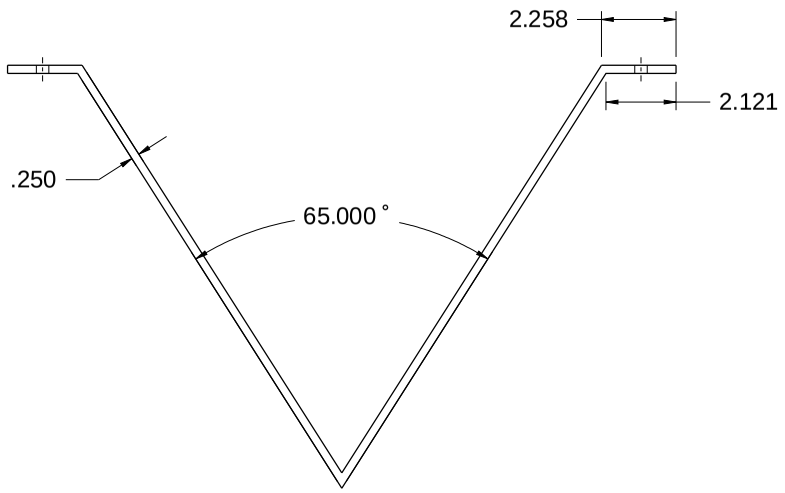

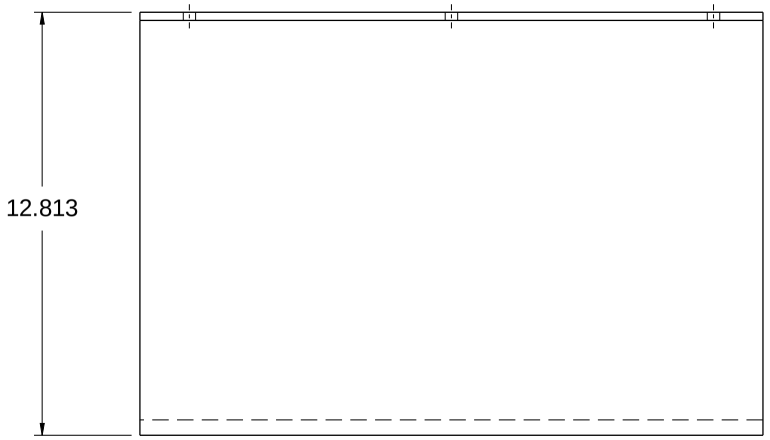

	DRAWN: John Barber	DATE: 4 May 2015	
	CHECKED		
	QA		Wedge - 65 Degrees
	MFG		SIZE: C / FSCM NO. / DWG NO.: SK-012 / REV
	APPROVED		SCALE / SHEET

REVISIONS				
ZONE	REV	DESCRIPTION	DATE	APPROVED

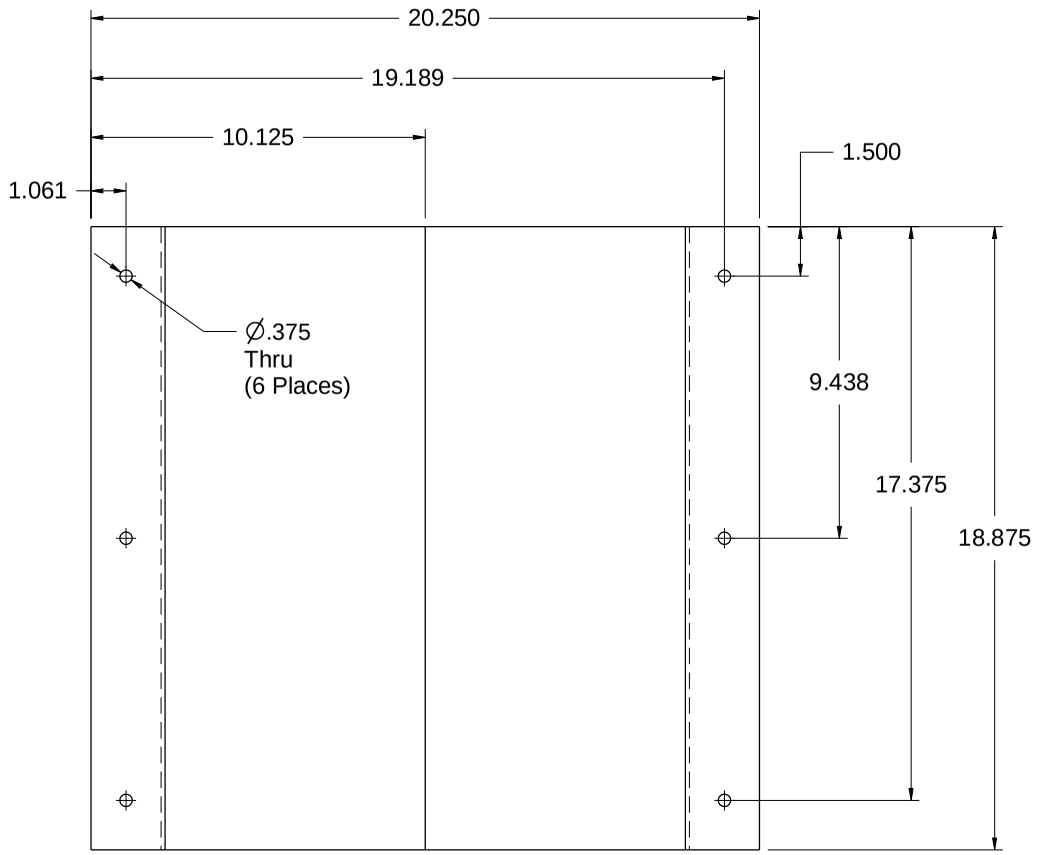

NOTES

1. Material - Steel Plate, 1/4 Inch
2. Finished Weight - 41 Pounds
3. Quantity Required - 1 Each

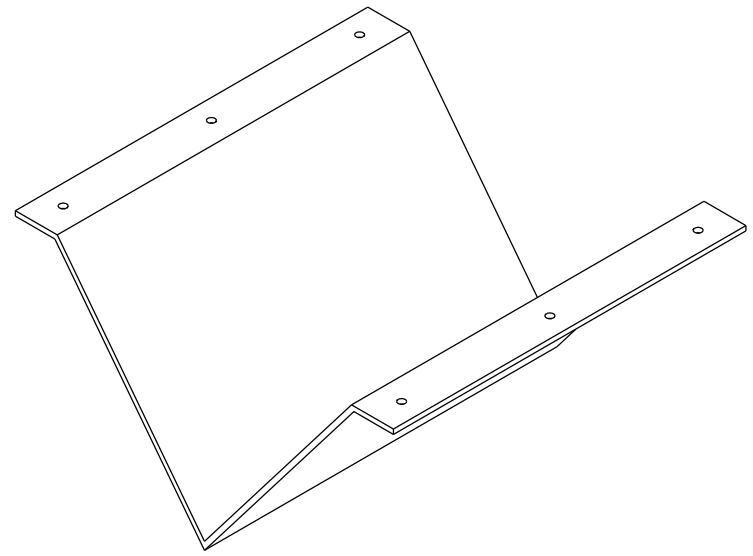

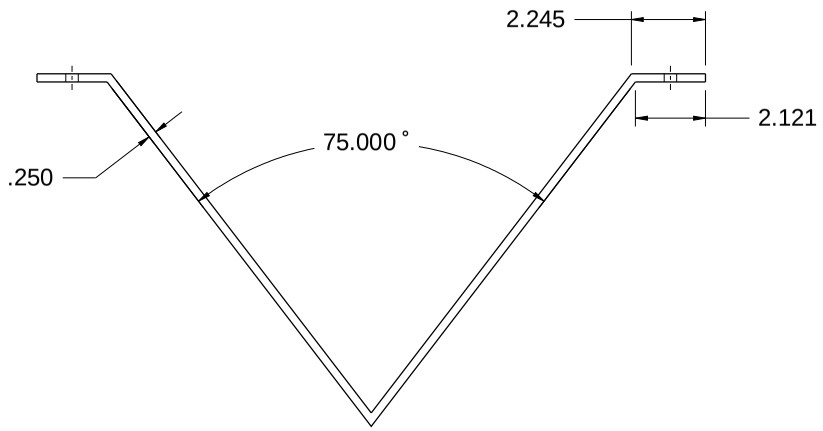

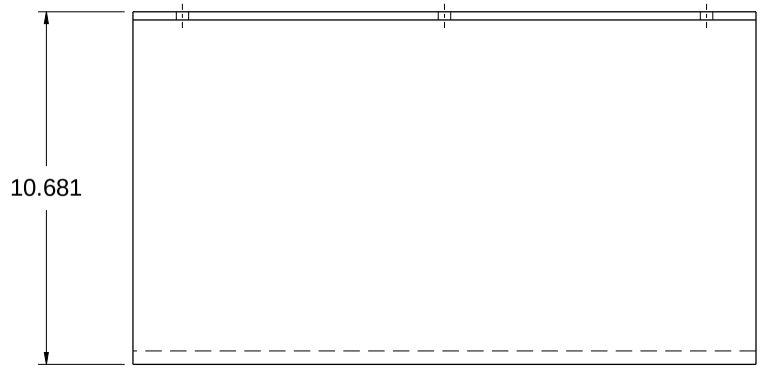

	DRAWN: John Barber	DATE: 10 May 2015	
	CHECKED		
	QA		Wedge - 75 Degrees
	MFG		SIZE: C / FSCM NO. / DWG NO.: SK-015 / REV
	APPROVED		SCALE / SHEET

REVISIONS				
ZONE	REV	DESCRIPTION	DATE	APPROVED

Notes

1. Material - Steel Plate, 1/4 Inch
2. Finished Weight - 29 Pounds
3. Quantity Required - 7 Each

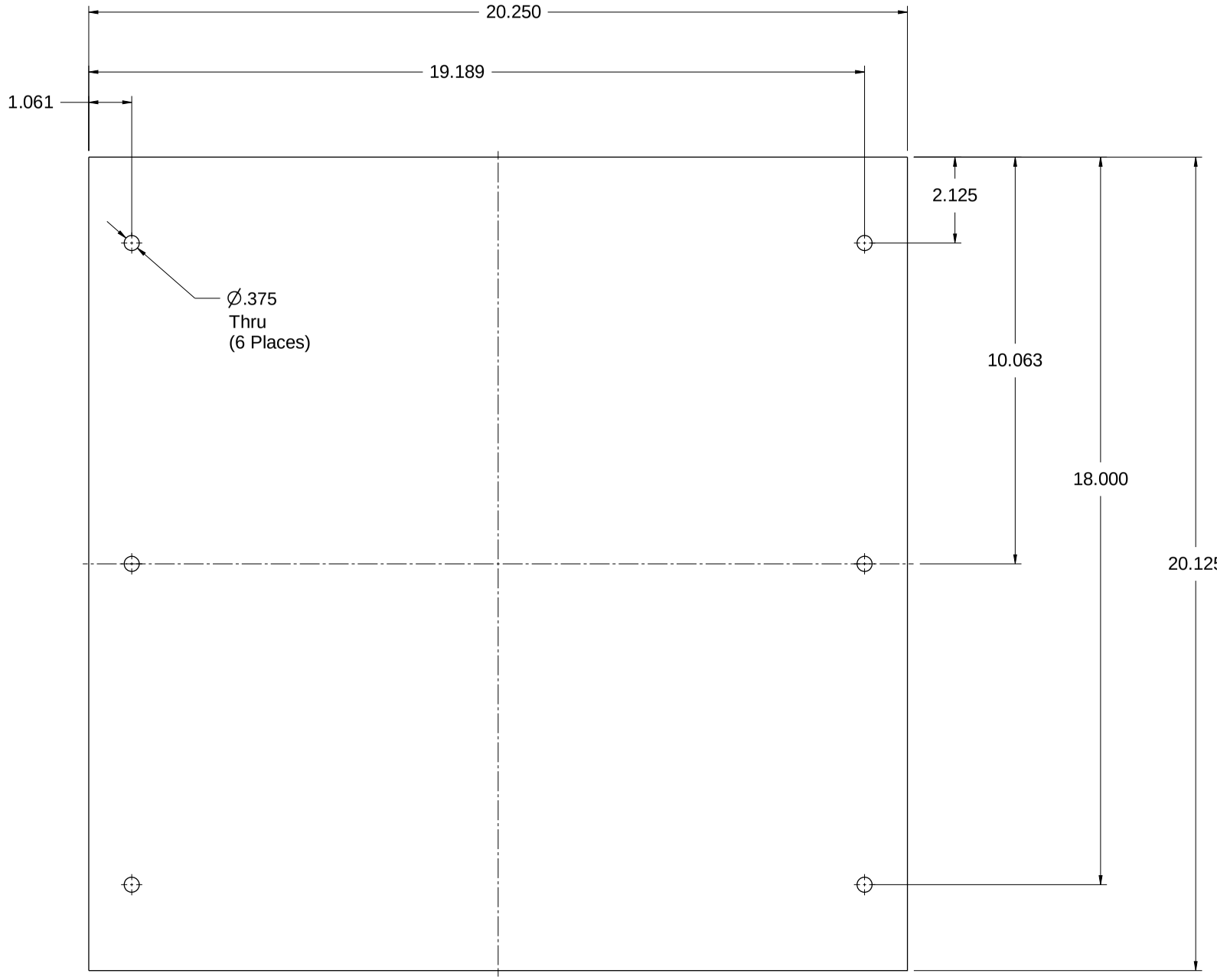

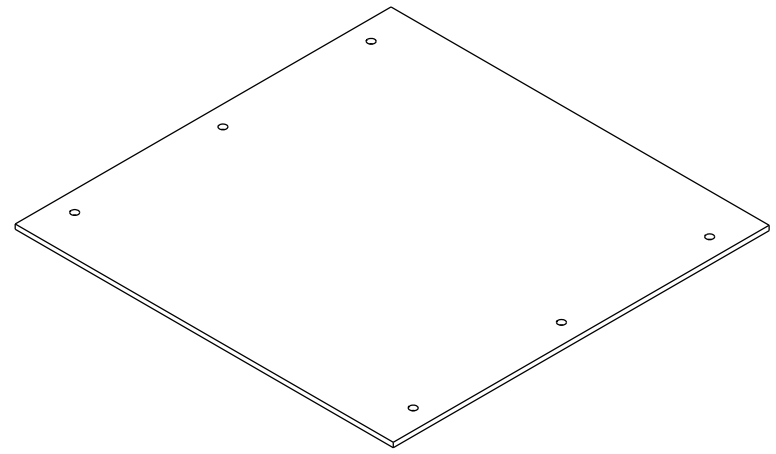

	DRAWN	John Barber	DATE 2 May 2015
	CHECKED		
	QA		
	MFG		
	APPROVED		

Top Plate

SIZE	FSCM NO.	DWG NO.	REV
C		SK-003	

SCALE		SHEET

REVISIONS				
ZONE	REV	DESCRIPTION	DATE	APPROVED

NOTES

1. Material - Steel Plate, 1/4 Inch
2. Finished Weight - 3 Pounds
3. Quantity Required - 2 Each

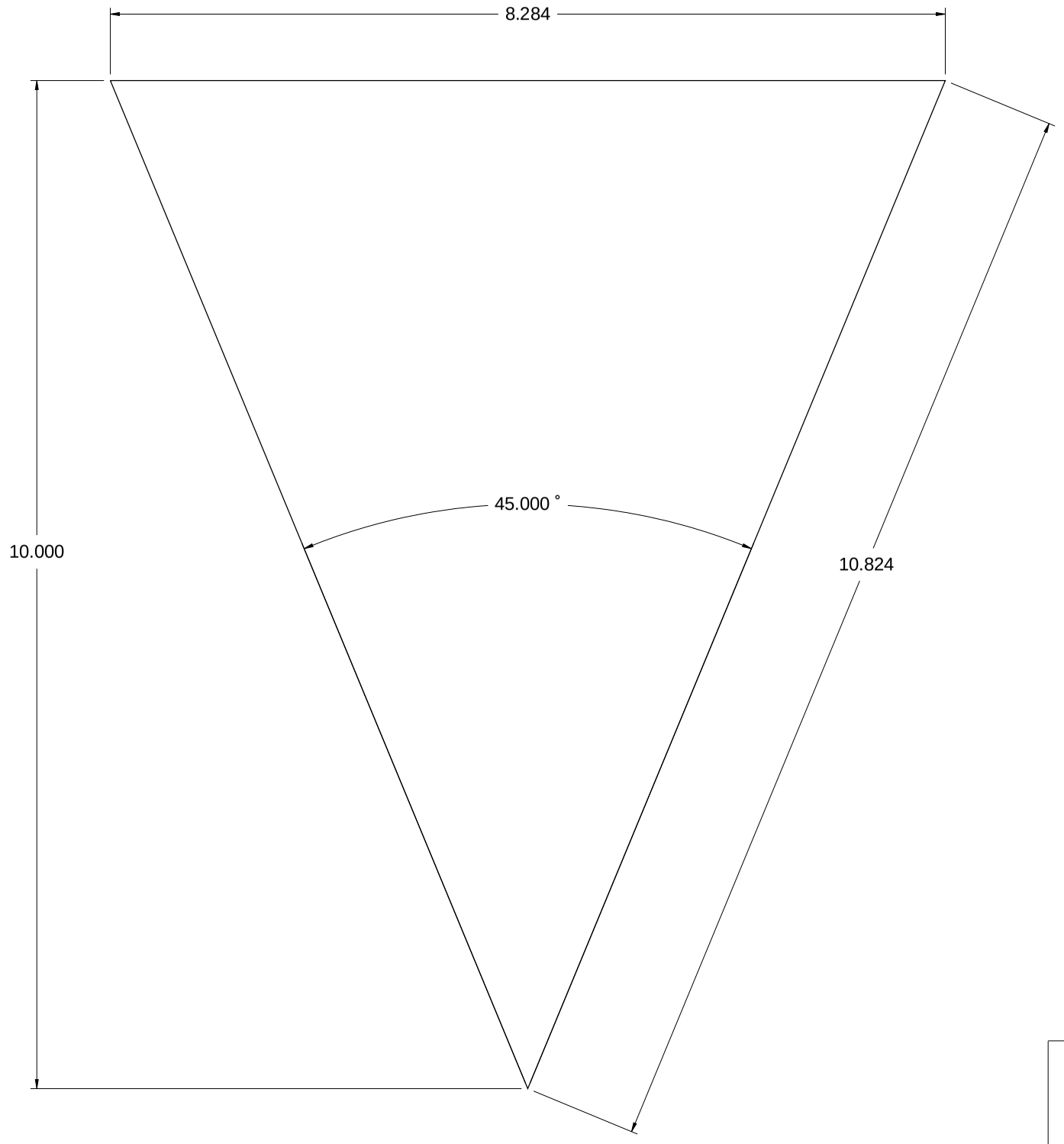

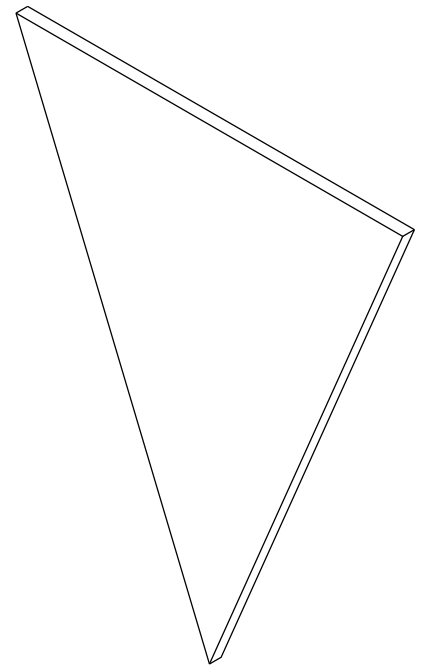

	DRAWN: John Barber	DATE: 2 May 2015	
	CHECKED		End Plate - 45 Degrees
	QA		
	MFG		SIZE: C / FSCM NO. / DWG NO.: SK-005 / REV
	APPROVED		SCALE / SHEET

REVISIONS				
ZONE	REV	DESCRIPTION	DATE	APPROVED

NOTES

1. Material - Steel Plate, 1/4 Inch
2. Finished Weight - 3 Pounds
3. Quantity Required - 2 Each

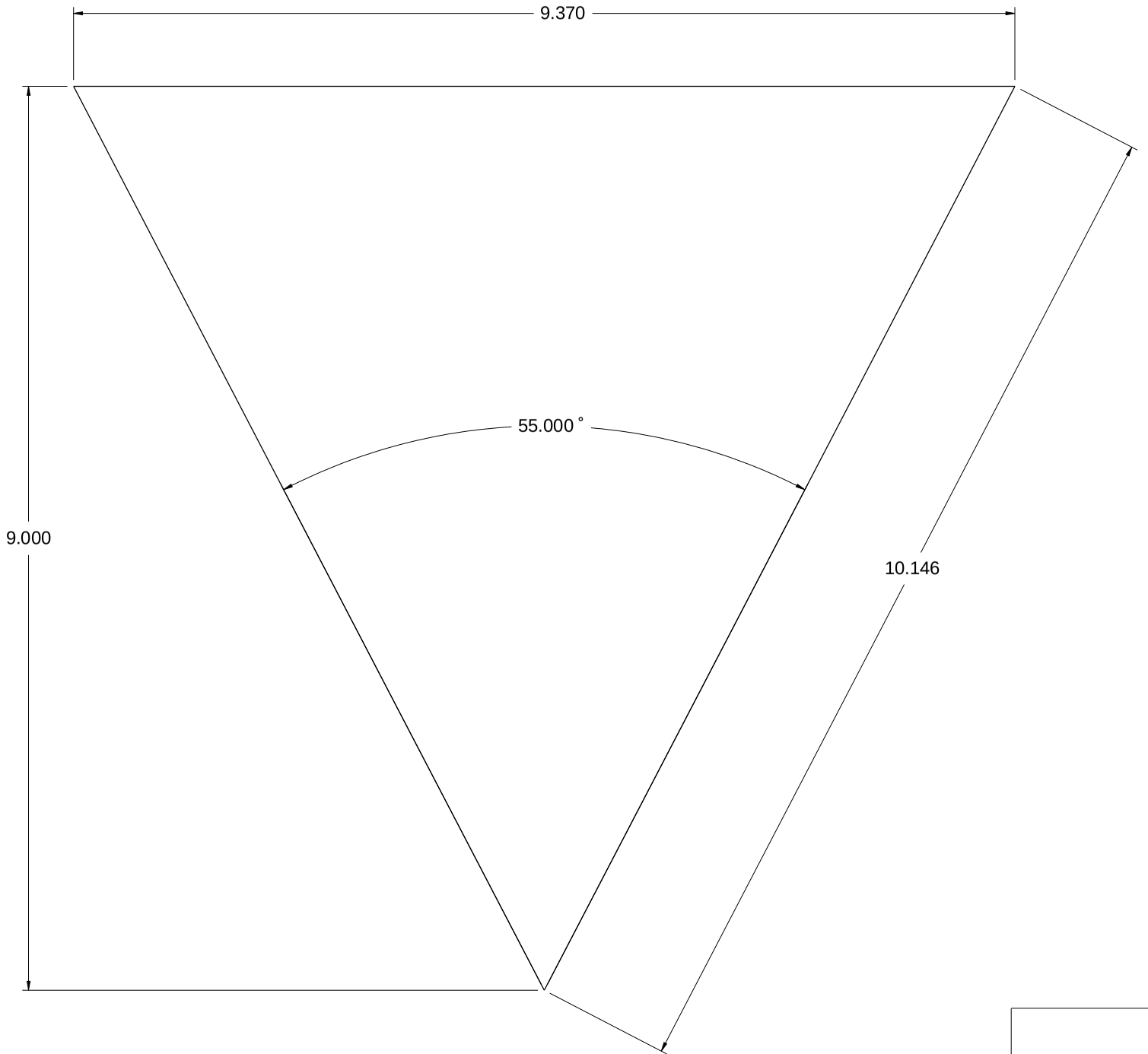

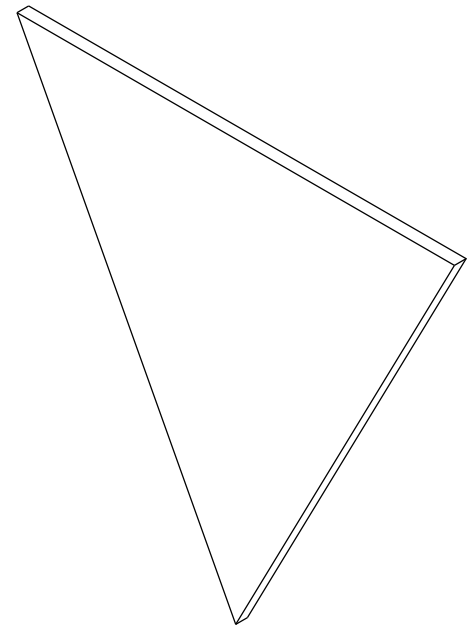

	DRAWN	John Barber	DATE	2 May 2015
	CHECKED			
	QA			
	MFG			
	APPROVED			

End Plate - 55 Degrees

SIZE	FSCM NO.	DWG NO.	REV
C		SK-010	

SCALE | SHEET

NOTES

1. Material - Steel Plate, 1/4 Inch
2. Finished Weight - 3 Pounds
3. Quantity Required - 2 Each

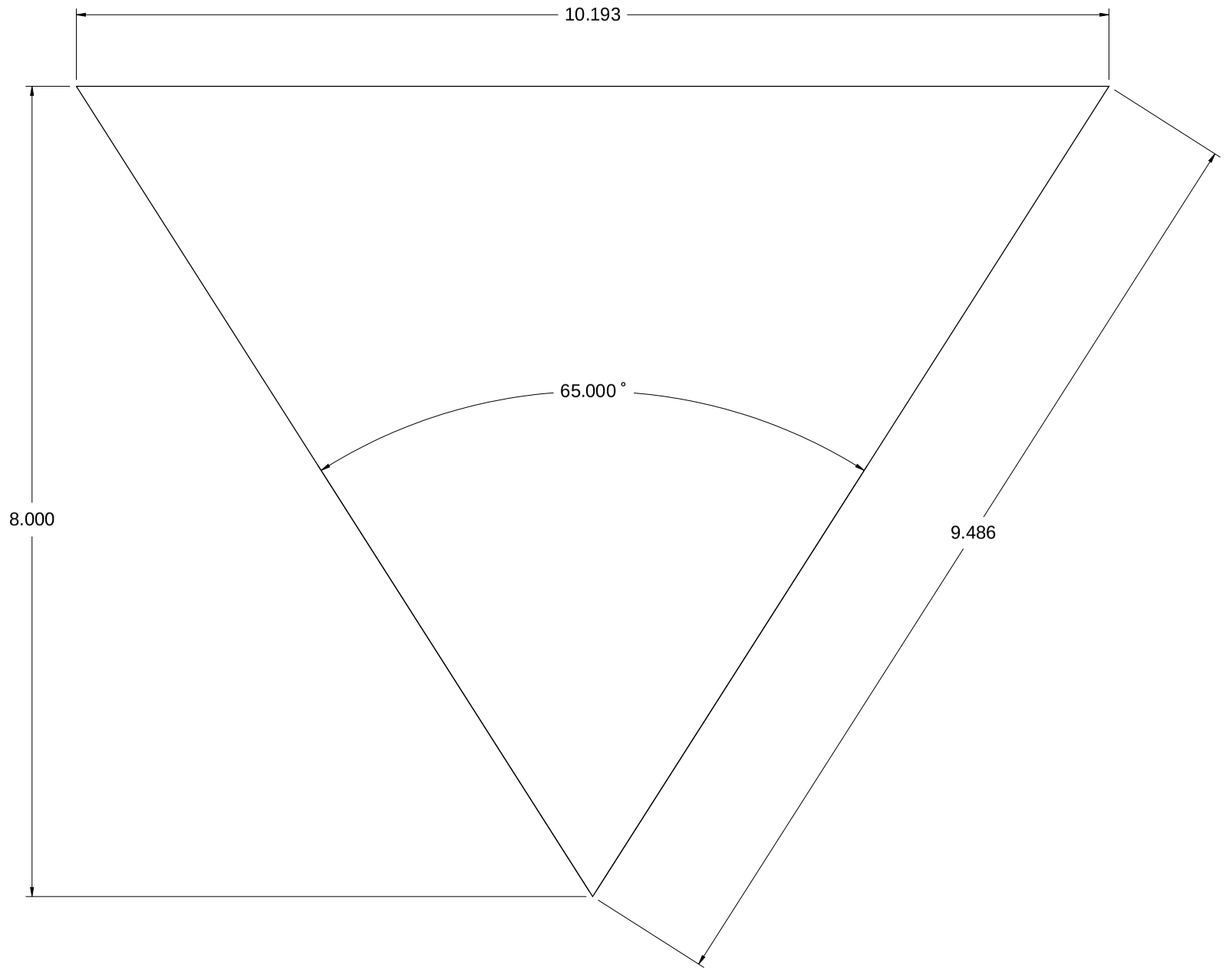

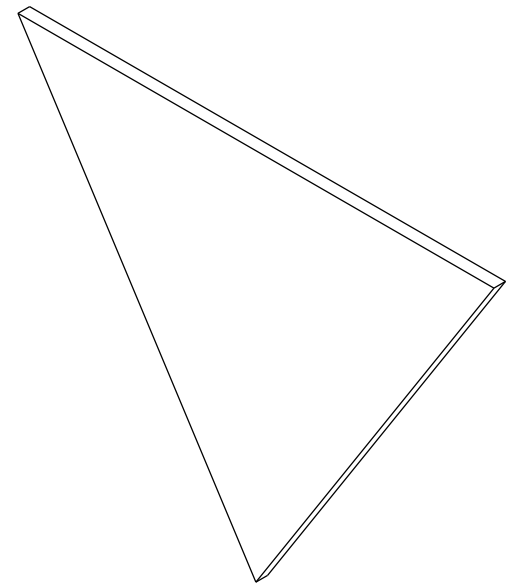

REVISIONS				
ZONE	REV	DESCRIPTION	DATE	APPROVED

	DRAWN: John Barber	DATE: 4 May 2015	
	CHECKED		End Plate - 65 Degrees
	QA		
	MFG		SIZE: C / FSCM NO. / DWG NO.: SK-013 / REV
	APPROVED		SCALE / SHEET

REVISIONS				
ZONE	REV	DESCRIPTION	DATE	APPROVED

NOTES

1. Material - Steel Plate, 1/4 Inch
2. Finished Weight - 4 Pounds
3. Quantity Required - 2 Each

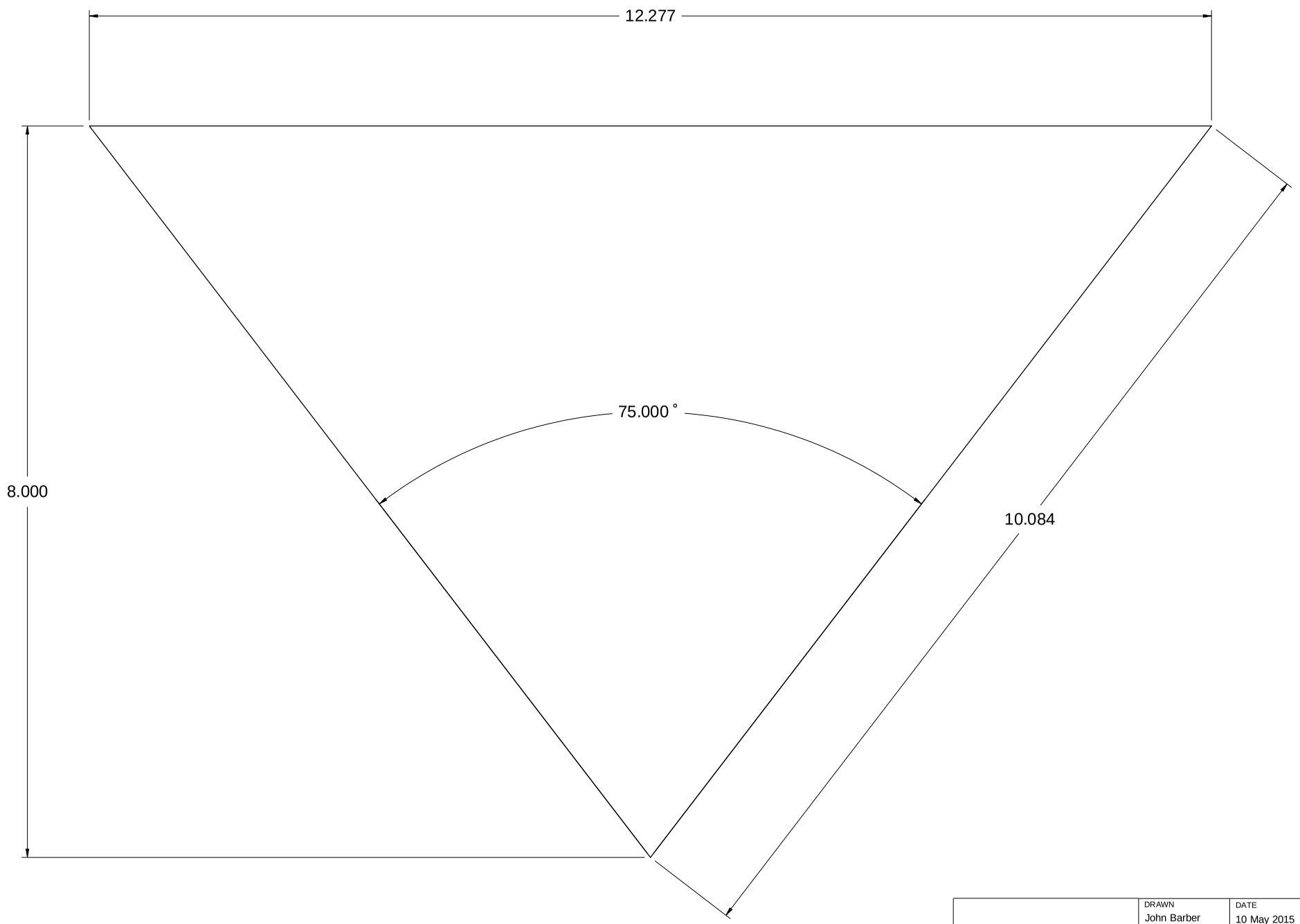

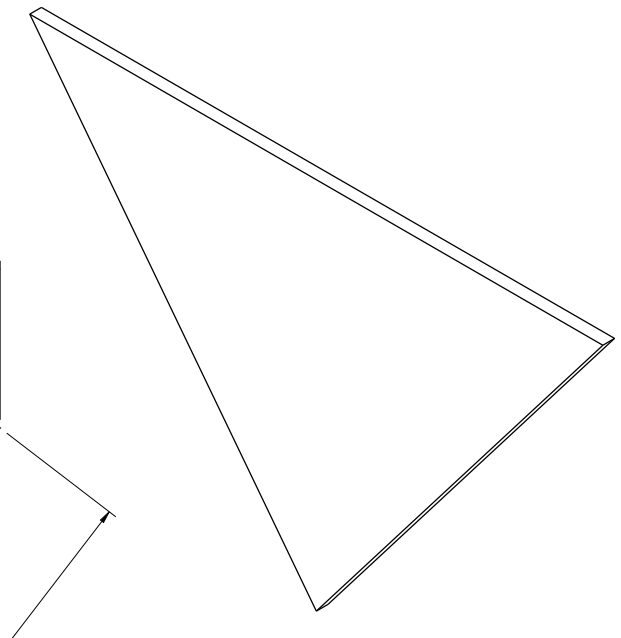

	DRAWN	John Barber	DATE	10 May 2015
	CHECKED			
	QA			
	MFG			
	APPROVED			

End Plate - 75 Degrees

SIZE	FSCM NO.	DWG NO.	REV
C		SK-016	

SCALE		SHEET

NOTES

1. Source - McMaster Carr, Part Number 3014T63

2. Quantity Required - 6 Each

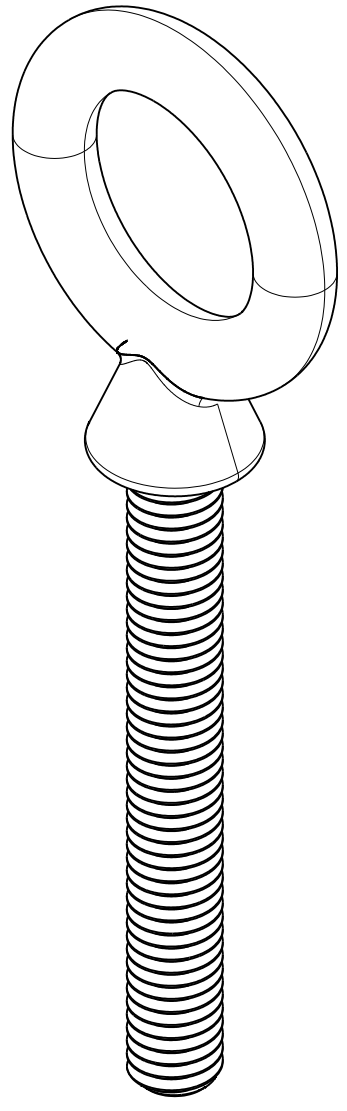

REVISIONS				
ZONE	REV	DESCRIPTION	DATE	APPROVED

DRAWN John Barber	DATE 2 May 2015	
CHECKED		
QA		
MFG		
APPROVED		

Eye Bolt, 3/8 Inch - 16 UNC x 3 Inch Long

SIZE	FSCM NO.	DWG NO.	REV
B		SK-004	

SCALE		SHEET

NOTES

1. Source - McMaster Carr, Part Number 92865A636

2. Quantity Required - 2 Each

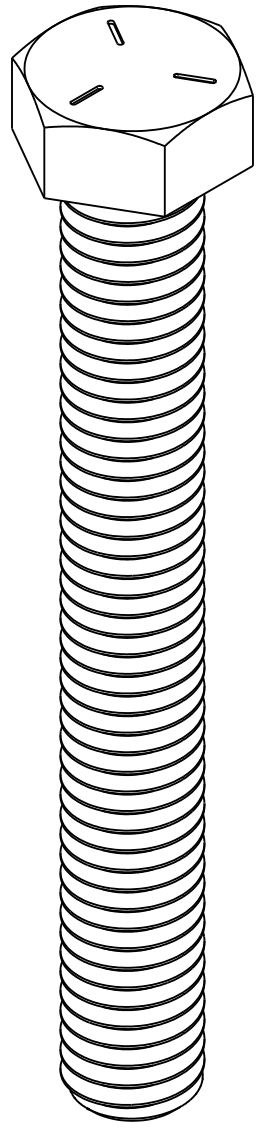

REVISIONS				
ZONE	REV	DESCRIPTION	DATE	APPROVED

DRAWN John Barber	DATE 2 May 2015	
CHECKED		
QA		
MFG		
APPROVED		

Hex Head Bolt - 3/8 Inch - 16 UNC x 3 Inch Long

SIZE	FSCM NO.	DWG NO.	REV
B		SK-006	

SCALE		SHEET

NOTES

1. Source - Open

2. Quantity Required - 6 Each

REVISIONS				
ZONE	REV	DESCRIPTION	DATE	APPROVED

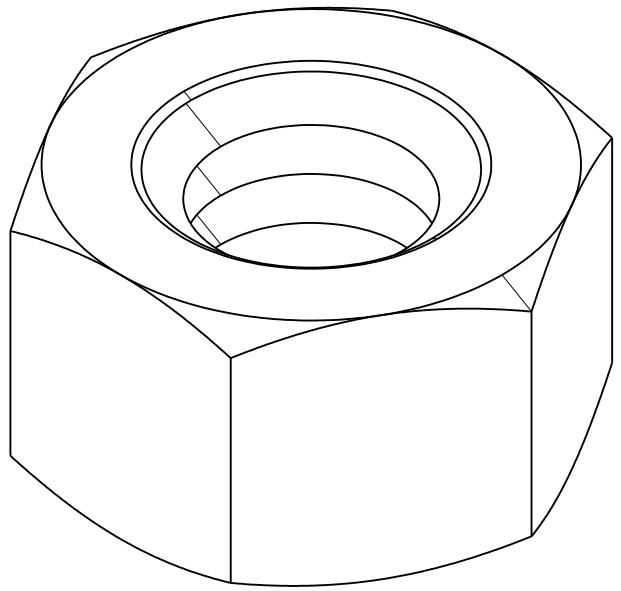

DRAWN	John Barber	DATE 2 May 2015
CHECKED		
QA		
MFG		
APPROVED		

Hex Nut - 3/8 Inch - 16 UNC

SIZE	FSCM NO.	DWG NO.	REV
B		SK-007	

SCALE		SHEET

Appendix B - Complete Raw Data Table

Drop Number	Wedge Angle (Degrees)	Number of Top Plates	Drop Height (Feet)	Weight (Lbs)	Sand Penetration Depth (Inches)	Actual Impulse Magnitude (G's)	Actual Impulse Duration (Milliseconds)	Impact Velocity (Ft/Sec)	Pitch at Impact (deg)	Roll at Impact (deg)	Strain Right Vertical	Strain Left Vertical	Strain Right Horizontal	Strain Left Horizontal
1	45	1	3	104.0	6.0	9.9	83.5	13.6	2.2	0.3	19.0	10.0	7.0	7.0
2	45	1	3	100.2	4.0	6.7	122.5	13.4	-1.1	1.8	<5	8.0	<5	6.0
3	45	1	3	100.2	4.5	6.6	117.5	13.6	-5.0	-0.7	<5	8.0	7.0	<5
4	45	1	3	100.2	4.5	6.3	133.0	13.5	-1.4	-2.3	<5	10.0	<5	<5
5	45	1	3	100.2	5.0	6.2	136.0	13.7	-3.4	1.6	<5	7.0	<5	<5
6	45	2	3	130.0	8.0	10.3	98.5	13.2	1.2	4.9	21.0	14.0	8.0	13.0
7	45	2	3	137.0	6.0	5.9	137.0	13.0	-2.1	-6.1	7.0	-	6.0	-
8	45	2	3	137.0	6.0	6.1	147.9	13.2	-1.2	-0.8	<5	-	<5	-
9	45	2	3	137.0	5.5	5.9	175.9	13.7	-3.7	-0.7	9.0	15.0	7.0	10.0
10	45	2	3	137.0	6.0	5.8	149.9	13.1	2.4	3.2	8.0	11.0	<5	9.0
11	45	3	3	159.0	9.0	9.5	112.5	13.6	-1.8	-5.9	19.0	30.0	9.0	16.0
12	45	3	3	165.5	6.0	5.9	148.0	13.7	-0.9	2.9	<5	29.0	<5	20.0
13	45	3	3	165.5	6.5	5.7	189.5	13.6	-2.0	1.3	<5	14.0	<5	<5
14	45	3	3	165.5	7.0	5.6	162.5	13.6	0.3	4.7	<5	20.0	6.0	<5
15	45	3	3	165.5	7.0	5.5	162.5	13.6	0.5	6.1	<5	28.0	7.0	18.0
16	45	4	3	189.0	9.0	9.4	112.0	13.4	-1.3	-9.2	24.0	61.0	16.0	24.0
17	45	4	3	194.2	7.0	5.5	163.0	13.7	-1.6	6.1	11.0	35.0	7.0	14.0
18	45	4	3	194.2	6.5	5.6	157.0	13.8	2.0	5.0	11.0	20.0	7.0	21.0
19	45	4	3	194.2	7.5	5.5	151.5	13.7	-0.2	1.1	8.0	13.0	7.0	<5
20	45	4	3	194.2	7.0	5.5	143.0	13.7	1.4	-0.6	8.0	16.0	6.0	6.0
21	45	5	3	218.0	9.5	8.6	116.0	13.1	-1.0	-3.1	18.0	35.0	23.0	21.0
22	45	5	3	225.4	6.8	5.7	139.5	13.7	3.2	5.6	<5	20.0	8.0	155.0
23	45	5	3	225.4	7.0	5.6	120.0	13.7	3.1	5.6	13.0	25.0	10.0	15.0
24	45	5	3	225.4	6.8	5.7	156.0	13.7	0.6	1.2	10.0	11.0	9.0	8.0
25	45	5	3	225.4	7.0	5.5	151.0	13.7	2.8	6.4	13.0	40.0	9.0	39.0
26	45	6	3	247.0	10.5	8.9	102.5	13.3	-4.9	-3.9	22.0	24.0	36.0	35.0
27	45	6	3	251.7	7.0	5.4	144.5	13.6	-1.5	7.7	44.0	86.0	11.0	25.0
28	45	6	3	252.0	7.3	5.5	153.5	13.6	1.4	4.8	52.0	57.0	11.0	12.0
29	45	6	3	252.0	7.8	5.3	139.0	13.7	-0.7	2.4	44.0	35.0	7.0	<5
30	45	6	3	252.0	7.8	5.4	129.5	13.8	2.6	3.3	36.0	42.0	6.0	<5
31	45	7	3	277.0	11.5	8.1	119.0	13.6	-2.9	-6.0	38.0	25.0	52.0	62.0
32	45	7	3	281.0	7.5	5.4	123.0	13.5	1.1	5.1	15.0	56.0	22.0	23.0
33	45	7	3	281.0	7.8	5.2	159.5	13.7	1.4	2.3	23.0	47.0	13.0	24.0
34	45	7	3	281.0	8.0	5.4	156.0	13.8	1.6	4.1	18.0	42.0	17.0	16.0
35	45	7	3	281.0	8.0	5.2	163.0	13.7	1.7	5.5	18.0	44.0	14.0	21.0
36	55	1	3	93.0	8.0	8.2	112.0	13.3	-3.5	-13.2	-	-	-	-
37	55	2	3	122.0	7.5	9.2	105.0	13.2	-0.1	-9.8	33.0	13.0	-	12.0
38	55	3	3	150.0	7.0	8.0	108.0	13.2	-0.4	-5.5	38.0	13.0	-	11.0
39	55	4	3	180.0	7.0	7.7	119.0	13.1	-3.3	-5.1	-	-	-	-
40	55	5	3	210.0	8.0	7.0	107.0	13.0	-4.1	-3.2	56.0	17.0	-	15.0

Drop Number	Wedge Angle (Degrees)	Number of Top Plates	Drop Height (Feet)	Weight (Lbs)	Sand Penetration Depth (Inches)	Actual Impulse Magnitude (G's)	Actual Impulse Duration (Milliseconds)	Impact Velocity (Ft/Sec)	Pitch at Impact (deg)	Roll at Impact (deg)	Strain Right Vertical	Strain Left Vertical	Strain Right Horizontal	Strain Left Horizontal
41	55	6	3	239.0	8.0	6.7	134.0	13.2	-3.0	-11.6	56.0	24.0	-	26.0
42	55	7	3	268.0	7.5	8.4	105.5	13.2	-0.9	-1.7	55.0	24.0	-	28.0
43	65	1	3	85.0	4.0	9.8	81.0	13.1	1.0	3.4	7.0	5.0	6.0	6.0
44	65	2	3	115.0	6.0	10.3	101.0	13.1	-3.4	-4.5	17.0	30.0	13.0	10.0
45	65	3	3	144.0	5.0	9.5	88.5	13.1	-1.5	-5.1	23.0	28.0	4.0	14.0
46	65	4	3	172.0	6.5	8.2	121.5	13.2	-4.4	-6.2	22.0	25.0	14.0	3.0
47	65	5	3	201.0	6.5	9.2	105.0	13.2	-2.1	-2.2	48.0	62.0	10.0	7.0
48	65	6	3	230.0	7.0	9.2	107.0	13.3	-3.8	-2.2	53.0	40.0	22.0	18.0
49	65	7	3	259.0	8.5	8.6	108.0	13.3	-3.0	-4.6	66.0	75.0	17.0	31.0
50	75	1	3	86.0	4.5	11.8	82.0	12.8	-3.9	-3.1	22.0	11.0	14.0	5.0
51	75	2	3	111.0	3.5	10.4	88.0	13.4	-	-	10.0	24.0	15.0	12.0
52	75	3	3	140.0	5.0	9.9	92.0	13.4	-0.9	3.0	25.0	40.0	17.0	17.0
53	75	4	3	170.0	6.0	9.6	116.0	13.5	0.9	-3.5	62.0	59.0	19.0	16.0
54	75	5	3	198.0	6.0	9.3	101.0	13.5	-	-	38.0	50.0	23.0	20.0
55	75	6	3	228.0	5.5	9.0	98.0	13.6	-0.6	2.8	70.0	54.0	15.0	23.0
56	75	7	3	257.0	7.0	8.5	123.5	13.6	-2.5	-2.1	103.0	110.0	18.0	20.0
57	45	1	5	104.0	6.3	13.5	80.5	17.3	1.4	3.5	21.0	17.0	10.0	10.0
58	45	1	5	101.0	6.0	8.6	114.0	17.7	-3.5	-2.1	<5	<5	<5	<5
59	45	1	5	101.0	6.0	8.3	153.0	17.7	-2.9	1.4	<5	<5	<5	9.0
60	45	1	5	101.0	6.0	8.5	151.0	17.6	-3.1	1.0	6.0	<5	<5	7.0
61	45	1	5	101.0	6.0	8.3	136.0	17.7	-1.4	3.4	11.0	<5	<5	<5
62	45	2	5	130.0	8.5	12.8	89.5	17.3	1.3	-4.3	13.0	-	8.0	-
63	45	2	5	137.0	7.0	7.5	150.7	17.6	2.2	1.0	19.0	32.0	13.0	13.0
64	45	2	5	137.0	7.0	7.5	159.0	17.7	0.9	4.0	15.0	29.0	9.0	15.0
65	45	2	5	137.0	7.0	7.6	156.5	17.6	0.2	5.7	13.0	36.0	8.0	11.0
66	45	2	5	137.0	7.0	7.6	152.0	17.6	-1.8	2.8	19.0	26.0	10.0	17.0
67	45	3	5	159.0	10.0	12.5	108.5	17.5	-0.7	-6.8	17.0	32.0	10.0	18.0
68	45	3	5	165.5	7.3	7.5	158.5	17.6	-2.3	5.5	9.0	12.0	6.0	17.0
69	45	3	5	165.5	7.3	7.2	153.0	17.7	3.2	22.7	27.0	100.0	15.0	36.0
70	45	3	5	165.5	7.3	7.3	151.5	17.6	3.4	10.1	17.0	52.0	11.0	21.0
71	45	3	5	165.5	7.5	7.6	153.5	17.6	2.3	5.6	12.0	45.0	9.0	14.0
72	45	4	5	189.0	10.0	12.4	89.0	17.7	-3.7	-11.8	27.0	74.0	17.0	23.0
73	45	4	5	194.7	8.0	7.4	155.0	17.6	1.1	4.0	9.0	23.0	8.0	27.0
74	45	4	5	194.7	8.3	7.2	157.5	17.7	-1.0	4.5	14.0	35.0	11.0	18.0
75	45	4	5	194.7	8.0	7.5	146.5	17.6	1.3	5.0	17.0	42.0	14.0	19.0
76	45	4	5	194.7	8.0	7.2	158.0	17.7	2.3	6.7	18.0	38.0	12.0	6.0
77	45	5	5	218.0	10.5	11.3	128.5	17.4	-1.8	-5.9	24.0	65.0	27.0	24.0
78	45	5	5	224.5	8.5	6.7	157.0	17.6	2.5	12.2	41.0	121.0	18.0	43.0
79	45	5	5	224.5	7.8	7.5	139.5	17.6	1.2	0.7	9.0	10.0	10.0	11.0
80	45	5	5	224.5	7.8	7.5	195.5	17.6	1.0	3.7	12.0	24.0	13.0	13.0

Drop Number	Wedge Angle (Degrees)	Number of Top Plates	Drop Height (Feet)	Weight (Lbs)	Sand Penetration Depth (Inches)	Actual Impulse Magnitude (G's)	Actual Impulse Duration (Milliseconds)	Impact Velocity (Ft/Sec)	Pitch at Impact (deg)	Roll at Impact (deg)	Strain Right Vertical	Strain Left Vertical	Strain Right Horizontal	Strain Left Horizontal
81	45	5	5	224.5	7.8	7.6	147.0	17.6	-1.3	1.3	9.0	20.0	14.0	12.0
82	45	6	5	247.0	11.5	10.8	113.0	17.4	-5.3	-8.3	26.0	26.0	37.0	40.0
83	45	6	5	252.0	8.0	7.3	160.0	17.6	0.2	8.5	57.0	110.0	11.0	21.0
84	45	6	5	252.0	8.5	7.1	151.0	17.5	1.8	8.0	49.0	84.0	13.0	33.0
85	45	6	5	252.0	8.5	7.4	145.0	17.6	1.0	2.7	63.0	75.0	12.0	12.0
86	45	6	5	252.0	8.8	7.2	162.0	17.7	1.7	7.2	51.0	75.0	17.0	8.0
87	45	7	5	277.0	12.0	9.9	125.5	17.7	-2.6	-12.4	37.0	99.0	51.0	38.0
88	45	7	5	281.0	9.5	7.0	148.0	17.6	2.1	13.1	40.0	118.0	25.0	41.0
89	45	7	5	281.0	9.5	6.3	157.0	17.6	2.1	19.0	64.0	184.0	28.0	64.0
90	45	7	5	282.0	10.0	6.2	151.0	17.4	-2.9	36.7	80.0	237.0	34.0	77.0
91	45	7	5	282.0	9.5	7.3	142.0	17.4	5.4	10.0	29.0	78.0	30.0	37.0
92	55	1	5	93.0	7.5	14.3	108.0	17.4	-6.1	-17.9	-	-	-	-
93	55	2	5	122.0	7.5	13.3	92.0	17.4	-4.2	-4.8	-	-	-	-
94	55	3	5	150.0	8.5	12.2	130.5	17.4	-0.8	-15.8	34.0	14.0	-	13.0
95	55	4	5	180.0	8.5	11.3	146.5	17.4	-4.7	-14.3	67.0	26.0	-	22.0
96	55	5	5	210.0	9.0	11.1	121.5	17.3	-2.3	-8.8	42.0	26.0	-	20.0
97	55	6	5	239.0	9.5	10.7	136.0	17.4	-2.2	-12.8	71.0	34.0	-	40.0
98	55	7	5	268.0	9.0	10.9	125.0	17.5	-2.4	-10.3	72.0	41.0	-	32.0
99	65	1	5	85.0	5.0	15.4	88.5	17.4	-1.7	-11.1	8.0	5.0	16.0	11.0
100	65	2	5	115.0	6.0	14.9	114.0	17.4	-1.7	-9.3	23.0	39.0	11.0	19.0
101	65	3	5	144.0	7.0	14.4	111.5	17.3	-3.1	-7.2	54.0	56.0	16.0	24.0
102	65	4	5	172.0	7.5	13.2	127.5	17.4	-1.5	-14.8	60.0	52.0	16.0	15.0
103	65	5	5	201.0	8.0	12.9	127.5	17.5	-2.5	-14.1	93.0	82.0	16.0	20.0
104	65	6	5	230.0	8.0	12.6	101.0	17.4	2.7	2.0	46.0	63.0	18.0	32.0
105	65	7	5	259.0	8.5	11.3	121.0	17.3	0.8	6.6	46.0	102.0	15.0	21.0
106	75	1	5	86.0	5.0	16.1	108.5	17.2	2.8	14.7	20.0	27.0	23.0	14.0
107	75	2	5	111.0	4.5	15.0	87.5	17.6	1.4	0.4	24.0	34.0	20.0	15.0
108	75	3	5	140.0	6.0	13.8	96.5	17.7	-	-	53.0	56.0	15.0	14.0
109	75	4	5	170.0	7.0	13.7	121.0	17.7	-1.0	-6.5	76.0	56.0	26.0	15.0
110	75	5	5	198.0	6.5	12.5	116.0	17.7	-	-	72.0	69.0	13.0	23.0
111	75	6	5	228.0	6.5	12.3	117.0	17.6	0.1	-0.9	89.0	72.0	28.0	22.0
112	75	7	5	257.0	8.0	13.0	123.5	17.7	-2.0	-3.2	97.0	118.0	27.0	38.0
113	45	1	7	104.0	8.0	16.7	83.5	20.9	2.2	3.3	17.0	19.0	18.0	20.0
114	45	1	7	101.0	6.5	10.3	132.0	20.8	-1.8	9.3	15.0	6.0	6.0	<5
115	45	1	7	101.0	6.5	10.0	136.0	21.0	-1.2	13.7	27.0	12.0	11.0	<5
116	45	1	7	101.0	6.5	10.0	134.5	20.9	-1.1	13.5	28.0	13.0	13.0	7.0
117	45	1	7	101.0	6.5	9.8	138.0	20.8	-1.3	11.8	27.0	<5	9.0	<5
118	45	2	7	130.0	9.5	16.6	86.0	20.8	5.6	-0.7	35.0	45.0	17.0	21.0
119	45	2	7	137.0	7.8	9.1	148.5	20.8	3.2	-0.3	26.0	32.0	17.0	18.0
120	45	2	7	137.0	7.8	9.3	145.5	20.7	1.9	-0.9	19.0	33.0	12.0	16.0

Drop Number	Wedge Angle (Degrees)	Number of Top Plates	Drop Height (Feet)	Weight (Lbs)	Sand Penetration Depth (Inches)	Actual Impulse Magnitude (G's)	Actual Impulse Duration (Milliseconds)	Impact Velocity (Ft/Sec)	Pitch at Impact (deg)	Roll at Impact (deg)	Strain Right Vertical	Strain Left Vertical	Strain Right Horizontal	Strain Left Horizontal
121	45	2	7	137.0	7.8	9.3	143.0	20.8	2.4	-1.1	22.0	29.0	13.0	17.0
122	45	2	7	137.0	8.0	9.4	123.5	20.8	-2.2	1.6	26.0	35.0	16.0	23.0
123	45	3	7	159.0	10.5	15.4	81.0	20.8	-2.1	-9.6	33.0	63.0	18.0	28.0
124	45	3	7	165.5	8.5	9.1	155.5	20.9	0.7	8.8	16.0	50.0	14.0	9.0
125	45	3	7	165.5	8.0	8.6	154.5	20.9	6.8	18.4	31.0	93.0	14.0	31.0
126	45	3	7	165.5	8.3	8.8	159.0	20.9	1.5	3.9	14.0	44.0	11.0	11.0
127	45	4	7	189.0	11.5	15.4	125.0	20.7	-3.1	-9.8	31.0	71.0	16.0	21.0
128	45	4	7	195.2	9.0	8.4	161.0	20.9	4.6	19.3	32.0	76.0	22.0	40.0
129	45	4	7	195.2	9.0	8.9	157.0	20.8	2.8	10.9	21.0	69.0	8.0	32.0
130	45	4	7	195.2	8.8	9.1	158.0	21.0	1.9	3.1	18.0	43.0	15.0	13.0
131	45	4	7	195.2	8.8	8.2	155.0	21.0	0.4	1.6	14.0	33.0	13.0	14.0
132	45	5	7	218.0	11.5	14.4	123.5	20.7	-6.8	-8.3	38.0	91.0	49.0	49.0
133	45	5	7	225.1	9.0	8.8	142.0	20.9	-1.3	6.8	21.0	53.0	15.0	31.0
134	45	5	7	225.1	8.5	9.1	141.5	20.9	1.2	5.8	17.0	50.0	25.0	30.0
135	45	5	7	225.1	9.0	9.0	131.5	20.8	-1.2	6.1	32.0	84.0	20.0	45.0
136	45	5	7	225.1	8.8	9.0	157.0	21.0	1.0	4.4	16.0	50.0	23.0	33.0
137	45	6	7	247.0	12.0	13.4	123.5	20.8	-4.6	-12.2	21.0	51.0	58.0	68.0
138	45	6	7	252.5	9.5	8.9	158.0	21.0	2.0	4.4	60.0	98.0	14.0	14.0
139	45	6	7	252.5	9.5	8.9	169.5	21.0	3.9	4.4	58.0	97.0	11.0	26.0
140	45	6	7	252.5	9.5	8.7	150.5	21.0	1.2	9.9	51.0	121.0	19.0	32.0
141	45	6	7	252.5	9.8	8.9	150.5	21.0	1.4	11.7	78.0	142.0	17.0	23.0
142	45	7	7	277.0	13.5	13.0	135.0	20.8	-2.9	-19.8	41.0	91.0	80.0	78.0
143	45	7	7	282.0	10.0	7.4	150.0	20.9	4.4	28.2	76.0	201.0	32.0	59.0
144	45	7	7	282.0	10.0	7.4	156.5	20.9	6.3	34.8	94.0	240.0	41.0	65.0
145	45	7	7	282.0	10.0	8.6	153.5	21.0	3.6	21.7	60.0	168.0	50.0	39.0
146	45	7	7	281.0	10.0	7.9	157.5	21.0	1.5	7.8	42.0	127.0	49.0	47.0
147	55	1	7	93.0	7.0	17.8	96.5	20.7	-5.9	-25.0	35.0	17.0	-	7.0
148	55	2	7	122.0	8.5	17.1	109.0	20.6	-4.7	-7.5	-	-	-	-
149	55	3	7	150.0	9.0	16.8	126.0	20.6	-1.8	-17.4	44.0	23.0	-	24.0
150	55	4	7	180.0	9.0	15.1	127.0	20.8	-7.7	-19.4	58.0	14.0	-	36.0
151	55	5	7	210.0	9.5	15.0	121.5	20.7	-1.2	-6.6	59.0	36.0	-	34.0
152	55	6	7	239.0	10.0	14.1	133.5	20.8	-2.8	-15.5	89.0	52.0	-	60.0
153	55	7	7	268.0	10.0	14.4	130.0	21.0	-3.7	-19.0	101.0	56.0	-	57.0
154	65	1	7	85.0	6.0	18.9	87.0	20.5	-4.4	-17.7	20.0	18.0	9.0	16.0
155	65	2	7	115.0	7.0	18.8	116.5	20.6	-1.6	-9.8	52.0	77.0	29.0	28.0
156	65	3	7	144.0	7.5	18.4	95.0	20.7	-1.9	-2.1	68.0	89.0	37.0	28.0
157	65	4	7	172.0	8.5	16.9	124.0	20.7	-2.0	-12.5	65.0	83.0	26.0	36.0
158	65	5	7	201.0	9.0	16.5	155.0	20.7	-4.4	-9.3	124.0	121.0	27.0	22.0
159	65	6	7	230.0	9.5	15.8	122.0	20.5	-5.5	-13.9	142.0	67.0	58.0	28.0
160	65	7	7	259.0	9.0	15.9	109.5	20.7	-3.8	-4.1	131.0	149.0	34.0	21.0

Drop Number	Wedge Angle (Degrees)	Number of Top Plates	Drop Height (Feet)	Weight (Lbs)	Sand Penetration Depth (Inches)	Actual Impulse Magnitude (G's)	Actual Impulse Duration (Milliseconds)	Impact Velocity (Ft/Sec)	Pitch at Impact (deg)	Roll at Impact (deg)	Strain Right Vertical	Strain Left Vertical	Strain Right Horizontal	Strain Left Horizontal
161	75	1	7	86.0	5.5	20.5	86.0	20.5	-3.9	-10.8	45.0	17.0	12.0	12.0
162	75	2	7	111.0	5.5	18.3	94.0	20.8	-0.9	-0.6	37.0	47.0	18.0	10.0
163	75	3	7	140.0	6.0	17.8	96.5	20.9	-1.6	-0.7	62.0	92.0	26.0	24.0
164	75	4	7	170.0	7.0	16.8	123.0	20.9	-0.5	-6.0	103.0	94.0	38.0	13.0
165	75	5	7	198.0	7.5	16.5	125.5	20.9	-1.3	-7.1	129.0	106.0	40.0	44.0
166	75	6	7	228.0	7.0	16.4	116.5	21.0	-	-	139.0	127.0	31.0	43.0
167	75	7	7	257.0	8.5	16.9	139.0	21.0	-1.0	-	197.0	154.0	29.0	24.0
168	45	1	9	104.0	8.5	19.8	88.5	24.1	0.2	-20.5	28.0	60.0	3.0	17.0
169	45	1	9	102.5	7.0	11.5	136.3	23.1	-0.8	2.1	98.0	-	37.0	-
170	45	1	9	102.5	7.0	11.2	132.2	23.1	-0.5	-5.2	91.0	-	35.0	-
171	45	1	9	102.5	7.5	11.5	120.1	23.1	-0.5	4.1	88.0	-	30.0	-
172	45	1	9	102.5	7.0	11.1	137.4	23.8	0.3	1.9	98.0	-	34.0	-
173	45	2	9	130.0	10.5	19.0	108.0	24.0	-5.1	-8.3	50.0	71.0	27.0	31.0
174	45	2	9	137.0	7.5	11.5	134.5	23.7	0.1	4.7	25.0	31.0	13.0	15.0
175	45	2	9	137.0	7.8	11.0	147.0	23.8	2.2	3.9	25.0	35.0	18.0	28.0
176	45	2	9	137.0	8.0	11.2	138.5	23.7	-0.9	0.2	17.0	31.0	19.0	24.0
177	45	2	9	137.0	8.8	11.0	146.5	23.8	0.9	5.1	27.0	41.0	19.0	15.0
178	45	3	9	159.0	11.5	18.3	81.0	24.0	-1.9	-6.6	28.0	54.0	17.0	23.0
179	45	3	9	165.5	9.0	10.4	149.0	23.9	5.2	17.9	29.0	91.0	14.0	28.0
180	45	3	9	165.5	9.0	10.4	156.5	23.7	1.7	8.0	21.0	63.0	11.0	19.0
181	45	3	9	165.5	9.5	10.4	150.0	23.8	6.1	14.6	30.0	60.0	13.0	31.0
182	45	3	9	165.5	9.5	11.0	152.5	24.0	3.6	6.8	17.0	27.0	13.0	29.0
183	45	4	9	189.0	11.8	17.6	104.0	23.7	2.3	-4.0	33.0	57.0	58.0	37.0
184	45	4	9	196.0	8.5	10.6	153.0	23.7	5.2	13.8	24.0	70.0	17.0	32.0
185	45	4	9	196.0	9.0	10.5	150.5	24.0	4.2	7.2	19.0	51.0	19.0	201.0
186	45	4	9	196.0	9.0	10.2	154.5	23.8	5.8	11.8	24.0	62.0	13.0	420.0
187	45	4	9	198.3	9.0	10.4	150.0	23.8	5.8	16.2	29.0	85.0	21.0	55.0
188	45	5	9	218.0	12.8	17.0	130.0	24.0	-1.7	-12.0	41.0	104.0	80.0	77.0
189	45	5	9	225.8	9.8	10.6	146.0	23.8	-0.2	6.8	19.0	61.0	32.0	110.0
190	45	5	9	225.8	9.5	10.5	148.5	23.7	2.1	5.7	20.0	47.0	28.0	17.0
191	45	5	9	225.8	9.3	10.7	133.5	23.8	2.1	0.7	14.0	21.0	31.0	18.0
192	45	5	9	225.7	9.8	10.8	154.0	23.8	0.9	6.6	29.0	97.0	27.0	40.0
193	45	6	9	247.0	13.5	16.3	109.0	24.0	-8.5	-20.7	38.0	104.0	110.0	171.0
194	45	6	9	253.0	10.0	9.6	153.0	23.7	2.4	13.8	94.0	130.0	16.0	26.0
195	45	6	9	253.0	10.0	10.9	146.5	23.8	1.0	8.6	112.0	79.0	32.0	120.0
196	45	6	9	253.0	10.0	10.4	151.0	23.8	0.8	13.0	106.0	67.0	29.0	280.0
197	45	6	9	253.0	10.0	10.3	148.5	23.8	0.2	15.5	115.0	173.0	22.0	173.0
198	45	7	9	277.0	14.8	15.1	139.5	24.0	-5.3	-23.2	36.0	153.0	118.0	159.0
199	45	7	9	281.0	10.0	9.5	151.5	23.7	3.1	31.9	84.0	210.0	42.0	65.0
200	45	7	9	281.0	10.0	10.0	156.5	23.8	2.1	23.9	64.0	180.0	58.0	49.0

Drop Number	Wedge Angle (Degrees)	Number of Top Plates	Drop Height (Feet)	Weight (Lbs)	Sand Penetration Depth (Inches)	Actual Impulse Magnitude (G's)	Actual Impulse Duration (Milliseconds)	Impact Velocity (Ft/Sec)	Pitch at Impact (deg)	Roll at Impact (deg)	Strain Right Vertical	Strain Left Vertical	Strain Right Horizontal	Strain Left Horizontal
201	45	7	9	281.0	10.0	9.6	157.0	23.8	1.6	12.7	55.0	161.0	59.0	50.0
202	45	7	9	281.0	10.0	10.3	154.5	23.6	2.4	23.1	85.0	204.0	64.0	176.0
203	55	1	9	93.0	8.0	22.0	99.0	23.9	-3.0	-25.4	36.0	22.0	-	24.0
204	55	2	9	122.0	9.0	20.2	117.5	23.9	-1.4	-12.6	47.0	23.0	-	31.0
205	55	3	9	150.0	9.5	19.4	135.5	23.9	-3.3	-18.4	46.0	31.0	-	37.0
206	55	4	9	180.0	9.5	19.4	104.5	23.8	0.3	6.4	60.0	69.0	-	70.0
207	55	5	9	210.0	10.5	17.9	121.0	23.9	-4.2	-14.4	70.0	58.0	-	58.0
208	55	6	9	239.0	11.5	17.7	131.0	23.9	-2.3	-12.2	94.0	91.0	-	88.0
209	55	7	9	268.0	10.5	17.1	118.0	24.1	-5.1	-20.5	168.0	105.0	-	165.0
210	65	1	9	85.0	6.5	23.3	81.0	23.8	-3.2	-9.4	-	-	-	-
211	65	2	9	115.0	7.5	22.3	61.0	23.8	-2.1	-11.7	83.0	93.0	22.0	23.0
212	65	3	9	144.0	8.5	21.5	110.5	23.8	-3.5	-8.2	138.0	134.0	70.0	46.0
213	65	4	9	172.0	9.0	19.7	130.5	23.8	-4.9	14.6	159.0	102.0	55.0	30.0
214	65	5	9	201.0	9.5	20.2	140.5	23.9	-3.5	-11.5	279.0	186.0	69.0	31.0
215	65	6	9	230.0	9.5	19.2	117.0	23.8	-2.3	-5.7	202.0	148.0	64.0	55.0
216	65	7	9	259.0	9.5	19.3	91.5	24.0	-5.4	0.0	198.0	240.0	26.0	69.0
217	75	1	9	86.0	6.0	23.4	77.5	23.7	-2.8	-16.7	47.0	21.0	16.0	4.0
218	75	2	9	111.0	6.0	21.5	93.5	24.1	1.5	4.9	57.0	84.0	23.0	52.0
219	75	3	9	140.0	7.0	21.4	97.5	24.2	-1.7	-1.0	95.0	113.0	58.0	29.0
220	75	4	9	170.0	8.0	20.4	119.0	24.2	-	-	151.0	158.0	47.0	19.0
221	75	5	9	198.0	8.0	20.5	129.5	24.3	-	-	178.0	157.0	60.0	37.0
222	75	6	9	228.0	8.0	20.1	122.0	24.3	-	-	140.0	185.0	32.0	30.0
223	75	7	9	257.0	8.5	19.9	139.5	24.2	-4.4	-5.4	268.0	239.0	29.0	56.0

VITA

John D. Barber

C/O

Batten College of Engineering and Technology

1105 Engineering Systems Building

Norfolk, VA 23529

Cell Phone: (757) 617-1546, E-mail: jbarber20@Verizon.net

Education: University of Evansville, Mechanical Engineering, B.S., Jun 1985

Old Dominion University, Mechanical Engineering, M.S., Dec. 2016

General Experience:

2007 – Present	Naval Surface Warfare Center, Carderock Division, Mechanical Engineer
2007 - 2007	Booz Allen Hamilton, Associate
2006 - 2007	Scientific Research Corporation, Senior Analyst
2000 - 2006	Naval Special Warfare Development Group, Mechanical Engineer
1985 - 2000	Naval Surface Warfare Center, Crane Division, Mechanical Engineer

Experience Summary:

Extensive experience in test and evaluation, test program planning and execution, test and evaluation logistics support, test fixture design, demolition application software design and support. Test and evaluation experience includes, small arms, small arms ammunition, shoulder fired anti-tank weapons, hand emplaced demolition and small combatant craft.